

# Masterthesis

## EEG-Based Characterization Of Different Upper Limb Movements For The Control Of Prosthetic Hands

Ahmad Sasah  
Matriculation Number 3202980

Summer Semester 2019  
Hannover, August 5, 2019

First Examiner: Prof. Dr.-Ing. Tobias Ortmaier  
Second Examiner: Prof. Dr.-Ing. Christof Hurschler  
Supervisors: Dr. Sc. hum. Eike Jakubowitz  
M. Sc. Max-Heinrich Laves

# Contents

<b>1</b>	<b>Introduction and Motivation</b>	<b>1</b>
1.1	The State of the Art Prosthetic Hands nowadays . . . . .	2
1.2	Targeted Muscle Reinnervation . . . . .	3
1.3	The synergy between EMG, EEG, and cable driven hand . . . . .	3
1.4	Brain Computer Interface System . . . . .	4
1.5	Comparison between EEG, and ECG Signals . . . . .	6
1.6	Overview of the Project . . . . .	6
1.7	The main Objectives in this thesis . . . . .	7
1.8	The Kinematics-Data Acquisition System . . . . .	9
1.9	The EEG-Data Acquisition System . . . . .	10
1.9.1	Neuron Activity . . . . .	11
1.9.2	The Brain Lobes . . . . .	12
1.9.3	The Brodmann Areas . . . . .	13
1.9.4	The EEG Montage and the Measurement Modes . . . . .	14
1.9.5	The Frequency Bands of the EEG . . . . .	14
<b>2</b>	<b>Methods</b>	<b>16</b>
2.1	The used Tasks in this Study . . . . .	16
2.1.1	Gestures 1-10 . . . . .	17
2.1.2	Grasps 11-30 . . . . .	18
2.1.3	Precision vs. Power Grasps . . . . .	21
2.1.4	Dividing EEG Data into Classes . . . . .	22
2.2	Events Extraction . . . . .	22
2.3	EEG Data Filtering . . . . .	22
2.4	EEG Artifacts Removal . . . . .	23
2.4.1	Independent Component Analysis ICA . . . . .	25
2.5	Epoching . . . . .	26
2.6	Machine Learning Classifiers with CSP . . . . .	28
2.6.1	Common Spatial Pattern . . . . .	28
2.6.2	Logistic Regression . . . . .	30
2.6.3	Support Vector Machine . . . . .	31
2.6.4	Kernel Trick . . . . .	31
2.6.5	Support Vector Machine RBF Kernel . . . . .	31
2.6.6	Support Vector Machine Parameters . . . . .	31
2.6.7	Random Forest . . . . .	32
2.6.8	Linear Discriminant Analysis . . . . .	32
2.7	Machine Learning on Riemannian Manifold . . . . .	32
2.7.1	Covariance Matrices . . . . .	33
2.7.2	Classification in Tangent Space . . . . .	33
2.7.3	Classification with Minimum Distance to the Mean . . . . .	34
2.8	Cross Validation . . . . .	35

2.9	Multi-Grasps Classification . . . . .	35
2.9.1	The Confusion Matrix and Classification Report Parameters . . . . .	36
2.10	Cross-Subjects Classification . . . . .	37
2.10.1	Deep Learning Methods . . . . .	37
2.10.2	The Boosting Methods . . . . .	42
2.11	Classification using 31 and 16 Channels . . . . .	43
<b>3</b>	<b>Results</b>	<b>45</b>
3.1	Filtering . . . . .	45
3.2	EEG Artifacts Removal . . . . .	48
3.3	Epoching . . . . .	52
3.4	Binary Classification of Individual Subjects . . . . .	61
3.4.1	Classification Results for Gestures vs. Grasps . . . . .	61
3.4.2	Classification Results for Precision vs. Power Grasps . . . . .	64
3.4.3	Comparison between ML Algorithms . . . . .	67
3.4.4	Common Spatial Pattern . . . . .	70
3.4.5	Covariance Matrices for Gestures vs. Grasps . . . . .	71
3.5	Multi-Grasps Classification . . . . .	72
3.5.1	Multi-Grasps Classification Results . . . . .	72
3.5.2	Confusion Matrices and Classification Reports . . . . .	73
3.5.3	Covariance Matrices for different Grasps . . . . .	84
3.6	Cross-Subjects Classification . . . . .	88
3.6.1	Cross-Subjects Gestures vs. Grasps Classification . . . . .	88
3.6.2	Cross-Subjects Classification for Precision vs. Power Grasps . . . . .	91
<b>4</b>	<b>Discussion</b>	<b>93</b>
4.1	Comparison between Machine Learning methods . . . . .	94
4.2	Comparison between Machine Learning and Deep Learning Methods . . . . .	95
4.3	Comparison according to the Gender, and the Age of the Subject . . . . .	95
4.4	Common Spatial Pattern . . . . .	95
4.5	Confusion Matrices . . . . .	95
<b>5</b>	<b>Conclusion, Limitations, and Future Outlook</b>	<b>97</b>
5.1	Conclusion . . . . .	97
5.2	Limitations . . . . .	97
5.3	Future Outlook . . . . .	98
<b>References</b>		<b>i</b>

# List of Figures

1.0.1	The joints in human hand and the Degrees Of Freedom (DOF) [9] . . . . .	1
1.1.1	Controlling simple prosthetic hand with EMG Sensors [25] . . . . .	3
1.3.1	Tendon driven prosthetic hand [37] . . . . .	4
1.4.1	Comparison between different types of BCI's [38]. . . . .	5
1.6.1	Overview about the Project . . . . .	7
1.6.2	Overview about Orthogo project . . . . .	7
1.8.1	The subject wears spherical passive markers according to SoftPro project . . . . .	9
1.8.2	12 Stereo VICON cameras according to the SoftPro project . . . . .	10
1.9.1	A neuron making a synaptic connection with another neuron [55] . . . . .	11
1.9.2	4 Main Human Brain-Lobes . . . . .	12
1.9.3	Brodmann Areas . . . . .	14
1.9.4	Electroencephalography (EEG) bands [71] . . . . .	15
2.1.1	Grasps taxonomy [91] . . . . .	18
2.1.2	Gestures types according to SoftPro project . . . . .	18
2.1.3	Grasps Types according to SoftPro Project . . . . .	19
2.1.4	Left: precision grasps - Right: power grasps. According to SoftPro Project . . . . .	21
2.3.1	Temporal filters . . . . .	22
2.4.1	Eyes vertical movement [95] . . . . .	24
2.4.2	Eye-Blink Artifacts [96] . . . . .	24
2.4.3	ICA as Cocktail Party Problem . . . . .	26
2.6.1	Logistic Function [109] . . . . .	30
2.6.2	Kernel trick [115] . . . . .	31
2.7.1	Riemann tangent space at point $G$ . EEG trials are points[128] . . . . .	33
2.7.2	Riemann minimum distance to the mean [130] . . . . .	34
2.10.1	EEG signals are converted to 2D meshes [48] . . . . .	38
2.10.2	Cascade convolutional recurrent neural networks [48] . . . . .	39
2.10.3	Parallel convolutional recurrent neural networks [48] . . . . .	40
2.10.4	Series of topographical images are generated from EEG data and fed into RCNN	41
2.10.5	AdaBoost Method of combining weak learners [141] . . . . .	43
2.11.1	31 electrodes localization plotted in EEGLAB(Delorme and Makeig, 2004) . . . . .	44
2.11.2	16 electrodes localization plotted in EEGLAB(Delorme and Makeig, 2004) . . . . .	44
3.1.1	Average gestures vs. grasps classification results for different frequency-intervals .	46
3.1.2	Average precision vs. power grasps classification results for different frequency-intervals . . . . .	47
3.1.3	Average multi-grasps classification results for different frequency-intervals . . . . .	47
3.2.1	Independent Compondnet Analysis (ICA) components of 1st Subject (S1) plotted in EEGLAB(Delorme and Makeig, 2004) . . . . .	49
3.2.2	S1 ICA component as eye artifact plotted in EEGLAB(Delorme and Makeig, 2004)	49
3.2.3	S1 ICA component muscle artifact plotted in EEGLAB(Delorme and Makeig, 2004)	50
3.2.4	S1 ICA component as eye artifact plotted in EEGLAB(Delorme and Makeig, 2004)	50
3.2.5	S1 ICA component as eye artifact plotted in EEGLAB(Delorme and Makeig, 2004)	51

3.2.6	ICA components for 2nd Subject (S2) plotted in EEGLAB(Delorme, Makeig, 2004)	51
3.3.1	Average gestures vs. grasps classification results for different time intervals using Logistic Regression used with Common Spatial Patterns in this study (LogReg), Random Forest used with Common Spatial Patterns in this study (RF), Classification in Tangent Space (TS), and Classification with Minimum Distance to the Mean (MDM) . . . . .	54
3.3.2	Average gestures vs. grasps classification results for different time intervals using LogReg, RF, TS, and MDM . . . . .	55
3.3.3	Average power vs. precision grasps classification results for different time intervals using LogReg, RF, TS, and MDM . . . . .	56
3.3.4	Average precision vs. power grasps classification results for different time intervals using LogReg, RF, TS, and MDM in the case of using only 16 electrodes . . . . .	57
3.3.5	S2 multi-classification results for different time intervals using LogReg, RF, TS, and MDM . . . . .	58
3.3.6	10th Subject (S10) multi-classification results for different time intervals using LogReg, RF, TS, and MDM . . . . .	59
3.3.7	S1 multi-classification results for different time intervals using LogReg, RF, TS, and MDM . . . . .	60
3.4.1	Comparison between binary classification results (gestures vs. grasps) of individual subjects using TS, Support Vector Machine used with Common Spatial Patterns in this study (SVC) with linear kernel, SVC with Radial Basis Function (RBF) kernel, LogReg, RF, and Linear Discriminant Analysis used with Common Spatial Patterns in this study (LDA) . . . . .	62
3.4.2	Comparison between binary classification results (gestures vs. grasps) of individual subjects using TS, SVC with linear kernel, SVC with RBF kernel, LogReg, RF, and LDA in the case of using only 16 electrodes . . . . .	63
3.4.3	Comparison between binary classification results (precision vs. power grasps) of individual subjects using TS, SVC with linear kernel, SVC with RBF kernel, LogReg, RF, and LDA . . . . .	65
3.4.4	Comparison between binary classification results (precision vs. power grasps) of individual subjects using TS, SVC with linear kernel, SVC with RBF kernel, LogReg, and LDA using only 16 electrodes . . . . .	66
3.4.5	Comparison between different ML algorithms classification results (gestures vs. grasps) using 31-16 electrodes . . . . .	68
3.4.6	Comparison between different ML algorithms classification results (precision vs. power grasps) using 31-16 electrodes . . . . .	69
3.4.7	S2 spatial Patterns Gestures vs. Grasps . . . . .	70
3.4.8	S2 spatial patterns of precision vs. power grasps . . . . .	70
3.4.9	S2 mean covariance matrix in gestures using pyRiemann package [127] . . . . .	71
3.4.10	S2 mean covariance matrix in grasps using pyRiemann package [127] . . . . .	72
3.5.1	S2 normalized confusion matrix for 20 grasps . . . . .	74
3.5.2	S2 16-electrodes normalized confusion matrix for 20 grasps . . . . .	76
3.5.3	S10 normalized confusion matrix for 20 grasps . . . . .	78

3.5.4	S10 16-electrodes normalized confusion matrix for 20 grasps . . . . .	80
3.5.5	S1 normalized confusion matrix for 20 grasps . . . . .	82
3.5.6	S1 16-electrodes normalized confusion matrix for 20 grasps . . . . .	84
3.5.7	S2 mean covariance matrix for the Grasp Suitcase (Suitcase) task using pyRiemann package [127] . . . . .	86
3.5.8	S2 mean covariance matrix for the Grasp Small Cup (SmallCup) task using pyRiemann package [127] . . . . .	87
3.5.9	S2 mean covariance matrix for the Grasp Key to Extract (ExtractKey) task using pyRiemann package [127] . . . . .	88
3.6.1	Comparison between cross-subject classification methods for the gestures vs. grasps case using 31 and 16 electrodes . . . . .	90
3.6.2	Comparison between cross-subject classification methods for the precision vs. power grasps case using 31 and 16 electrodes . . . . .	92

## List of Tables

3.5.1	S2 Classification report for 20 grasps . . . . .	75
3.5.2	S2 Classification report for 20 grasps using 16 electrodes . . . . .	77
3.5.3	S10 Classification report for 20 grasps . . . . .	79
3.5.4	S10 Classification report for 20 grasps using 16 electrodes . . . . .	81
3.5.5	S1 Classification report for 20 grasps . . . . .	83
3.5.6	S1 Classification report for 20 grasps using 16 electrodes . . . . .	85

## List of Abbreviations

**actiCAP** Active Electrode Cap.

**actiCHamp** Active Channel Amplifier.

**Apple** Grasp Apple.

**Ball** Grasp Tennis Ball.

**Bat** Grasp Tennis Bat.

**BCI** Brain Computer Interface.

**Book** Grasp Book.

**Bottle** Grasp Bottle to Pour Water.

**BottleCap** Grasp Bottle Cap.

**Cap** Grasp Cap.

**CNN** Convolutional Neural Netowrk.

**CSP** Common Spatial Patterns.

**DL** Deep Learning.

**DOF** Degrees Of Freedom.

**DoorKnb** Grasp Doorknob.

**ECG** Electrocorticography.

**EEG** Electroencephalography.

**EMG** Electromyography.

**EOG** Electrooculography.

**ExtractKey** Grasp Key to Extract.

**FFT** Fast Fourier Transform.

**Glass** Grasp Glass to Drink.

**GND** Ground.

**ICA** Independent Compondnet Analysis.

**Laptop** Grasp Laptop.

**LargeCup** Grasp Large Cup.

**LDA** Linear Discriminant Analysis used with Common Spatial Patterns in this study.

**LED** Light Emitting Diode.

**LogReg** Logistic Regression used with Common Spatial Patterns in this study.

**LSTM** Long Short-Term Memory.

**MDM** Classification with Minimum Distance to the Mean.

**MEG** Magnetoencephalography.

**ML** Machine Learning.

**NCI** Neural Control Interface.

**PCA** Principal Component Analysis.

**PenDraw** Grasp Pen to draw.

**PenMove** Grasp Pen to move.

**Phone** Grasp Phone.

**PSD** Power Spectrum Density.

**RB<sub>F</sub>** Radial Basis Function.

**RCNN** Recurrent Convolutional Neural Network.

**ReceiveTray** Receive Tray.

**RF** Random Forest used with Common Spatial Patterns in this study.

**RNN** Recurrent Neural Network.

**S1** 1st Subject.

**S10** 10th Subject.

**S11** 11th Subject.

**S2** 2nd Subject.

**S3** 3rd Subject.

**S4** 4th Subject.

**S5** 5th Subject.

**S6** 6th Subject.

**S7** 7th Subject.

**S8** 8th Subject.

**S9** 9th Subject.

**SD** Standard Deviation.

**SmallCup** Grasp Small Cup.

**Suitcase** Grasp Suitcase.

**SVC** Support Vector Machine used with Common Spatial Patterns in this study.

**TeaBag** Grasp Tea-Bag.

**Toothbrush** Grasp Toothbrush.

**TS** Classification in Tangent Space.

**WHO** World Health Organization.

**Declaration of Academic Integrity:**

I hereby confirm, that the present masterthesis is solely my own work and that any text passages, pictures, or diagrams from books, papers, or other sources have been acknowledged and fully cited.

Name:

Date:

Signature:

# 1 Introduction and Motivation

The number of amputations is globally increasing due to injuries, diabetes, vascular attacks, and earthquakes [1], [2]. According to a joint study in 2001 by World Health Organization (WHO) and the World Bank, there are more than billion disabled people in the world [3]. There will be an estimated 3.6 million amputees in the U.S in 2050 [4]. Researches have shown, that the case of an amputee can be compared with the feeling of loss, self-stigma, and depression [5], [6]. The case of the amputee can be even compared with the case of someone who lost his wife [7].

The hand is the second most complex organ in the human body after the brain [8]. In healthy subjects, hand movement is achieved by about thirty muscles (intrinsic, extrinsic) [8]. Extrinsic muscles are responsible for flexion and extension movements, whereas the intrinsic muscles are responsible for fine motoric control [8].

A human hand has about twenty DOF as in 1.0.1. According to [9], the human hand can be divided into three functional components: The thumb, that has a vital role in interactions with all other fingers on the hand, due to its movement of opposition with respect to other fingers. The index and middle fingers, that help making the precision grasp with the help of the thumb. The ring and little fingers, that help the other fingers to have a stronger grasp.

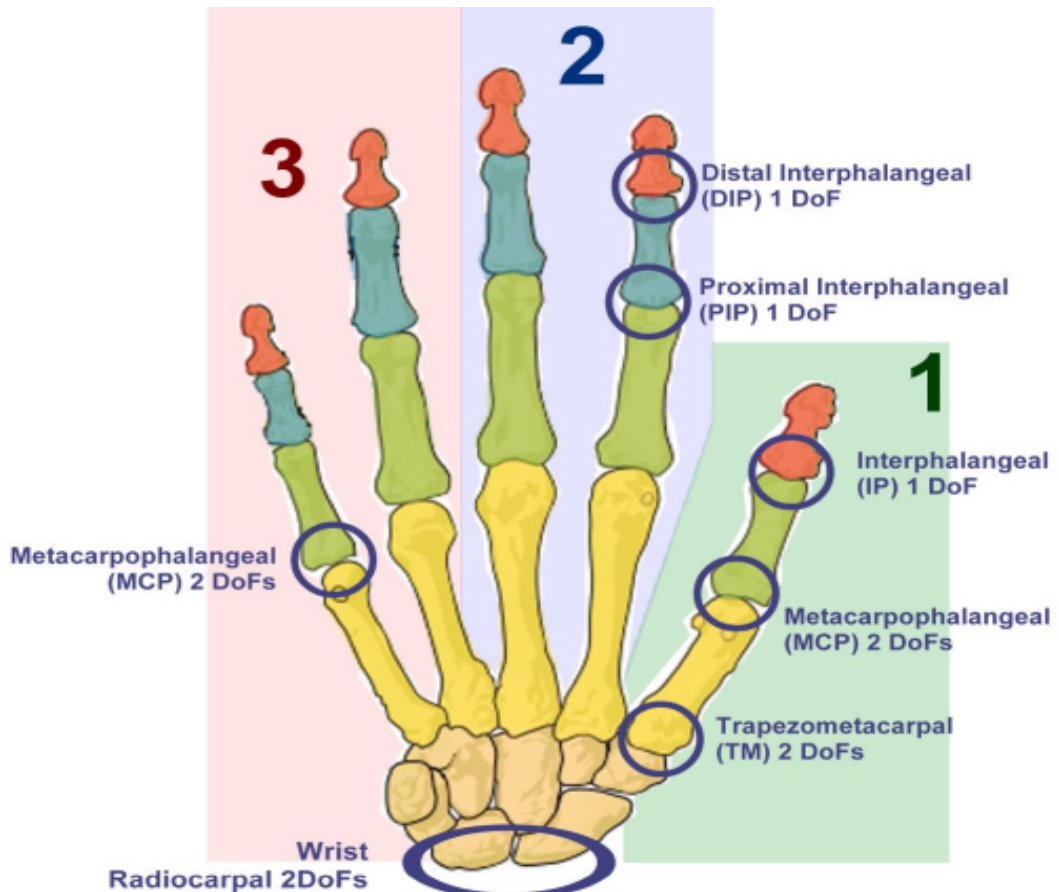


Figure 1.0.1: The joints in human hand and the DOF [9]

## 1.1 The State of the Art Prosthetic Hands nowadays

There are basically two categories of prosthetic hands: passive and active hands [10]. Passive hands are divided into: cosmetic, and functional types [10]. By cosmetic, it means that the prosthetic hand is only used to restore the symmetrical appearance of the amputee. This type will not be discussed in this study. By functional, it means that the hand is designed to facilitate doing different activities [10]. Active prosthetic hands are further divided into body-powered and external-powered [10]. The body-powered prosthetics are controlled via cables by a healthy limb of the human body, however in order to control this type of prosthetics, the patient should exert a high energy. That is why this type is not preferred [10]. Instead of using the energy of the human body itself, the external-powered prosthetics use the energy from external source (battery) [10]. In this case, the patient controls the prosthetic hand via Electromyography (EMG) sensors. The prosthetic hand itself can be normal or multiarticulated hand as in 1.3.1.

The prosthetic hands nowadays are still not comparable with the normal dexterous human hand. Most of the state of the art prosthetic hands nowadays are controlled via EMG sensors.

With the EMG sensors, the patient can control limited DOF with his arm muscles. This case gets worse when the patient has not only lost his hand but his arm as well. In this case, controlling a prosthetic hand can not be done through EMG sensors, but rather it should be done directly through thoughts using Brain Computer Interface (BCI) techniques such as EEG.

Typical prosthetic hands nowadays are still limited to EMG and they can provide simple On/Off control (flexion, extension) [11] as in 1.1.1. By using only two surface EMG channels, this kind of hands can only do two kinds of movement: extension which corresponds to an Open Hand, and flexion which corresponds to Close Hand. To use more EMG sensors, there is a need for more sites to extract EMG signals. There is also another solution to control the prosthetic hand with limited number of EMG sensors by using different activation thresholds as in [12], but this solution is irritating for the patient. Another solution was also found in [13] by using a pair of EMG sensors on an agonist-antagonist muscle pair, this co-contraction function gives the ability to switch from one function to another. Also, using EMG signals with co-contraction method, the prosthetic hand can be controlled with proportional speed/force as in [14]. Although the mentioned methods enhanced the control of the prosthetic hands and found new solutions, they still could not answer the needs of the patients of having functionally unlimited hand [15], [16]. They are still irritating to control as in [15], [16], [17], [18]. Also according to users reports as in [19], [20], [21], [22], [23], and [24], the upper limb prosthesis users perform less than 50% comparing with healthy people.

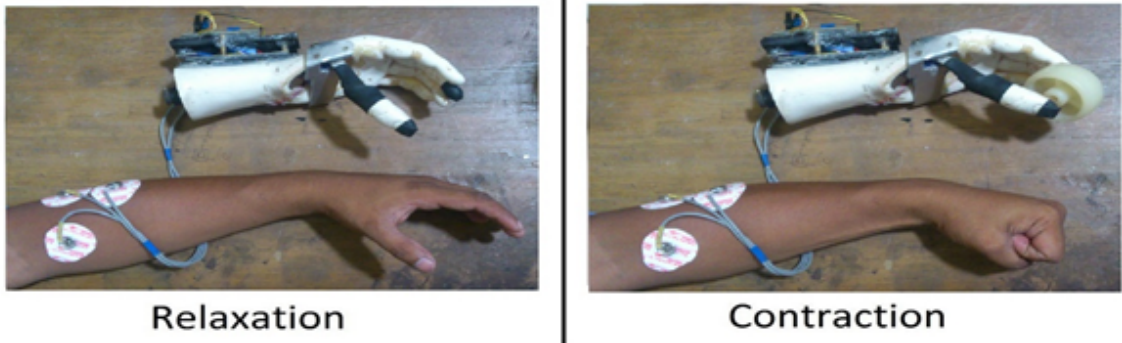


Figure 1.1.1: Controlling simple prosthetic hand with EMG Sensors [25]

## 1.2 Targeted Muscle Reinnervation

Targeted Muscle Reinnervation (TMR) was firstly introduced by Dr. Todd Kuicken and Dr. Gregory Dumanian in 2004 [26]. This method is based on transferring the residual nerves from the amputated limb to reinnervate new muscle targets [27]. In this way, the EMG signals from the healthy target muscles are the motoric inputs which will be used to control the prosthetic hand. TMR is based on the fact that, the brain still sends motoric signals to the damaged nerves even after the amputation as in [28]. Although TMR method seems to be a good solution for the amputees, it has disadvantages. Some of these disadvantages are: the high risk associated with this kind of surgical operations including the permanent paralysis of the targeted muscle, and the physical therapy needed after the operation [29].

## 1.3 The synergy between EMG, EEG, and cable driven hand

There is always a need to make the prosthetic hands more natural for the patients. By natural, it means that there is always a need for more smooth, and continuous movement for the patient. Even the state of the art prosthetic hands nowadays are still irritating for the patients. To make the prosthetic hands more functional, the synergy from the kinematics, the EMG and the EEG can be used. By using hybrid control from EMG and EEG, it is possible to increase the DOF and this, in turn, will increase the smoothness of the control.

Tendon-driven prosthetic hands:

The idea of the underactuated prosthetic hands was firstly discussed in the 19th century [30]. Since the human hand is designed to have many DOF, there is always a need to increase the output signals to control the whole hand by giving limited number of input signals. This can be achieved to control the tendon-driven hand by giving only one input signal [31], [32], [33]. This type of control is also from the mechanical point of view defined as Mechanical Intelligence [34]. Thanks to the Continuum Robotics science, a tendon driven prosthetic hand has been invented as in 1.3.1 to give mechanically smooth grasping for different sizes of objects, and this mechanical flexibility in the tendon driven hand also simplifies the EMG control of the prosthetic hand as the patient does not need to give sequence of discrete muscle activations to close or open the prosthetic hand to the desired shape [35]. This method has shown to be effective in reach to grasp hand movement as in [36]. However, even with EMG and the tendon driven hand control, it is still not possible to control different kinds of grasps, precision and power grasps.

By integrating the EEG control signals in this system, it is possible to use the signals from the EEG, with the signals from the EMG and the tendon driven hand 1.3.1 to control different types of grasps.



Figure 1.3.1: Tendon driven prosthetic hand [37]

In this Thesis, Shared Control is implemented, in which only a high-level goal (the type of the hand movement: gestures, grasps, precision grasps, power grasps, etc) is used. Low-level implementation is supposed to be done by the machine (the prosthetic hand in this study).

## 1.4 Brain Computer Interface System

BCI, also called Neural Control Interface (NCI), is a system that can read specific patterns from brain signals EEG to control external devices. In this study, BCI for prosthetics will be used. When BCI is used for prosthetics, then it is called neuroprosthetics. BCI is used in the neuroprosthetics to help patients who have lost their arms, legs, sight, or even their hearing. The Limbs of the human body are controlled by brain through the spinal cord, nerves, and muscles. When a damage occurs in the limbs, or even when a damage occurs in the nerves or the spinal cord, which connects the brain to the limbs, then to restore the function of the limbs, there is a need for controlling them directly through the brain. This is what the BCI system does. BCI combines different technologies: Biomedical Engineering, Computer Science, Signals Processing, Biomechanics, Neurosurgery, and Electronics.

The most used and relative types of BCI Systems as in 1.4.1 can be compared with their pros and cons as following:

## EEG

- Pros:
  - High temporal resolution
  - Safe, easy, and not expensive
- Cons: Low spatial resolution

## Magnetoencephalography (MEG)

- Pros:
  - High temporal resolution
  - Better spatial resolution than the EEG
- Cons: Bulky, and expensive

## Electrocorticography (ECG)

- Pros:
  - High temporal resolution
  - Best spatial resolution
- Cons: Dangerous, needs surgical operation, and expensive

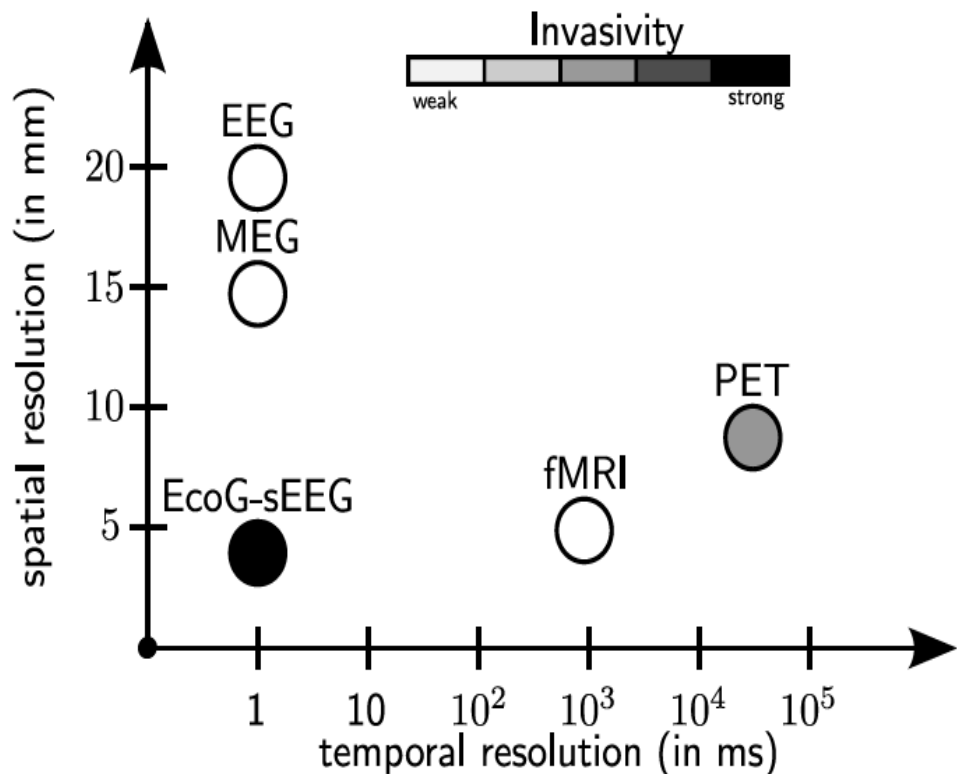


Figure 1.4.1: Comparison between different types of BCI's [38].

## 1.5 Comparison between EEG, and ECG Signals

From the comparison between the BCI methods, the EEG is the most suitable and practical BCI type to use. It has high temporal but low spatial resolution. The MEG type has also high temporal and better spatial resolution. However in order to use the MEG, there is a need for a large and bulky device. This makes it impractical for the neuroprosthetics. Also the ECG in comparison with the EEG, has both high temporal and spatial resolutions. ECG method has been successfully used in [39] to control individual prosthetic fingers. ECG is invasive (this is why it has high spatial resolution [40]). ECG has also the advantage of being able to record higher-frequency (10-200Hz) than EEG as in [41], and [42]. However, since the ECG is invasive, it has the disadvantage of being only available in clinical and medical operations. Another disadvantage of the invasive methods such as ECG is the encapsulation of the electrodes due to the connection between the electrodes and the tissues [43]. That is why in this thesis, EEG will be studied, and analyzed to see if it is possible to differentiate between different types of hand movements.

## 1.6 Overview of the Project

The goal of this thesis is to find out if it is possible by using EEG in combination with machine learning methods to have an additional decision tool to differentiate between different types of hand movement (grasp vs. gesture, power vs. precision grasp, and multi-grasps), in order to add this info to prosthetic hands to further underactuate them. The underactuated hand should know what the user will do next with the hand in order to have the hand ready for the next task and therefore give the user a feeling of an intuitive control.

This thesis is based on measurements from the Orthogo Laboratory in MHH (Medizinische Hochschule Hannover) in the winter of 2018. In this thesis, a study will be done to define whether it is possible to differentiate between different hand movements of healthy subjects through thoughts, more specifically through EEG signals.

The main goal in this thesis is to analyze collected EEG Signals from 11 healthy subjects and classify them to get a prediction of different types of hand movements as in 1.6.1.

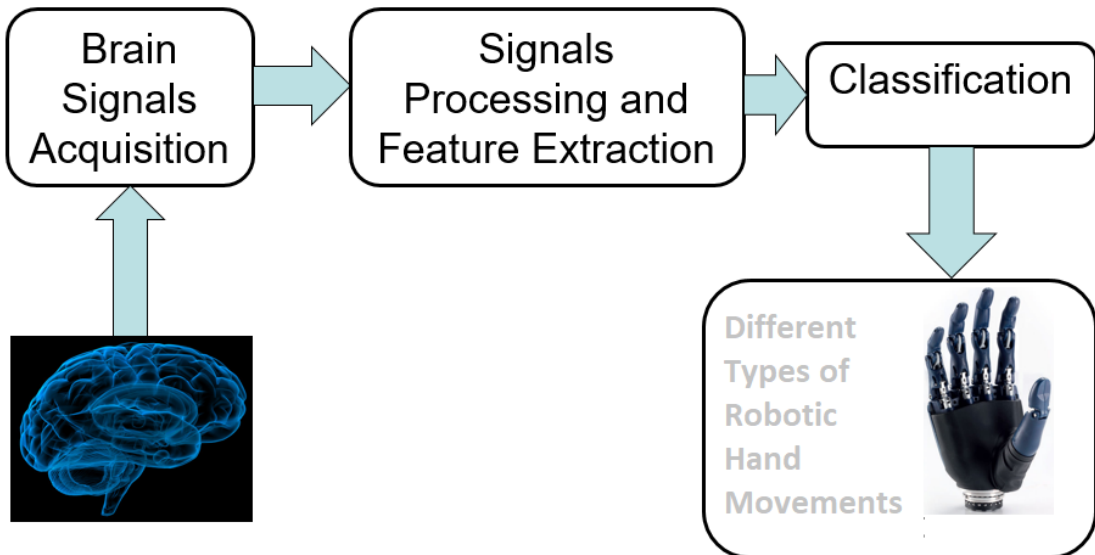


Figure 1.6.1: Overview about the Project

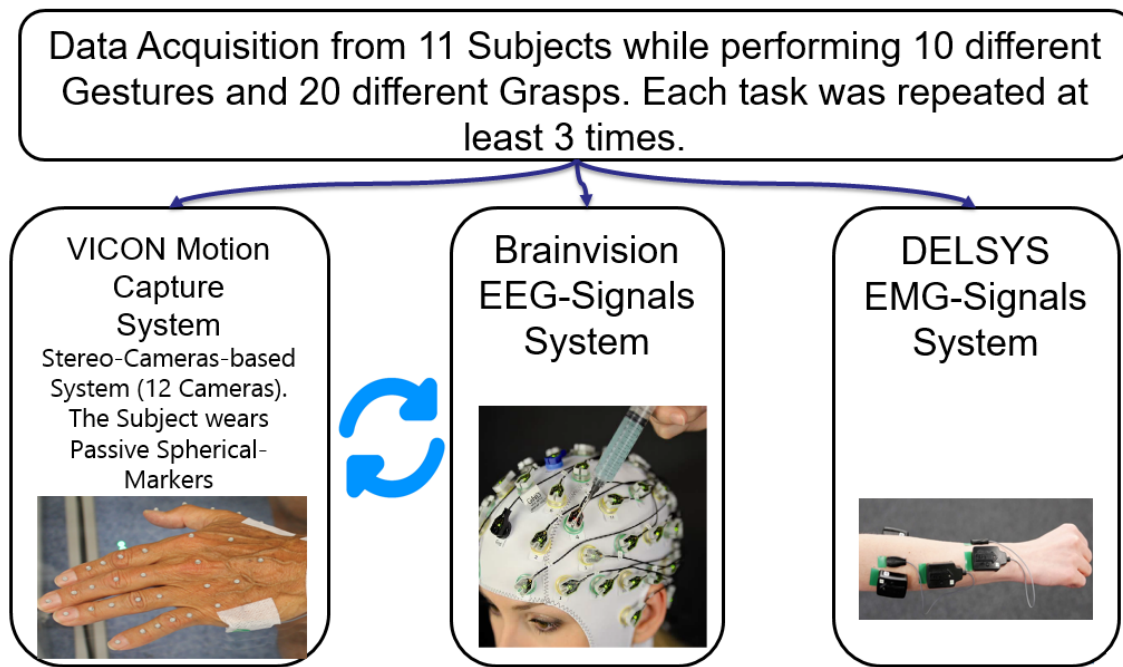


Figure 1.6.2: Overview about Orthogo project

In this Project, EEG, EMG, and Kinematics data has been measured as in 1.6.2 from 11 healthy subjects. This study will only focus on analyzing, extracting features, and classifying the EEG data as in 1.6.1.

## 1.7 The main Objectives in this thesis

This study will focus on the possibility of using non-invasive EEG Signals to differentiate between gestures and grasps types of hand movements. The EEG signals were successfully used in [44] to detect the intention to grasp during reaching movements from EEG data. This study will

also handle the possibility of using non-invasive EEG signals to differentiate between the most simple and important types of grasps in the prosthetics: precision and power grasps. This type of classification was successfully done in [45] to differentiate between power and precision pinch grasps. In this study, also the non-invasive EEG signals will be analyzed to see if it is possible to differentiate between different 20 grasps types. There is a similar study in [46] where the EEG signals could be used to differentiate between 9 different types of power-type grasps, and 7 different types of precision-type grasps. It is important to test if a trained model on subject or group of subjects. That is why, in this study the possibility of doing cross-subject binary classification will be studied for both gestures vs. grasps and precision vs. power grasps using transfer learning from subject to another, by training on 9 subjects and testing on the tenth subject (the reason of choosing only 10 subjects is explained in 2.8). Using the transfer learning will tell if a trained model on subjects can be applied on a new subject. Although the EEG signals differ from subject to subject as in [47], this method has been used with deep learning methods as in [48] and in [49] and achieved high classification results. In this thesis, 31 electrodes were used to measure the EEG signals. According to this, the possibility of using only 16 instead of 31 channels will be tested in all the classification cases. This approach will be tested in all the classification cases in this study (binary classification of gestures vs. grasps, binary classification of precision vs. power grasps, and multi-classification of 20 different types of grasps). This approach has been used in previous studies, as in [50], where only 8 out of 64 electrodes were used to classify between right and left hand movements, and in [51], where only 4 out of 62 electrodes were used to classify between three different types of arm movements (close, open arm, and close hand), and also in [52], where 3 different electrodes-layouts (5, 15, and 25 out of 61 electrodes) were used, and did the classification using 61, 25, 15, and 5 electrodes.

As a summary, this thesis is based on the following hypothesis:

- Main Hypothesis: Machine learning classified EEG signals should be sufficiently usable to differentiate between different movements of the hand (gestures vs. grasps, and precision vs. power grasps).
  - The EEG-based machine learning and deep learning classifiers can be transferred from a study cohort to another single subject with a sufficient accuracy.
  - All types of classification should be also solved with a reduced set of EEG electrodes.

## 1.8 The Kinematics-Data Acquisition System

There are commonly several methods to track the motion of the subject to extract the time intervals (events) to be then used in the EEG data Processing.

- Accelerometers based technologies.
- Flex Sensor Data Glove.
- Vision based technologies: This is the method that has been used in this study (VICON). The subject wears the passive markers as in 1.8.1 and an infrared system (12 cameras) as in 1.8.2 tracks the subject's hand movement.

Motion is tracked by the system by reflecting light off reflective markers attached to the subject's hand. Every VICON camera is surrounded by a ring of Light Emitting Diode (LED)'s. These LED's send infrared light. This light then is reflected by the markers, and is received by the VICON camera. The markers are made of a retroreflective material, which reflects back more light than other materials. In This way, the vision system identifies markers from all other reflecting objects in the area. Each of the VICON cameras sends a 2D image to the MX Ultranet HD. Based on the geometry of the room, and the positions of the cameras within it, the system uses trigonometry to approximate the position of each marker in 3D space. In order for a marker to be correctly localised, it needs to be seen by 2 or more cameras. The computer calculates each marker's position as a function of 12 2d camera picture per frame. The software used by VICON for visualising this data, performing motion capture, is called Vicon Nexus.



Figure 1.8.1: The subject wears spherical passive markers according to SoftPro project



Figure 1.8.2: 12 Stereo VICON cameras according to the SoftPro project

## 1.9 The EEG-Data Acquisition System

In this study, hardware (Active Channel Amplifier (actiCHamp), Active Electrode Cap (actiCAP)), and software (Brain Vision analyzer, and Brain Vision Recorder ver2.0) from Brainvision were used to measure the EEG signals from 31 electrodes, while the subject is doing different gestures and grasps tasks.

EEG signals have commonly small amplitude of less than  $100\mu\text{V}$  when measured from non-invasive electrodes and about 10 to 20mV when measured from invasive electrodes. This attenuation is due to the brain fluids, the skull, and the skin. The EEG signals of each electrode are then amplified, digitized (sampling frequency: 500Hz), and sent to the computer for further processing.

**Electrodes Impedance:** For every EEG electrode, a status LED with 3 different colors indicates the status of the connectivity between the electrode and the skull of the subject's head. The following color codes show the state of the impedance between the electrode and the skull of the head:

1. Green: Impedance  $<25\text{K}\Omega$ . This is the optimal impedance that should be shown for all electrodes in actiCAP.
2. Yellow: Impedance between 25 to  $60\text{K}\Omega$
3. Red: Impedance  $> 60\text{K}\Omega$

### 1.9.1 Neuron Activity

The average human brain contains about 100 billion neurons [53]. Neurons or nerve cells are kind of cells that can be electrically triggered. They communicate through synapses [54]. There are three types of neurons based on their function [54]:

1. Sensory neurons that respond to stimulation (sound, touch,...).
2. Motor neurons that receive signal from the brain and the spinal cord to control the muscles.
3. Interneurons that connect neurons to other neurons in the brain. A group of connected neurons is called neural circuit.

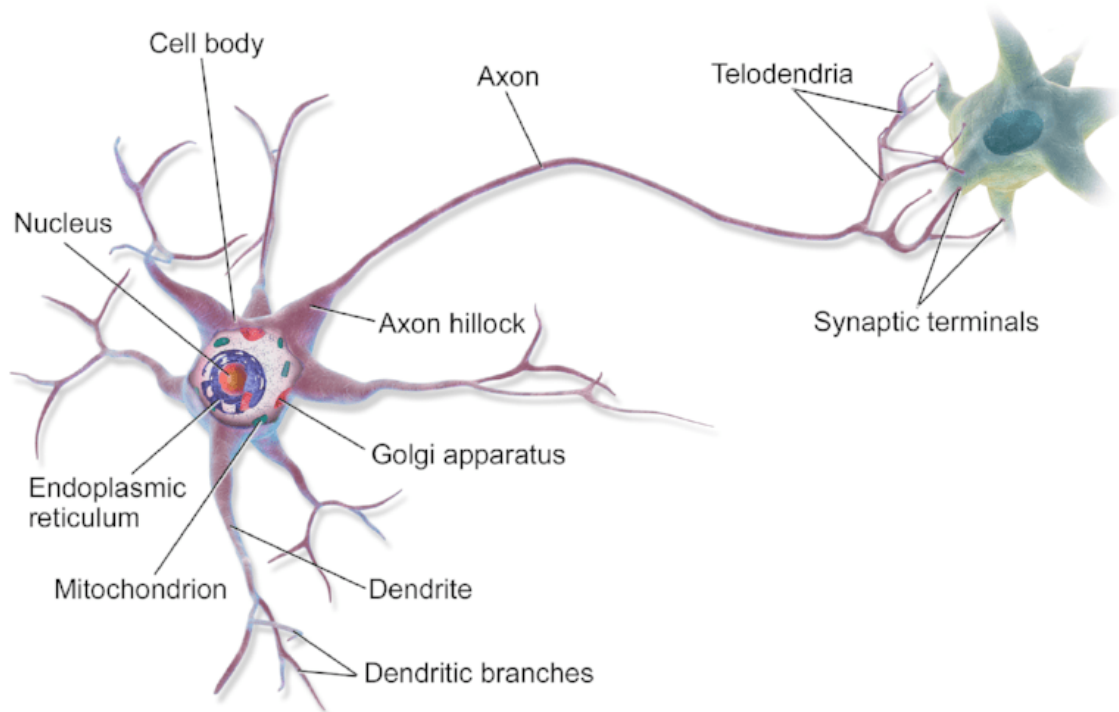


Figure 1.9.1: A neuron making a synaptic connection with another neuron [55]

### 1.9.2 The Brain Lobes

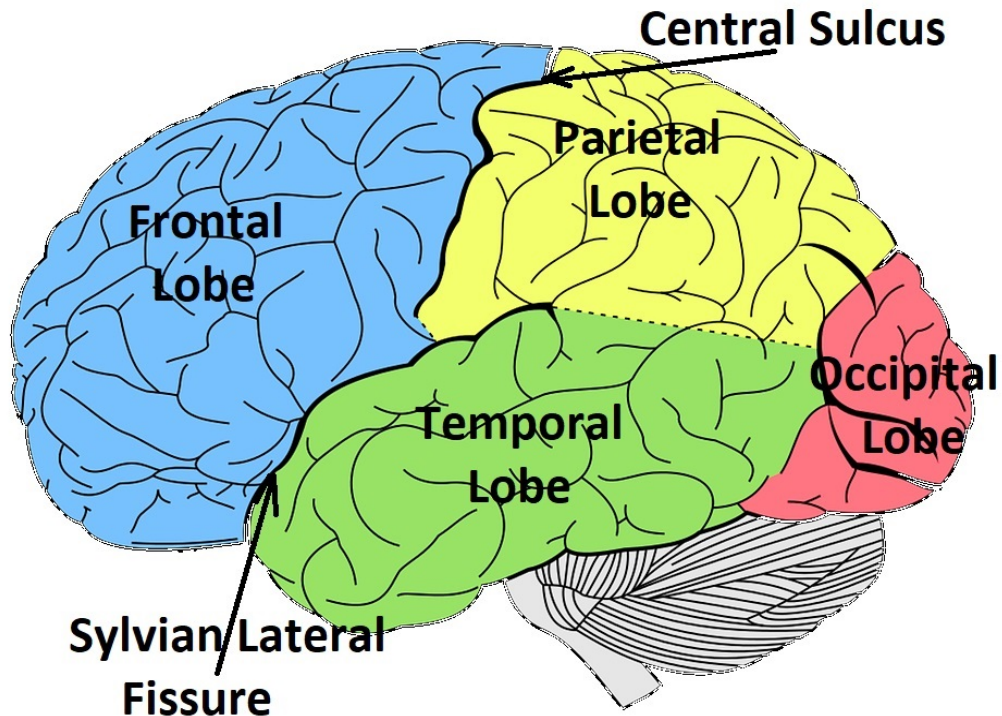


Figure 1.9.2: 4 Main Human Brain-Lobes

Each hemisphere is divided into the following 4 main brain lobes:

Frontal Lobe: It is the largest brain lobe. It is found at the front side of each hemisphere. All the EEG electrodes that start with the F letter: Fp1, Fp2, F3, F4, F7, F8, FC1, FC2, FC5, FC6, FT9, FT10 are located over this lobe. It is separated from the parietal lobe by the central sulcus tissue 1.9.2. It is also separated from the temporal lobe by lateral Sylvian fissure tissue 1.9.2. It contains the Primary Motor Cortex 1.9.3. The function of the frontal lobe is mostly action function, such as the skeletal movement, ocular movement, speech control [56]. It has also other functions, such as language, cognition, attention, and memory [56]. Patients who experienced problems in their frontal cortex were unable to express their emotions or were having difficulties in speech, coordination, and planning [57].

Parietal Lobe: The parietal lobe integrates sensory information like the spatial awareness, navigation, touch sense [58], temperature sense, and pain sense [59]. The parietal lobe is separated from the frontal lobe by the central sulcus. It is also separated from the temporal lobe by the lateral sulcus. The Posterior Parietal Cortex is a part of the motor system, it is also important for the visuomotoric [60], and it is important for special motor patterns like grasping [61]. A damage to this area in the left hemisphere may cause problems in the mathematics [62]. It has the electrodes that start with the P letter: P3, P4, P7, P8, Pz.

Occipital Lobe: The occipital lobe is the visual processing processor of the human brain [63]. It contains the the Primary Visual Cortex which is referred to as Brodmann area 17. The occipital lobe is the smallest between the major four brain lobes: Frontal Lobe, Parietal Lobe, and Temporal Lobe. If the occipital lobe in one hemisphere is damaged, this leads to a vision

loss on one side, visual hallucinations, color blindness, motion blindness, or even blindness [64]. It has the electrodes that start with the O letter: O1, O2, Oz.

Temporal Lobe: This region is responsible for the memory function [65], such as: visual memories [66]. It also contains auditory processing function, language recognition. Patients, who experience damage in this lobe, have problems in recalling memory, and failing to recognize faces, and familiar objects [67]. It has the electrodes that start with the T letter: T7, T8, TP10, TP9.

### 1.9.3 The Brodmann Areas

The human brain can be divided into Brodmann areas 1.9.3. Brodmann areas were defined by the German neurologist Korbinian Brodmann. The human brain can be divided into 52 Brodmann areas [68]. Following areas are the most related to this study:

1. Areas: 1,2,3 Primary Somatosensory Cortex: It is responsible for detecting touch, temperature, and pain. It is important for the contribution of the sensors signals to the motoric functions for skilled movements. Without the correct processing and translation of sensory inputs, the movements will be abnormal and inaccurate. [69].
2. Area: 4 Primary Motor Cortex: It is the part that is responsible for the movement of all human parts. It is responsible for generating neural signals to the spinal cord to execute a movement.
3. Area: 5 Somatosensory Association Cortex
4. Area: 6 Premotor Cortex (Secondary Motor Cortex): It is responsible for the preparation of the movement. [70]
5. Area: 7 Somatosensory Association Cortex
6. Area: 8 Frontal Eye Fields
7. Area: 17 Primary Visual Cortex
8. Area: 18 Secondary Visual Cortex
9. Area: 19 Associative Visual Cortex

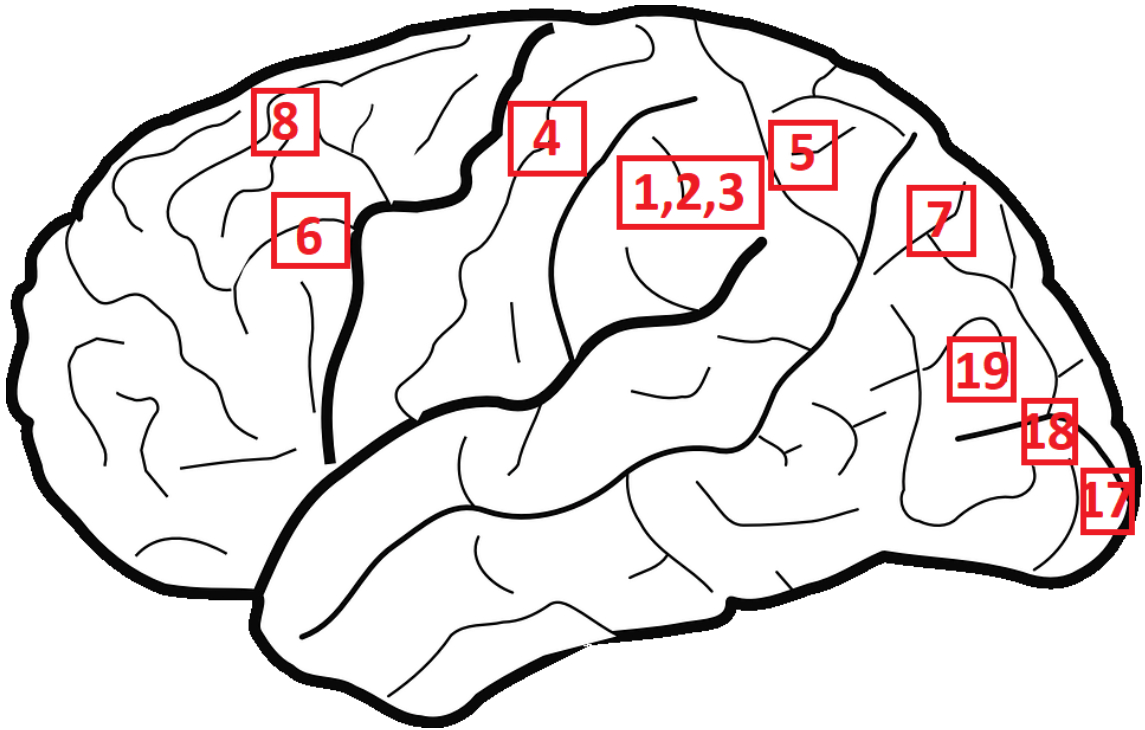


Figure 1.9.3: Brodmann Areas

#### 1.9.4 The EEG Montage and the Measurement Modes

The EEG electrode potential is measured by taking the difference between two electrodes. The modes of calculating the electrical potential for electrodes are called Montage. There are several kinds of montages:

- Sequential Montage: In this mode, the electrical potential for each electrode is calculated by taking the difference between two adjacent electrodes.
- Referential Montage: In this mode, the electrical potential in a channel is calculated by taking the difference between the voltage of the channel itself and the reference electrode. This is the mode that the Brainvision system uses in this study.
- Average Reference Montage: In this mode, all the signals are summed and averaged. Then, this averaged result is used as a common reference for all channels.
- Laplacian Montage: In this case, the electrical potential of each channel is calculated by taking the difference between voltage of the channel's electrode and the average of the adjacent electrodes.

#### 1.9.5 The Frequency Bands of the EEG

There are 5 Frequency Bands in EEG signals as in [71]. These frequency bands can be used to describe different tasks like: movements, thinking, dreaming, and sleeping.

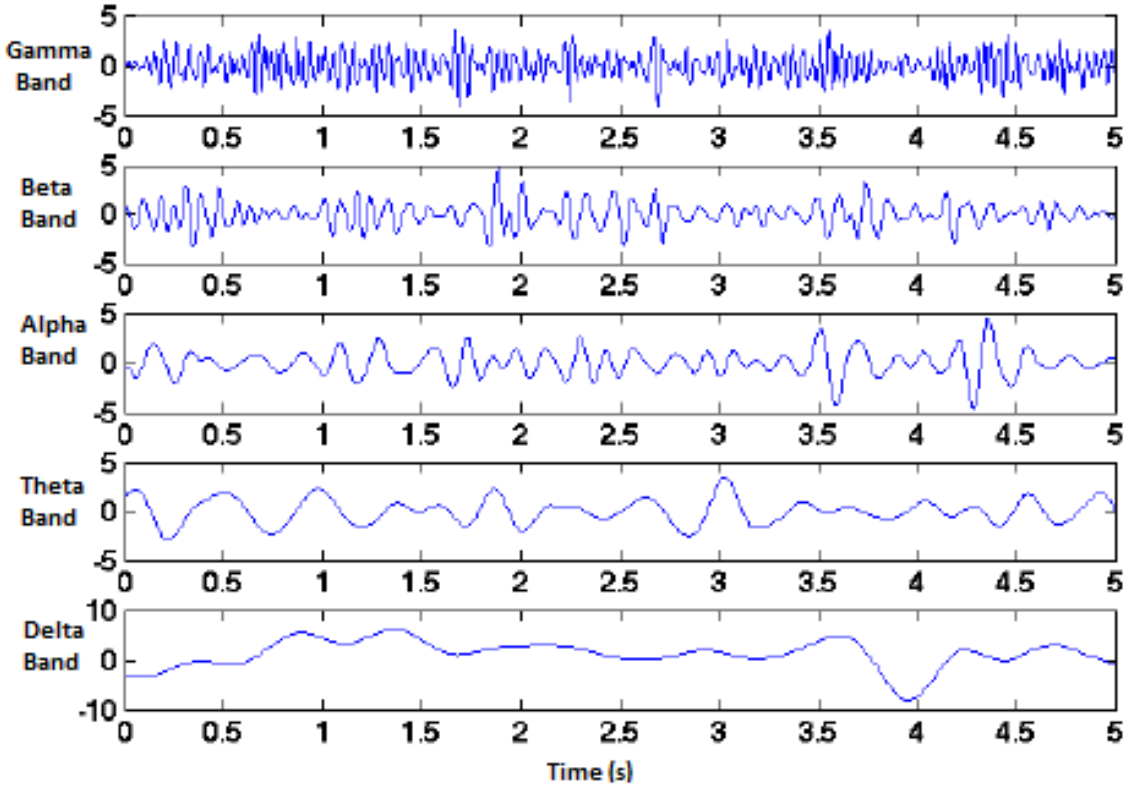


Figure 1.9.4: EEG bands [71]

**Delta waves (<4Hz):** These waves have the lowest frequency in EEG signals. Normally they are located frontally in adults and posteriorly in children [72]. They are normally observed in babies [73] and during sleep of adults [74]. They were also observed during the execution of continuous attention tasks as in [75]. Delta waves have the highest amplitude between EEG waves. **Sex Differences:** It has been found, that Delta waves are more present in women than in men [76].

**Theta waves (4-7Hz):** These EEG waves have the second lowest frequency in EEG signals. They have been observed in young children [74]. In adults, they were observed during drowsiness and sleeping [74], but not during deep sleep. They were observed in adults while doing short-term memory tasks [77].

**Alpha waves (8-12Hz):** Alpha waves mostly originate from the occipital lobe [74] during wakefullness whilst eyes closure [78]. And they get reduced by eyes opening [78]. It has been recently found, that Alpha waves play a role in the neural network coordination and communication [79].

**Beta waves (16-31Hz):** Beta waves have been observed during voluntary hand movements [80]. Beta waves are associated with motor planning and control of grasping tasks [81]. It has been found, that Beta waves with low amplitude are associated with anxiety and concentration [82]. It has been also found, that Beta waves increase when a resistance to the movement occur [83]. Beta waves also has been found to be active over the motor cortex during muscle contractions, and will be reduced before and during the movement [84]. Beta Waves also increase with the sensory feedback [85].

**Gamma waves (32-100Hz):** These are the waves that have the highest frequency between EEG bands. It has been found, that it is active over the somatosensory region, and during combination of more than one sense, like hearing and seeing [86]. Gamma waves are also believed

to be present while doing tasks which require network of neurons to be activated together [87]. Gamma activity is also increased in the human sensorimotor cortex while doing visuomotor tasks [88]. According to [89], [90], the amplitude of  $\gamma$  waves increases while executing a movement.

## 2 Methods

In this section, gestures, grasps, precision grasps, and power grasps tasks will be explained. The main work in this study is to classify EEG data. In order to classify the EEG data, the following steps should be done.

- EEG data events extraction.
- EEG data filtering
- EEG data artifacts removal
- EEG data epoching

After having the epochs, the classification methods can be used. To do the classification, the following methods were used:

- Classification using Common Spatial Patterns (CSP) and Machine Learning (ML).
- Classification with TS.
- Classification using deep learning methods.

To analyze the CSP's, the CSP of S2 in the case of gestures vs. grasps and the case of precision vs. power grasps will be plotted.

To analyze the covariance matrices in the Riemannian space, the covariance matrices of S2 will be also plotted.

To enhance the cross-subjects classification results, boosting methods will be used.

To test the classification using reduced number of electrodes, the classification using 31 and 16 electrodes will be used.

### 2.1 The used Tasks in this Study

In this study, the EEG signals were measured from 11 right-handed Subjects(S1, S2, 3rd Subject (S3), 4th Subject (S4), 5th Subject (S5), 6th Subject (S6), 7th Subject (S7), 8th Subject (S8), 9th Subject (S9), S10, 11th Subject (S11)). Mean age: 46 years with Standard Deviation (SD): 16 years and female:male: 3:8. In this study, EEG, and kinematics data has been measured. The kinematics data was measured using the VICON motion capture system. VICON motion systems company, with headquarters in Oxford, UK, and US headquarters, has been since 1984 providing tools for 3D human capture systems for research, medicine, sport, and engineering. The EEG data was measured using Brainvision system. Brainvision company with headquarter in Gilching (Munich) was founded in 1997 and has been since then providing the universities and the markets with hardware and software solutions in the neurophysiological researches. The

kinematics, and EEG data was synchronized. The kinematics data acquisition system is useful for extracting events or steps of the hand movements to be used for the epoching of the EEG data. The tasks are 10 Gestures, and 20 Grasps. The EEG Data is measured from 11 healthy subjects. Each task was repeated 3 times (trials) for S1, S4, S5, S7, S8, S9, S10, and S11. And it was repeated 5 times (trials) for the subjects: S2, S3, and S6.

### 2.1.1 Gestures 1-10

In this study, each subject performs 10 gestures. These 10 gestures types are taken according to the SoftPro project. SoftPro is a European project that study and design soft synergy-based robotic hands. For S1, S4, S5, S7, S8, S9, S10, and S11, each gesture was repeated 3 times (3 trials). For S2, S3, and S6, each gesture was repeated 5 times (5 trials). These gestures are as following:

- 1- OK. The subject moves his/her hand to the position in the picture 1 in 2.1.2, holds his/her hand for a while, and then releases his/her hand.
- 2- Thumb Down. The subject moves his/her hand with the thumb down as in the picture 2 in 2.1.2, holds his/her hand for a while, and then releases his/her hand.
- 3- Exultation. The subject moves his/her hand up as in the picture 3 in 2.1.2, holds his/her hand for a while, and then releases his/her hand.
- 4- Hitchhiking. The subject moves his/her hand to the side position as in the picture 4 in 2.1.2, holds his/her hand for a while, and then releases his/her hand.
- 5- Block out Sun from Own Face. The subject moves his/her hand to the front of his/her head as in the picture 5 in 2.1.2, holds his/her hand for a while, and then releases his/her hand.
- 6- Greet. The subject moves his/her hand to the position in the picture 6 in 2.1.2, waves his/her hand for a while, and then releases his/her hand.
- 7- Military Salute. The subject moves his/her hand to the position in the picture 7 in 2.1.2, holds his/her hand for a while, and then releases his/her hand.
- 8- Stop. The subject moves his/her hand to the position in the picture 8 in 2.1.2, holds his/her hand for a while, and then releases his/her hand.
- 9- Pointing. The subject moves his/her hand to the position as in the picture 9 in 2.1.2, holds his/her hand for a while, and then releases his/her hand.
- 10- Silence. The subject moves his/her hand to his/her nose as in the picture 10 in 2.1.2, holds his/her hand for a while, and then releases his/her hand.

## 2.1.2 Grasps 11-30

A grasp taxonomy as in 2.1.1 can be compared with the grasps types in this study.

		Power					Intermediate			Precision				
Opp:	Palm	Pad				Side			Pad				Side	
VF:	3-6	2-5	2	2-3	2-4	2-5	2	3	3-4	2	2-3	2-4	2-5	3
Thumb Abducted		1. Large Diameter Diameter	2. Small Diameter	31. Ring Finger	28. Sphere 3 Finger	18. Extension Type	19. Distal Type	23. Adduction Grip	21. Tripod Variation	9. Palmar Pinch	8. Prismatic 2 Finger	7. Prismatic 3 Finger	6. Prismatic 4 Finger	20. Writing Tripod
		3. Medium Wrap	10. Power Disk		26. Sphere 4 Finger					24. Tip Pinch	14. Tripod	27. Quadpod	12. Precision Disk	
		11. Power Sphere								33. Inferior Pincer		13. Precision Spheres		22. Parallel Extension
Adducted Thumb		17. Index Finger Extension	4. Adducted Thumb	5. Light Tool				16. Lateral	25. Lateral Tripod					
		15. Fixed Hook		30. Palmar				29. Stick						
								32. Ventral						
										Non-Prehensile				
										34. Lift	35. Push			

Figure 2.1.1: Grasps taxonomy [91]

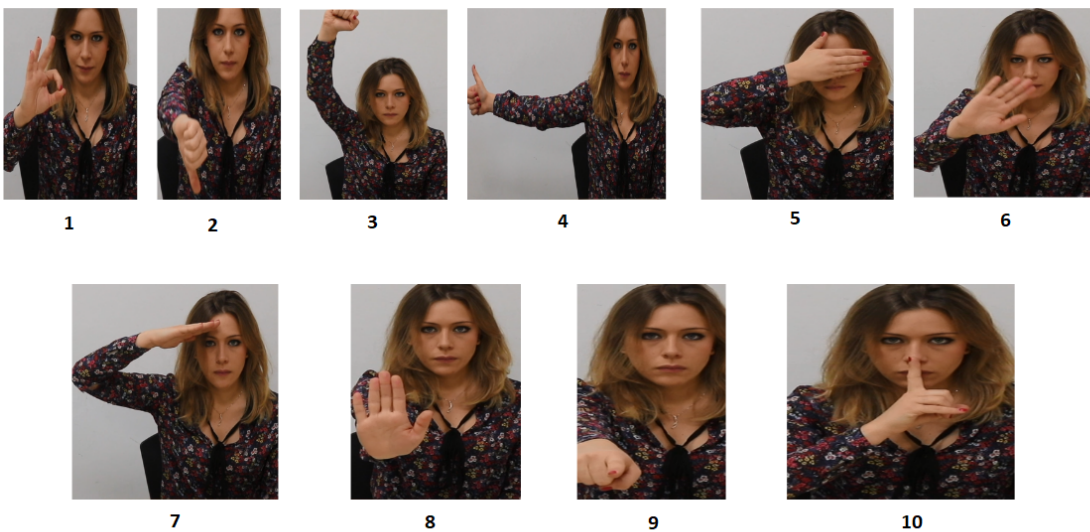


Figure 2.1.2: Gestures types according to SoftPro project

In this study, each subject does 20 grasps. The 20 grasps types are taken according to the

SoftPro project. For S1, S4, S5, S7, S8, S9, S10, and S11 subjects, each grasp was repeated 3 times (3 trials). For the S2, S3, and S6, each grasp was repeated 5 times (5 trials). While checking the EEG data, it has been found, that the S4 is missing time-intervals information in the 19th grasp. Hence, S4 has only 19 grasps. Also S6 is missing time-intervals information in the 5th trial of 19th grasp.



Figure 2.1.3: Grasps Types according to SoftPro Project

These grasps are as following:

- 11- Suitcase. The subject moves his/her hand to hold the suitcase as in the picture 11 in 2.1.3, holds the suitcase to put it somewhere, and then releases his/her hand.
- 12- Grasp Glass to Drink (Glass). The subject moves his/her hand to hold the glass as in the picture 12 in 2.1.3, moves the glass to his/her mouth, and then puts and releases his/her hand.
- 13- Grasp Phone (Phone). The subject moves his/her hand to hold the phone as in the picture 13 in 2.1.3, holds the phone to put it on his/her ear, and then put it back somewhere and releases his/her hand.
- 14- Grasp Book (Book). The subject moves his/her hand to hold the book as in the picture 14 in 2.1.3, holds the book to put it on the table, starts paging, and then releases his/her hand.
- 15- SmallCup. The subject moves his/her hand to hold the small cup as in the picture 15 in 2.1.3, moves the small cup to his/her mouth, and then puts and releases his/her hand.

- 16- Grasp Apple (Apple). The subject moves his/her hand to hold the cup as in the picture 16 in 2.1.3, moves the apple to his/her mouth, and then puts and releases his/her hand.
- 17- Grasp Cap (Cap). The subject moves his hand to hold the cap as in the picture 17 in 2.1.3, puts the cap on his/her head, and then releases his/her hand.
- 18- Grasp Large Cup (LargeCup). The subject moves his/her hand to hold the large cup as in the picture 18 in 2.1.3, moves the cup to his/her mouth, and then puts it back somewhere and release his/her hand.
- 19- Receive Tray (ReceiveTray). The subject moves his/her hand to receive a tray from a person as in the picture 19 in 2.1.3, puts it on the table, and then releases his/her hand.
- 20- ExtractKey. The subject moves his/her hand to hold the the key as in the picture 20 in 2.1.3, extracts the key, and then puts it somewhere and releases his/her hand.
- 21- Grasp Bottle to Pour Water (Bottle). The subject moves his/her hand to holds the bottle as in the picture 21 in 2.1.3, pours water from bottle in a glass, and then puts the bottle back on the table and releases his/her hand.
- 22- Grasp Tennis Bat (Bat). The subject moves his/her hand to hold the bat as in the picture 22 in 2.1.3, moves the bat as he/she smashes a tennis in the air, and then puts the bat back on the table and releases his/her hand.
- 23- Grasp Toothbrush (Toothbrush). The subject moves his/her hand to hold the brush as in the picture 23 in 2.1.3, moves the brush to his/her mouth, moves the brush as if he/she brushes his/her teeth, puts the brush back on the table and then releases his/her hand.
- 24- Grasp Laptop (Laptop). The subject moves his/her hand to hold the laptop cover as in the picture 24 in 2.1.3, opens the laptop cover, and then releases his/her hand.
- 25- Grasp Pen to draw (PenDraw). The subject moves his/her hand to hold the pen as in the picture 25 in 2.1.3, holds the pen to draw a vertical line, and then puts it back on the table and releases his/her hand.
- 26- Grasp Pen to move (PenMove) The subject moves his/her hand to hold the pen as in the picture 26 in 2.1.3, holds the pen to put it somewhere, and then releases his/her hand.
- 27- Grasp Tea-Bag (TeaBag). The subject moves his/her hand to hold the Tea-Bag as in the picture 27 in 2.1.3, holds the Tea-Bag to put it somewhere, and then release his/her hand.
- 28- Grasp Doorknob (DoorKnb). The subject moves his/her hand to hold the doorknob as in the picture 28 in 2.1.3, rotates the doorknob, and then releases his/her hand.
- 29- Grasp Tennis Ball (Ball). The subject moves his/her hand to hold the tennis ball as in the picture 29 in 2.1.3, holds the tennis ball to put it somewhere, and then releases his/her hand.

- 30- Grasp Bottle Cap (BottleCap). The subject moves his/her hand to hold the bottle cap, as in the picture 30 in 2.1.3, unscrews the bottle cap, and then puts the bottle cap on the table and release his/her hand.

### 2.1.3 Precision vs. Power Grasps

The most simple and important two types of grasps in the prosthetics are precision and power grasps. The grasps can be classified into two groups: precision and power grasps as in 2.1.4.

Precision grasps are chosen in this study as following (numbers are same as in 2.1.3):

- 11. Suitcase
- 15. SmallCup
- 20. ExtractKey
- 23. Toothbrush
- 25. PenMove
- 26. PenDraw

Power grasps are as following (numbers are same as in 2.1.3):

- 28. DoorKnb
- 12. Glass
- 21. Bottle
- 18. LargeCup
- 29. Ball
- 16. Apple

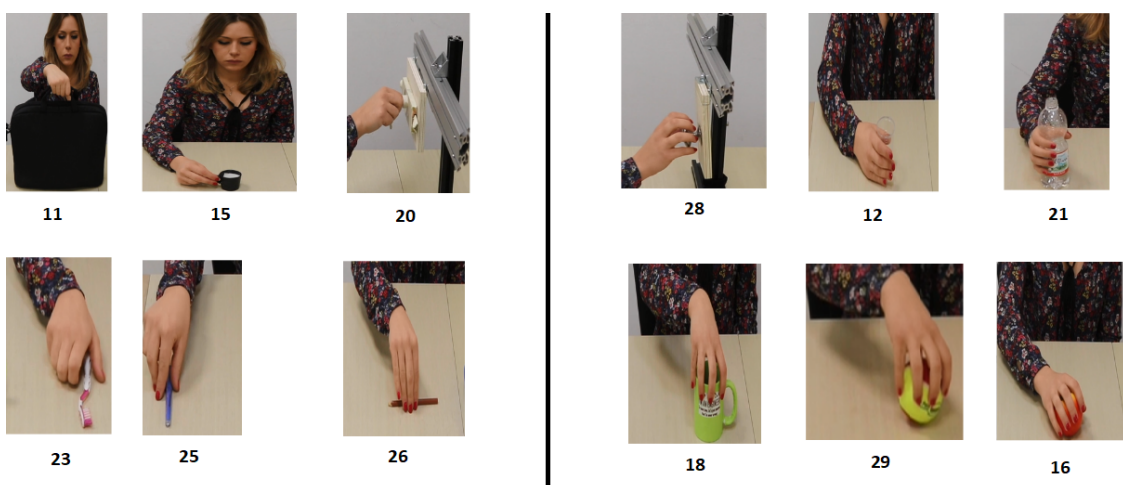


Figure 2.1.4: Left: precision grasps - Right: power grasps. According to SoftPro Project

#### 2.1.4 Dividing EEG Data into Classes

In this study, at first the filtering and the epoching will be done on the whole set of EEG data for every subject. Then in the classification step to get a better overview about the classification accuracy and the balance between the classes, the EEG data has been made equal in both classes: (30 gestures vs. 30 grasps) in the case of 3 trials for each task, and (50 gestures vs. 50 grasps) in the case of 5 trials for each task. Also in the case of cross-subjects classification, all the subjects have been made to have equal number of gestures and grasps in the case of gestures vs. grasps classification, and equal number of precision, and power grasps in the case of precision vs. power grasps classification.

## 2.2 Events Extraction

To use the events in the epoching of the EEG data, the recorded time intervals from the kinematics data acquisition system (VICON) have been extracted.

The sampling frequency of the kinematics data is 200Hz. The sampling frequency of the EEG data is 500Hz. The difference in the sampling frequency between the kinematics and the EEG data should be taken in the consideration in the following equation:

$$Events_{EEG}[TimePoints] = Events_{Kinematics}[TimePoints] \cdot 500Hz/200Hz. \quad (2.2.1)$$

The frequency of the kinematics is 200Hz, and the frequency of the EEG data is 500Hz.

## 2.3 EEG Data Filtering

There are different kinds of temporal, and spatial filters that can be applied on the EEG data. Below are some of the temporal filters that can be applied 2.3.1

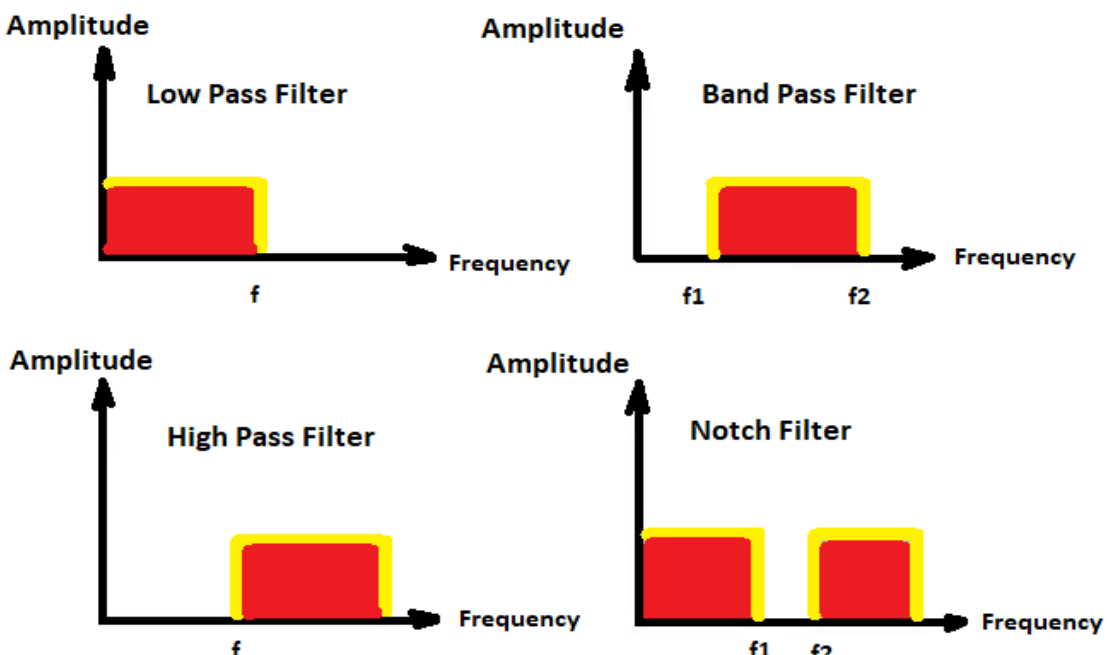


Figure 2.3.1: Temporal filters

1. Low pass filtering: In this kind of filtering, signals that contain less than a specific frequency  $f$  can be cut out. This is normally used to get rid of low frequency signals.
2. Band pass filtering: In this kind of filtering, all the frequencies will be cut out, and only a specified range between  $f_1$  and  $f_2$  will be kept. This is useful if the frequency-band of interest is known.
3. High pass filtering: In this kind of filtering, signals that have more than a specific frequency  $f$  can be cut out.
4. Notch filtering: In this kind of filtering, signals in a specific range between  $f_1$  and  $f_2$  can be cut out. This is useful to cut out electrical noise which is caused by any electrical source in or near the recording room.

For the EEG data in this study, a high pass filtering (0.5Hz), low pass filtering (100Hz), and notch filtering of 50Hz (The electrical frequency in Germany is 50Hz) have been applied. It is important to mention, that filtering should be done before the epoching step to avoid edge artifacts [92]. In this study, no band pass filtering is needed. If the classification should be done between a hand movement and a rest (no movement), then a band pass filtering for Beta (16-31)Hz and Alpha (8-12)Hz frequency range can be applied [93], [94]. Also in this study, the classification will be done using different kinds of hand movements, which means that all kinds of frequency bands are needed as explained in this study in 1.9.5. To prove, that there is no need to band-pass filter the EEG data in this study, a frequency-window filtering has been applied for the gestures vs. grasps classification using TS, the precision vs. power grasps classification using TS, and the multi-classification using TS. The classification is to be done using frequency-window approach from 0.5 to 100Hz. The number of bins(frequency-windows) has been chosen to be 9, and hence every frequency-window size is:  $(100\text{Hz} - 0.5\text{Hz})/9 = 11.056\text{Hz}$ . Then the accuracy has been calculated for every subject for every frequency-window. At the end, the average accuracy over all 11 subjects has been calculated for different frequency-bins (frequency-windows) between 0.5 and 100Hz.

## 2.4 EEG Artifacts Removal

EEG signals contain cerebral and non-cerebral activity. Since the EEG signals are measuring the brain activity, the non-cerebral part should be considered as artifacts. To remove these artifacts, ICA algorithm will be used.

Commonly there are several known EEG artifacts:

1. Eye artifacts: To understand the eye artifacts in the EEG data, they can be represented as negative and positive charges as in 2.4.1. The electrical charge of the cornea is positive. Since the Fp1, and Fp2 are the most affected electrodes by eye artifacts, they get positively charged by the cornea in the case of the eye vertical movement while the person is looking upwards [95]. They get also negatively charged when the cornea moves downwards [95] (the person looks downwards) as in 2.4.1.

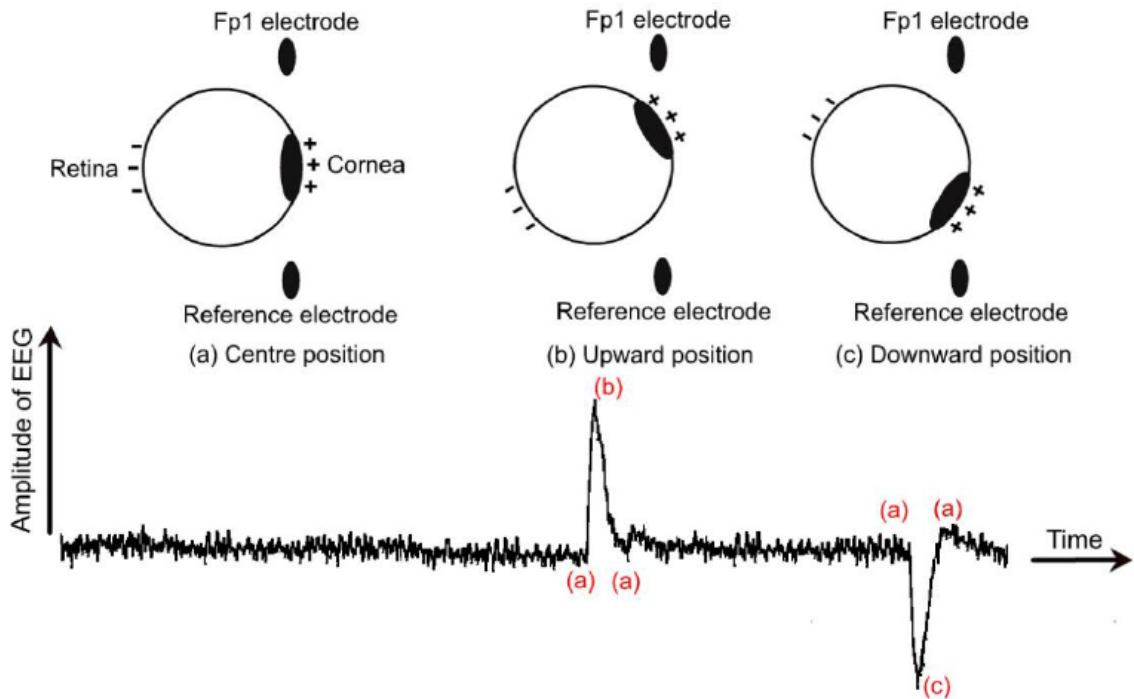


Figure 2.4.1: Eyes vertical movement [95]

Also another example of the eye artifacts is the eye-blink artifact as in 2.4.2. When the person closes his eye, the cornea moves upwards and hence the frontal electrodes Fp1, and Fp2 get positively charged [96], whereas when the person opens his/her eye, then the cornea moves downwards and so the electrodes Fp1, and Fp2 get negatively charged [96].

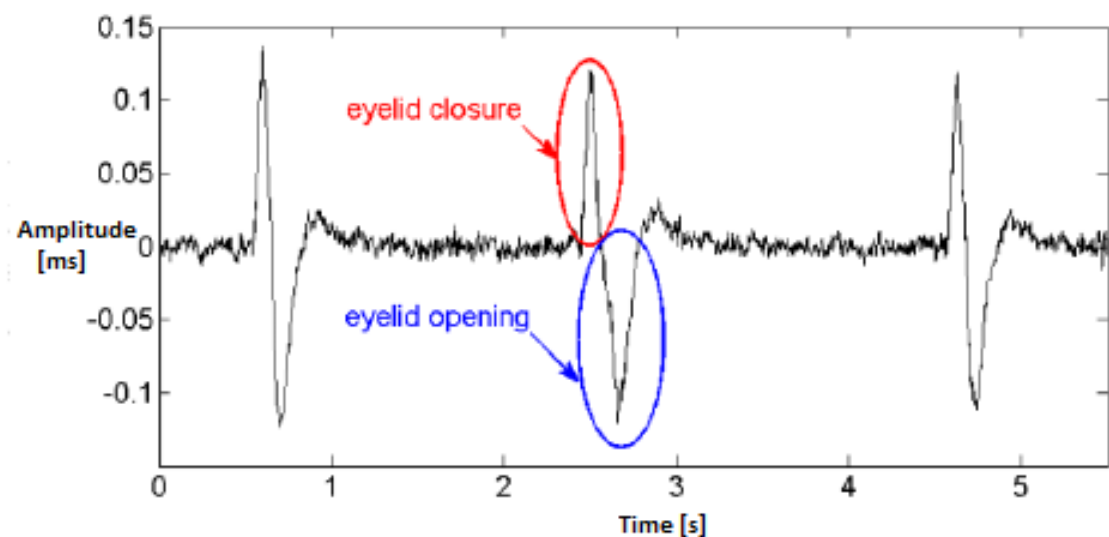


Figure 2.4.2: Eye-Blink Artifacts [96]

2. Muscle Artifacts: This type of artifacts is commonly seen on the sides of the head (neck artifacts, and near the ears artifacts)
3. Sweat Artifacts
4. Clenching Teath Artifacts

## 5. Electrode Artifacts

## 6. Cardiac Artifacts

### 2.4.1 Independent Component Analysis ICA

ICA is one of the algorithms that are used for blind source separation [97]. The blind source separation can be explained in the example below 2.4.3. In this picture, the ICA algorithm is explained as Cocktail Party Problem (CPP) [97]. In 2.4.3, there are many speakers (sources) and many microphones (channels, sensors, or electrodes), and also there is noise signal from the crowd. The microphones record the sound signals from the speakers, and the crowd. These microphones can not differentiate between sources. The ICA algorithm takes the signals from the microphone and does blind separation into sources. By using this algorithm in this case, it is possible to know which part of the signals corresponds to which speaker. This is exactly what the ICA does for the EEG signals. It takes the signals from many electrodes over the scalp of the head and separates them into potential sources. ICA algorithm is used in this study to remove artifacts. Principal Component Analysis (PCA) algorithm has been proposed to remove eye artifacts, however, PCA is not able to completely remove eye artifacts from neuro signals especially when the signals have similar amplitudes [98]. An important note to mention here is that, it is not possible to tell the ICA to give more sources than it takes. This means that the number of the sources can not be more than the number of the channels [99]. ICA assumes that the subcomponents are non-Gaussian signals and independent from each other [100]. According to the people who used the ICA, they claimed that the EEG signals are not Gaussian [100].

In this study, since there are 31 electrodes, the ICA algorithm has been applied to take 31 channels as an input, and give 31 sources as an output. ICA has been run and used for all subjects for the complete dataset: gestures and grasps. ICA components in this study will be visualized and analyzed for S1 (since it contains many artifacts). It will be also compared with the components of S2 (since S2 gave the best classification results in this study for all cases). ICA can be applied on continuous or discrete EEG data [101]. By continuous, it means that the EEG data is not yet epoched. Since in this study different time-windows have been tried, the ICA has been applied after the filtering step and before the epoching on continuous EEG data using the "runica" that runs slow ICA algorithm and by choosing the "extended" option since it is recommended to find sub-gaussians [102] in EEGLAB(Delorme and Makeig, 2004) software as in [101]. In this study, the ICA algorithm has been used once to remove the artifacts on the 31 electrodes. To test the 16 electrodes classification, the reduction from 31 to 16 electrodes has been done on the EEG data (31 electrodes) after the artifacts removal.

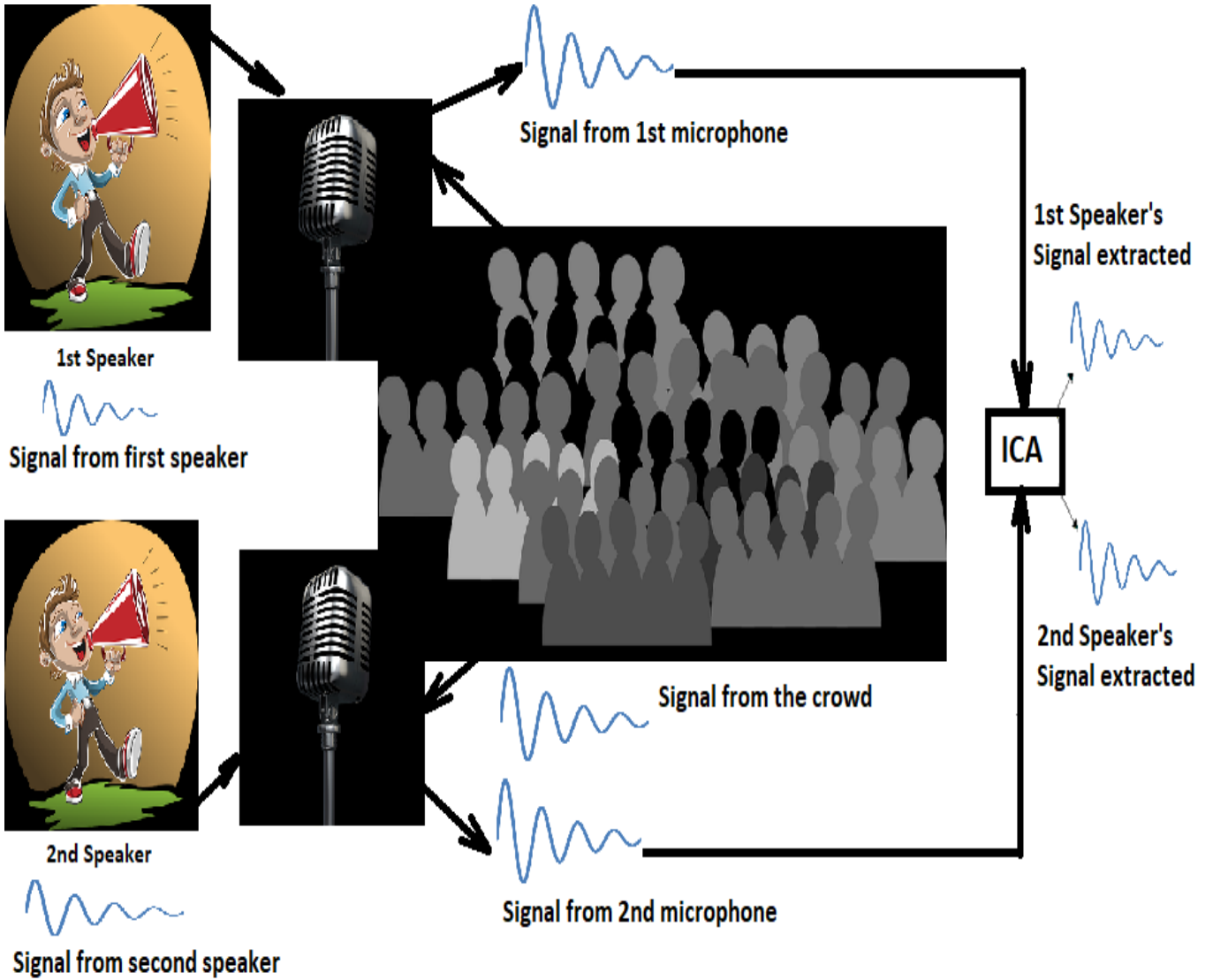


Figure 2.4.3: ICA as Cocktail Party Problem

## 2.5 Epoching

To classify the EEG data, it should be divided into equal epochs. These epochs will be chosen according to the time of interest and the highest possible accuracy. The time of interest here means, that there is an interest in differentiating between gestures and grasps before starting the gesture or starting the grasp and possibly also before starting the hand movement. In other words, it is important to predict the type of movement before the subject physically starts the movement but of course after he/she starts thinking about the desired kind of movement.

EEG Epoching is a method in which time series discrete EEG data are extracted from continuous data. Epoching continuous data gives epochs. These epochs are equally sized and are then needed for further processing. Epoching is done according to events. These events are normally recorded from other system. In this study, the events are extracted from the VICON Kinematics System. In the case of continuous data, the data-matrix has the shape [channels, time], whereas in case of epoched data, the data-matrix will have the shape [channels, time, epochs].

According to a study made about detecting the intention of grasping during the reaching phase as in [44], the grasp intention could be predicted about 400ms before the grasp movement. In the EEG data in this study, the event of starting the hand movement from the VICON motion capture system is extracted. However this event does not take in the consideration the thinking process which happens in the subject's brain before he/she takes the decision to move his/her hand. It is about the time between starting of thinking and making a decision. As in [103], thinking speed varies between different tasks. As an example, deciding to run for a runner after hearing the sound from the pistol takes about 150ms [103]. There are however more complex decision making tasks which take more time, like deciding when to change the street lane during driving, and finding out the way to solve a math problem after thinking [103]. Also, the travel distance of the signal from the brain to the body part which is executing the motion is important. It takes time until a signal from the brain will be transmitted to the part of the body which is executing a motion. The time it takes for a signal to move the hand is shorter than the time it takes to move a foot [103]. In most subjects in this study, it takes time about 400ms between starting the movement and starting the gesture/grasp. According to this, in this study a first epoching has been made between 400ms before and 600ms after starting the hand movement. In order to design a system that gives the right signal at the right time for an external controller to move the robotic hand according to the desired type of movement or the desired type of grasp, there is a need for choosing the correct time-window that has the highest classification-results. This signal also needs to be as predictable as possible. This means that it needs to be before starting the grasping action and possibly also before starting the hand movement. To do this, a sliding time-window approach with time-window-size of 100ms has been applied to the EEG data. This sliding time-window has been applied to start 400ms before and 600ms after the starting of the hand movement. This time-window has been taken equally from all the EEG datasets as following:

- Time-Window 1: -400ms to -300ms before starting the hand movement
- Time-Window 2: -300ms to -200ms before starting the hand movement
- Time-Window 3: -200ms to -100ms before starting the hand movement
- Time-Window 4: -100ms to starting the hand movement
- Time-Window 5: from starting the hand movement to +100ms after starting the hand movement
- Time-Window 6: +100ms to +200ms after starting the hand movement
- Time-Window 7: +200ms to +300ms after starting the hand movement
- Time-Window 8: +300ms to +400ms after starting the hand movement
- Time-Window 9: +400ms to +500ms after starting the hand movement
- Time-Window 10: +500ms to +600ms after starting the hand movement

The epoch then will be chosen by concatenating the time-windows which have the best classification accuracies.

## 2.6 Machine Learning Classifiers with CSP

Machine Learning Classification with CSP:

EEG classification with CSP has proved to be one of the best methods for the EEG data classification [94]. It has also proved that it is not only suitable for binary classification, but also for the multi-classification [104]. In this study, the following algorithms will be tested with CSP to classify the EEG data:

- LogReg
- SVC with Linear and RBF Kernel
- RF
- LDA

### 2.6.1 Common Spatial Pattern

CSP method was firstly used by H. Ramoser [94]. CSP: is a mathematical method used in signal processing and especially in EEG signal processing for separating a multivariate signal into components which have maximum difference in variance [94].

CSP is calculated by taking two equally sized windows from two different conditions and calculating the variance between them. It uses a linear transform to project multi-channel EEG data into low-dimensional spatial subspace with a projection matrix [105].

By taking the case of the binary classification between gestures and grasps: In this case, two equally sized windows for two different conditions (gestures vs. grasps):  $X_{GST}$  and  $X_{GSPs}$  are taken.  $X_{GST}$  and  $X_{GSPs}$  are the EEG matrices for gestures, and grasps. With dimensions  $m \times n$  where:  $m$ : the number of channels.  $n$ : the number of samples. The normalized spatial covariance matrices of EEG are calculated from [105] as following:

$$R_{GST} = \frac{X_{GST} \cdot X_{GST}^T}{\text{trace}(X_{GST} \cdot X_{GST}^T)} \quad (2.6.2)$$

$$R_{GSPs} = \frac{X_{GSPs} \cdot X_{GSPs}^T}{\text{trace}(X_{GSPs} \cdot X_{GSPs}^T)} \quad (2.6.3)$$

$X^T$  is the transpose of  $X$  and  $\text{trace}(X \cdot X^T)$  is the sum of the diagonal elements of the matrix  $X$ .

The averaged normalized covariances  $\overline{R_{GST}}$  and  $\overline{R_{GSPs}}$  are calculated by averaging over all the trials of each class. The overall spatial covariance can be calculated as following [105]:

$$R = \overline{R_{GST}} + \overline{R_{GSPs}} = E_0 \cdot \Sigma \cdot E_0^T \quad (2.6.4)$$

Where  $E$  and  $E_0$ : are the matrices of eigenvectors and  $\Sigma$  is the diagonal matrix of eigenvalues.

Then the whitening transformation matrix is calculated as following [105]:

$$W = \Sigma^{-1/2} \cdot E_0^T \quad (2.6.5)$$

By using the whitening transformation matrix  $W$ , the average covariance matrices can be calculated [105]:

$$R_{\text{Av}(\text{GST})} = W \cdot \overline{R_{\text{GST}}} \cdot W^T \quad (2.6.6)$$

$$R_{\text{Av}(\text{GSPs})} = W \cdot \overline{R_{\text{GSPs}}} \cdot W^T \quad (2.6.7)$$

These average covariance matrices share the same eigenvectors  $E$  and can be calculated as following [105]:

$$R_{\text{Av}(\text{GST})} = E \cdot \Sigma_H \cdot E^T \quad (2.6.8)$$

$$R_{\text{Av}(\text{GSPs})} = E \Sigma_H \cdot E^T \quad (2.6.9)$$

Then the Projection matrix can be calculated as following [105]:

$$Proj = E^T \cdot W \quad (2.6.10)$$

$Proj^{-1}$ : is the inverse projection matrix and it contains the spatial patterns which are then used to classify between the EEG windows of different conditions.

The EEG source components can be calculated from the projection matrix  $Proj$  and the EEG matrix  $X$  as following [105]:

$$Source = Proj \cdot X \quad (2.6.11)$$

The original EEG matrices can be calculated back from the Source components as following [105]:

$$X = Proj^{-1} \cdot Source \quad (2.6.12)$$

Although CSP is designed for binary classification, it can also be used for multi-classification (more than two classes) by using the One-Versus-Rest Concept [104].

Defining the Common Spatial Filters number :

In this study, at first arbitrarily 20 spatial filters were used for all subjects, in all algorithms, and all cases for the classification in the epoching step. Then, to define the right number of CSP filters for every classification case and for every classifier, the cross-validation has been used [106]. Using the cross validation, the number of CSP filters will be chosen according to the highest classification accuracy the classifier can achieve. If the classifier has another parameters, that need to be optimized, then these parameters can be chosen in combination with the CSP number using Grid Search Algorithm with cross validation to achieve the highest accuracy. For individual subjects binary classification, the following CSP filters numbers are tested using the cross validation: 3, 6, 10, 20, 30, 40, 50. After doing the classification for individual subjects, it has been found, that the most CSP filters numbers which achieve the best classification results are in the range between 3 and 30 filters. That is why, for the case of cross-subjects classification, the following CSP filters numbers were tested: 3, 6, 10, 20, 30.

## 2.6.2 Logistic Regression

LogReg has been used successfully by the first Grasp and Lift Kaggle Competition winner: Alexandre Barachant [107] in the grasp-and-lift-EEG-challenge [108], to classify between hand movement and rest (no-movement). Logistic Regression is a linear classifier [109]. It uses the Logit function to classify data as in 2.6.1.

The Logistic function is defined as following [109]:

$$\sigma(t) = \frac{e^t}{e^t + 1} = \frac{1}{1 + e^{-t}} \quad (2.6.13)$$

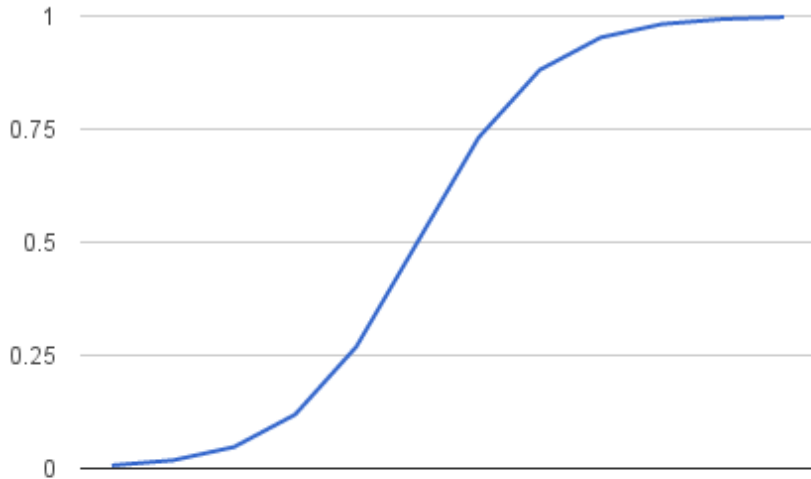


Figure 2.6.1: Logistic Function [109]

Logistic Regression Regularization Parameter:

The same as in Support Vector Machine, Logistic Regression uses regularization parameter  $C$  to classify the data. In the epoching step, this number has been set as default:  $C=1$ . However, in the classification step, this regularization parameter needs to be optimized to achieve the highest possible classification accuracy [110]. Grid search [111] with cross-validation as explained in this study in 2.8 is used to define both the CSP filters as explained in 2.6.1 and the regularization parameter  $C$ .

The regularization number range for individual subjects gestures vs. grasps and precision vs. power grasps has been chosen to be:

$$C_{\text{range}} = [0.01, 0.1, 1, 10, 100, 1000, 10^4, 10^5, 10^6, 10^7, 10^8, 10^9, 10^{10}].$$

After running the classification for the aforementioned cases and according to the best classification results, a new range for  $C$  has been chosen to be used in the cross-subjects classification case (gestures vs. grasps, precision vs. power grasps):  $C_{\text{range}} = [1, 10, 100, 1000, 10^4]$ .

### 2.6.3 Support Vector Machine

SVC method with CSP was used successfully in [112] to classify between left and right hand movement using EEG data. It was also used in [113] to classify between left and right imagined hand movements using EEG data by applying the linear and RBF kernel.

In this study, two types of SVC will be used in the classification step. SVC with linear kernel, and SVC with RBF kernel. SVC or SVM is support vector machine algorithm that uses support vectors and hyperplanes to classify data. Support vector machine with linear-kernel is the simplest SVC algorithm that is used for the classification in general.

### 2.6.4 Kernel Trick

The kernel trick is based on the idea that mapping non-linear separable data into higher dimensional space (non-linear) as in 2.6.2 will make the data better non-linearly separable [114].

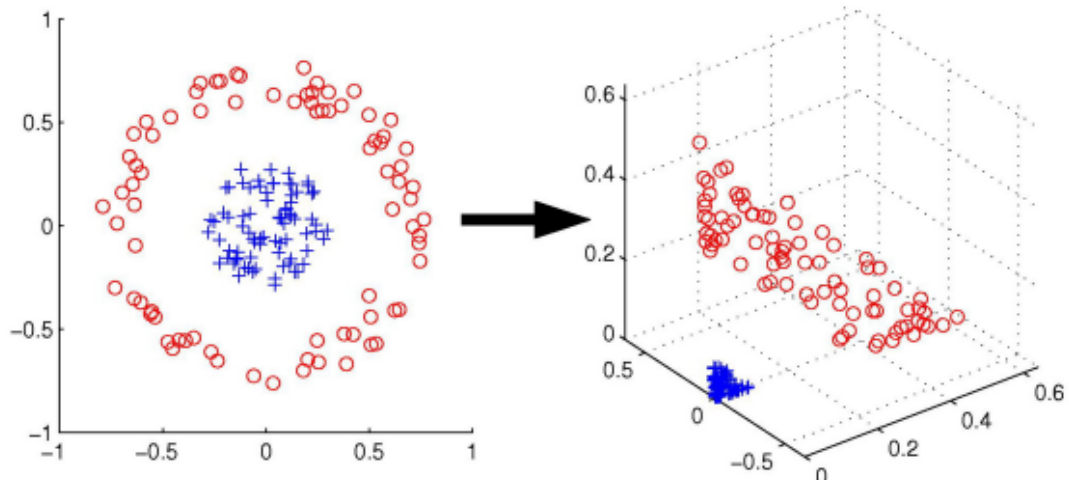


Figure 2.6.2: Kernel trick [115]

### 2.6.5 Support Vector Machine RBF Kernel

The idea of using a kernel in SVC is that, the data which is not separable in one space might be separable in a higher space [114]. That is why, a mapping of the datasets to a higher dimensional space is applied. The equation that explains the RBF kernel is as following [116]:

$$K(X_1, X_2) = \exp\left(-\frac{\|X_1 - X_2\|^2}{2\sigma^2}\right) \quad (2.6.14)$$

$X_1, X_2$ : are vectors of datasets in the features space,  $\sigma$  is a free parameter.

### 2.6.6 Support Vector Machine Parameters

In this study, in the classification step, the regularization parameter  $C$  and the overfitting Parameter  $\gamma$  need to be optimized by using the Grid Search algorithm with cross validation (Grid-

SearchCV) [111] in scikit-learn [117]. Grid Search algorithm does the optimization of the SVC parameters ( $C$ ,  $\gamma$ ) using the cross validation [111]. For the SVC with linear-kernel, only the  $C$  parameter needs to be optimized [111]. For the SVC with RBF kernel, both  $C$  and  $\gamma$  parameters need to be optimized. To have the best SVC classification results, the Grid Search algorithm with cross validation has been used for the number of CSP components as explained in 2.6.1, the overfitting parameter  $\gamma$ , and the regularization parameter  $C$ , by testing different values of  $C$  and  $\gamma$  in combination with CSP components for the case of individual subjects gestures vs. grasps and precision vs. power grasps classification for the following  $C$ , and  $\gamma$  values:

$$C_{\text{range}} = [0.01, 0.1, 1, 10, 100, 1000, 10^4, 10^5, 10^6, 10^7, 10^8, 10^9, 10^{10}].$$

$$\gamma_{\text{range}} = [10 - 9, 10^{-8}, 10^{-7}, 10^{-6}, 10^{-5}, 10^{-4}, 10^{-3}, 10^{-2}, 0.1, 1, 10, 100, 1000].$$

After running the classification for individual subjects and according to the best classification results, a new reduced range for  $C$  and  $\gamma$  has been chosen to be used then in the cross-subjects classification case:

$$C_{\text{range}} = [1, 10, 100, 1000, 10^4].$$

$$\gamma_{\text{range}} = [10^{-6}, 10^{-5}, 10^{-4}, 10^{-3}, 10^{-2}].$$

The used cross-validation number is chosen as explained in this study in 2.8.

### 2.6.7 Random Forest

This method has been used in [118] to classify motor-imagery EEG data of the right hand and the feet using CSP features and could outperform the LDA algorithm according to [118]. RF algorithm uses multi decision trees as classifiers on different sub-sets of the dataset and implements averaging to improve the accuracy and control over-fitting [119]. In the epoching step, the number of the estimators has been arbitrarily chosen to be 150. However, the number of the estimators can also be optimized. Using the Scikit-Learn package [117], the number of the estimators (decision trees) of RF, and the number of CSP filters as explained in 2.6.1 has been chosen using Grid Search algorithm with cross-validation (GridSearchCV) [111], [120]. The number of cross-validation number is chosen as explained in this study in 2.8.

### 2.6.8 Linear Discriminant Analysis

This method was successfully used in [118] to classify motor-imagery EEG data of the right hand and the feet using the CSP features. LDA stands for Linear discriminant analysis, It is a machine learning method to find the linear combination of features in order to classify them into classes [121]. LDA is similar to PCA in that they both try to find the linear combination of features which best describe the data [122]. The difference between LDA and PCA is, that LDA tries to find the variances between the classes [123]. LDA in this study is not used in the epoching step. In this study LDA will be tested on different CSP filters as explained in 2.6.1 using cross-validation as explained in 2.8.

## 2.7 Machine Learning on Riemannian Manifold

Riemannian geometry is named after the German mathematician Bernhard Riemann [124]. Unlike the classification with CSP, the classification in Riemannian space uses Riemannian distance

instead of the Euclidean one [125]. The classification in the Riemannian space is done by mapping the data to the Riemannian space to be classified [125].

Classification in Riemannian geometry with covariance matrices is a newer approach than the CSP one for the classification of the EEG data [125]. It has also recently proved to be one of the best algorithms for the classification of EEG data and especially in the case of multi-classification [126].

For the covariance matrices  $P_1$  and  $P_2$ , if  $P_1$  and  $P_2$  are the means of two classes, then the Riemannian distance can be calculated as following[125]:

$$\delta^2(P_1, P_2) = \sum_n \log^2 \lambda_n(P_1^{-1}P_2) \text{ while } \lambda_n : \text{ eigenvalues} \quad (2.7.15)$$

### 2.7.1 Covariance Matrices

Covariance matrices show exactly where the covariances between electrodes exist. In other words, they show which electrodes are more activated for specific tasks. Both TS, and MDM methods use the covariance matrices to classify the EEG data. In this study, covariance matrices for S2 using pyRiemann package [127] for the gestures, the grasps, and for 3 out of 20 grasps (the Suitcase, the SmallCup, and the ExtractKey grasps) using 31 electrodes will be plotted and analyzed. The reason, why the covariance matrices will be plotted for S2, is that S2 achieved the highest classification results in both gestures vs. grasps case in 3.4.1 and multi-classification case in 3.3.5.

### 2.7.2 Classification in Tangent Space

In this study, TS algorithm have been tested in the epoching and the classification step.

For the Riemann manifold  $M$  In the figure below, 2.7.1, the geodesic curve  $\gamma(t)$  between the two covariance matrices  $P_1$  and  $P_2$  is given as following [125]:

$$\gamma(t) = P_1^{1/2}(P_1^{-1/2}P_2P_1^{-1/2})^tP_1^{1/2} \text{ with } t \in [0 : 1] \quad (2.7.16)$$

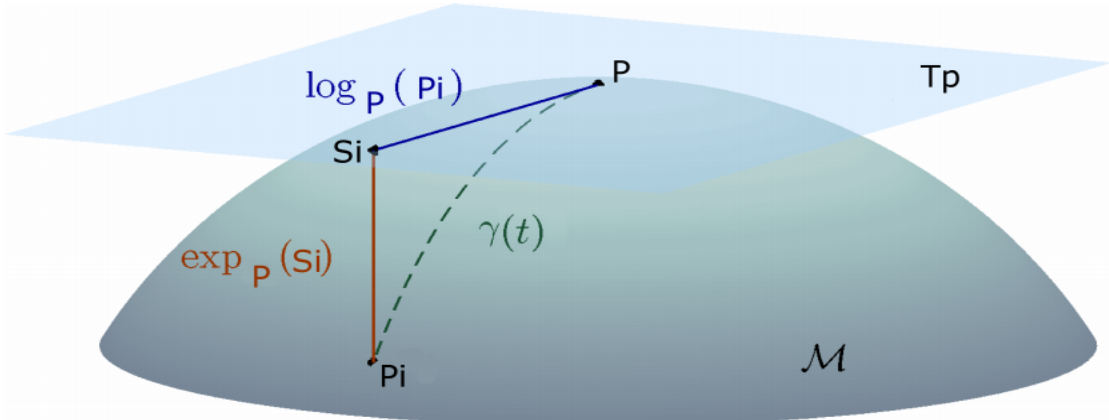


Figure 2.7.1: Riemann tangent space at point  $G$ . EEG trials are points[128]

for every point  $P \in P(n)$ , it is possible to have a tangent vector  $S_i \in S(n)$ . All the tangent vectors make the tangent space. This tangent space is Euclidean [125]. EEG data can be mapped to the tangent space using Logarithmic map [125]:

$$S_i = \text{Log}_p(P_i) = P^{1/2} \text{Log}(P^{-1/2} P_i P^{-1/2}) P^{1/2} \quad (2.7.17)$$

Due to the fact that the tangent space is Euclidean, the arithmetic mean can be calculated [125]. Then using the Riemannian exponential mapping, the computed arithmetic mean can be projected back into the covariance matrices space[125]. This is done by using iterations computations [125]:

$$\text{Exp}_p(S_i) = P^{1/2} \text{Exp}(P^{-1/2} S_i P^{-1/2}) P^{1/2} \quad (2.7.18)$$

In this study, the algorithm used to classify the data in TS is LogisticRegression in tangent space. The difference between LogisticRegression and the LogReg is that LogReg in this study classifies the EEG data using the CSP whereas the LogisticRegression in TS classifies the EEG data in the tangent space.

### 2.7.3 Classification with Minimum Distance to the Mean

MDM was only used in the epoching step, because it did not outperform other algorithms such as TS, and LogReg in the epoching step as in the results of the epoching of gestures vs. grasps classification 3.3.1, and precision vs. power grasps classification 3.3.3. MDM could outperform LogReg when doing the multi-classification in the epoching step as in the case of S2 3.3.5, and S10 3.3.6, however TS was better suitable for the multi-classification case.

In this type of classification, as in 2.7.2, there are two different datasets: the green and the blue ones. Each dataset has a center of mass  $G_1$  and  $G_2$ . Then a new data which is labeled with the question mark is assigned to one of these two classes, whose center of mass is the closest. By calculating the Riemannian distance in 2.7.15, the center of mass  $G$  of a set of  $P_1, P_2, \dots$  matrices can be calculated.  $G$  is called the geometric mean. The geometric mean is similar to the arithmetic mean. The difference between the geometric and arithmetic mean is that, the geometric mean is calculated in the Riemannian space, whereas the arithmetic mean is calculated in the Euclidean space [129].

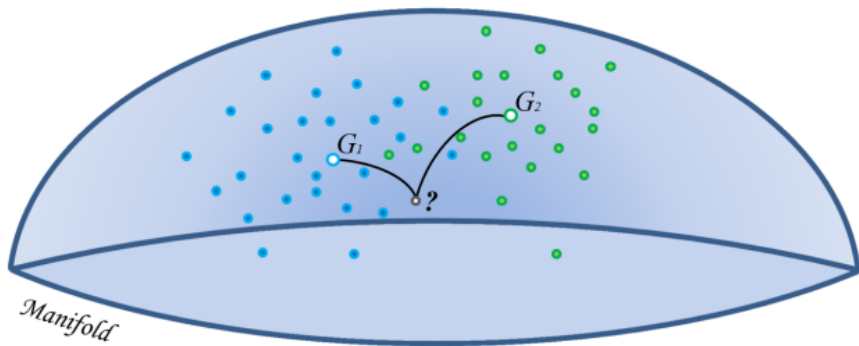


Figure 2.7.2: Riemann minimum distance to the mean [130]

## 2.8 Cross Validation

Cross validation is useful to avoid over-fitting problem [131]. To classify the EEG data, the  $k$ -fold cross validation method has been used in this study.  $K$ -fold cross validation is a method to split the data into training and test data. It is also called rotation estimation [132]. It splits the dataset into  $k$  folds of almost the same size. For each fold, the data is trained on all the folds except one fold to be further tested on it [132]. The accuracy is calculated by dividing the sum of the accuracies over all folds by the number of folds [132]. For calculating the  $k$ fold cross validation, the scikit-learn [117] package has been used. According to [133], using cross validation number of 10 is best suitable for most applications when the number of trials is large enough. According to this, the following numbers of cross validation have been used in this study:

- Cross validation of 10 for the case of gestures vs. grasps binary classification for individual subjects.
- Cross validation of 10 for both cases of gestures vs. grasps binary classification and precision vs. power grasps binary classification using the transfer learning of all 10 subjects. For this, 10 subjects have been used by training on 9 folds (subjects) and testing on the 10th fold (subject). The EEG data for every subject in this type of classification has been made to be equal to have equal folds. To have equal EEG data for all subjects, 2 out of 5 trials for S2, S3, S6 were removed.
- Since the number of the EEG data in the precision vs. grasps binary classification case in individual subjects is smaller than the number of the EEG data in the gestures vs. grasps binary classification case for every subject, the Cross validation number has been chosen to be 5.
- In the case of multi-grasps classification the following cross validation number have been used:
  - The cross validation number for the subjects who have 5 trials for every grasp has been chosen to be 5, by dividing the EEG trials to 5 folds: training has been done on 4 folds and testing was done on the 5th fold.
  - The cross validation number for the subjects who have 3 trials for every grasp has been chosen to be 3, by dividing the EEG trials to 3 folds: training on 2 folds and testing on the 3rd fold.

## 2.9 Multi-Grasps Classification

In this type of classification, 20 different types of grasps in S2, S10, and S1 will be classified. To analyze the results, and the classification performance, the confusion matrices, and the classification reports for S2, S10, and S1 will be used. The S2 and S10 were chosen because they could achieve the best classification results in the epoching step in the case of the multi-classification as in 3.3.5 for S2 and 3.3.6 for S10. The multi-classification results in S1 were not good enough as in 3.3.7, however the S1 has been chosen to compare with the best results of the S2 and S10.

### 2.9.1 The Confusion Matrix and Classification Report Parameters

The confusion matrix is a table of (True Labels x Predicted Labels), that can be used to measure the performance of the classifier. In this study, the confusion matrix will be plotted for the multi-grasps classification case, to show exactly in which labels the classifier makes errors. Also the classification report analyzes the following classification parameters to be then used with the accuracy to better evaluate the performance of the model [134]:

- Precision: It is calculated in the following equation:

$$Precision = \frac{TP}{TP + FP} \quad (2.9.19)$$

*TP*: True Positive which describes the number of correctly identified class labels.

*FP*: False Positive which describes the number of incorrectly identified class labels.

A high value of the precision indicates that the model has learned correctly. Precision is the measure of the classifier's exactness [135].

- Recall: It is calculated in the following equation:

$$Recall = \frac{TP}{TP + FN} \quad (2.9.20)$$

*TP*: True positives

*FN*: False negatives which describe the number of unidentified class labels.

Recall can be explained as the completeness of the classifier [135].

- F1 Score: The F1 Score is calculated as following:

$$\frac{2 \cdot precision \cdot recall}{precision + recall} \quad (2.9.21)$$

The F1 score indicates the balance between the precision and the recall [135].

- Micro Precision: It is the same as the precision but is used in the multi-classification case.

$$MicroPrecision = \frac{\sum_{i=1}^n TP_i}{\sum_{i=1}^n (TP_i + FP_i)} \quad (2.9.22)$$

- Micro Recall: It is the same as the recall but for more than two classes case.

$$MicroRecall = \frac{\sum_{i=1}^n TP_i}{\sum_{i=1}^n (TP_i + FN_i)} \quad (2.9.23)$$

- Micro F1 Score: It is the same as the F1 Score but for the multi-classification case.

$$\frac{MicroPrecision \cdot MicroRecall}{MicroPrecision + MicroRecall} \quad (2.9.24)$$

## 2.10 Cross-Subjects Classification

In order to test if the model can be transferred from a subject to another, the cross-subject classification on the gestures vs. grasps and precision vs. power grasps is performed. In this type of classification, a cross validation of 10 has been used, by training on 9 subjects and testing on the 10th one. The reason, why only 10 subjects have been used is explained in 2.8. In this type of classification, the typical machine learning with CSP and TS methods as in gestures vs. grasps, precision vs. power grasps will be used. In this type of classification, since there is big data, the Deep Learning (DL) methods will be also tested. Also to enhance the classification results of the ML with CSP and with TS methods, the boosting methods will be used.

### 2.10.1 Deep Learning Methods

Although deep learning proved to be the best method for the classification of images using the convolutional layers [136], and in other domains such as the text recognition [137] using the recurrent layers, and also in the classification of video (series of images) [138], it could not show that high performance in the EEG field. This is due to the following reasons:

- Deep learning always needs big data to classify correctly [139]. It is hard to collect big EEG data.
- EEG data varies from subject to another [47]. This makes it harder to use EEG data from many subjects or to transfer trained model from subject to another.
- EEG Data contains many artifacts. This makes it harder to classify with deep learning methods without using special temporal, and spatial filtering methods such as CSP.

In this study based on researches which have been done in [49] and [48], the following deep learning algorithms will be applied on cross-subjects classification of EEG data to test if the trained model on some subjects can be transferred to a new subject:

- Cascade Recurrent Convolutional Neural Network [48].
- Parallel Recurrent Convolutional Neural Networks [48].
- Power Spectrum Density (PSD) Recurrent Convolutional Neural Networks [49].

Cascade RCNN:

In this method, the EEG data vectors from many channels are converted to 2D meshes according to the electrodes map as in 2.11.1 for the case of 31 electrodes and 2.11.2 for the case of 16 electrodes. By using Recurrent Convolutional Neural Network (RCNN) as in 2.10.1. The algorithm works as following [48]:

- The EEG data is segmented into equal segments (time-windows) with each segment chosen to be 10 time points.
- Each of the segments is processed with 3 2D-convolutional neural networks, fully connected layer, and Long Short-Term Memory (LSTM) layer as in 2.10.2.

- 1st 2D convolutional Layer with kernel size (3,3), and stride 1. Output channels number: 31 or 16 depending on the number of electrodes used.
- 2nd 2D convolutional Layer with kernel size (3,3), and stride 1. Input channel number: 31, or 16, output channels number: 62 or 32 depending on the number of electrodes used.
- 3rd 2D convolutional Layer with kernel size (3,3), and stride 1. Input channel number: 124, or 64, output channels number: 256, or 224 depending on the number of electrodes used.
- No pooling layers were used as they are supposed to reduce the data dimensions at the cost of losing information as in [48].
- After the 3 2D-convolutional layers and before using the LSTM-layer, a fully connected layer, and dropout layer to avoid the overfitting are applied.
- Then for every time-window, two LSTM-layers are applied, followed by dropout layer.
- All the outputs of the LSTM cells and dropout layers are then processed with fully connected layer, followed by dropout layer.
- At the end, softmax layer is used to predict the class type.

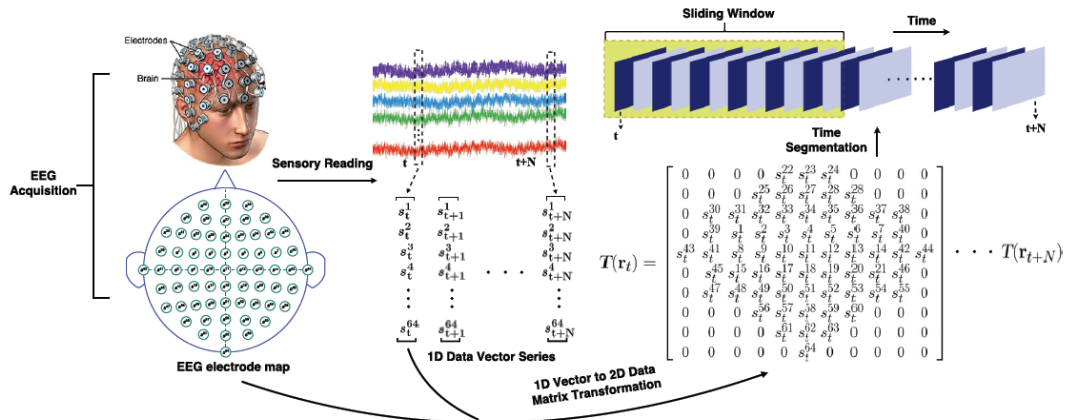


Figure 2.10.1: EEG signals are converted to 2D meshes [48]

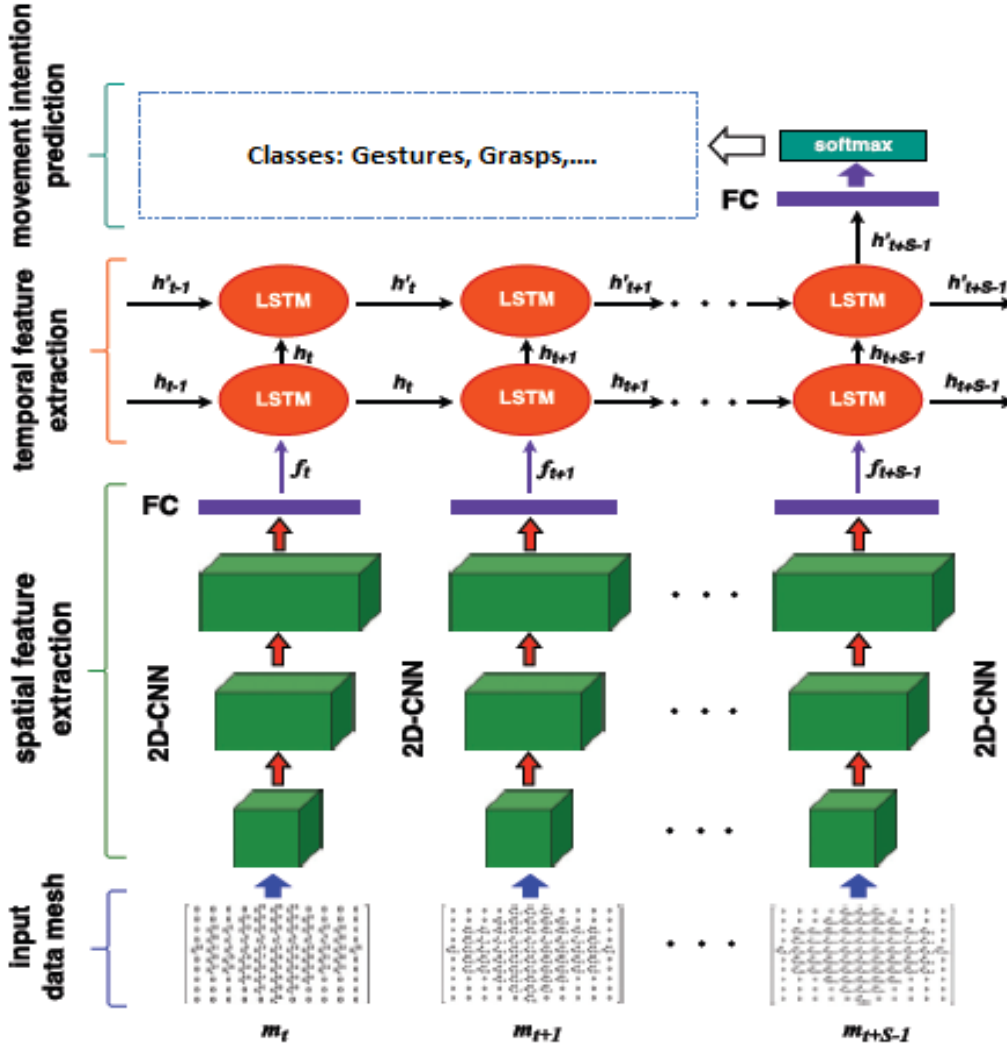


Figure 2.10.2: Cascade convolutional recurrent neural networks [48]

#### Parallel RCNN:

This method is very similar to the cascade RCNN method. It works as following [48]:

- The EEG data is segmented into equal segments (time-windows) with each segment is chosen to be 10 time points.
- Each of the segments is processed in two ways: one way with 3 2D-convolutional neural networks as in 2.10.3 and the other way is processed with 2 LSTM-cells. That is why it is called parallel.
- After the 3 2D-convolutional layers, a fully connected layer followed by a dropout layer are used for each segment. Also after 2 LSTM-cells, a fully connected layer with dropout layer are applied for each segment.
- Then both the fully connected layers from the Convolutional Neural Network (CNN) and the Recurrent Neural Network (RNN) ways are concatenated and a softmax layer is used to predict the type of the class.

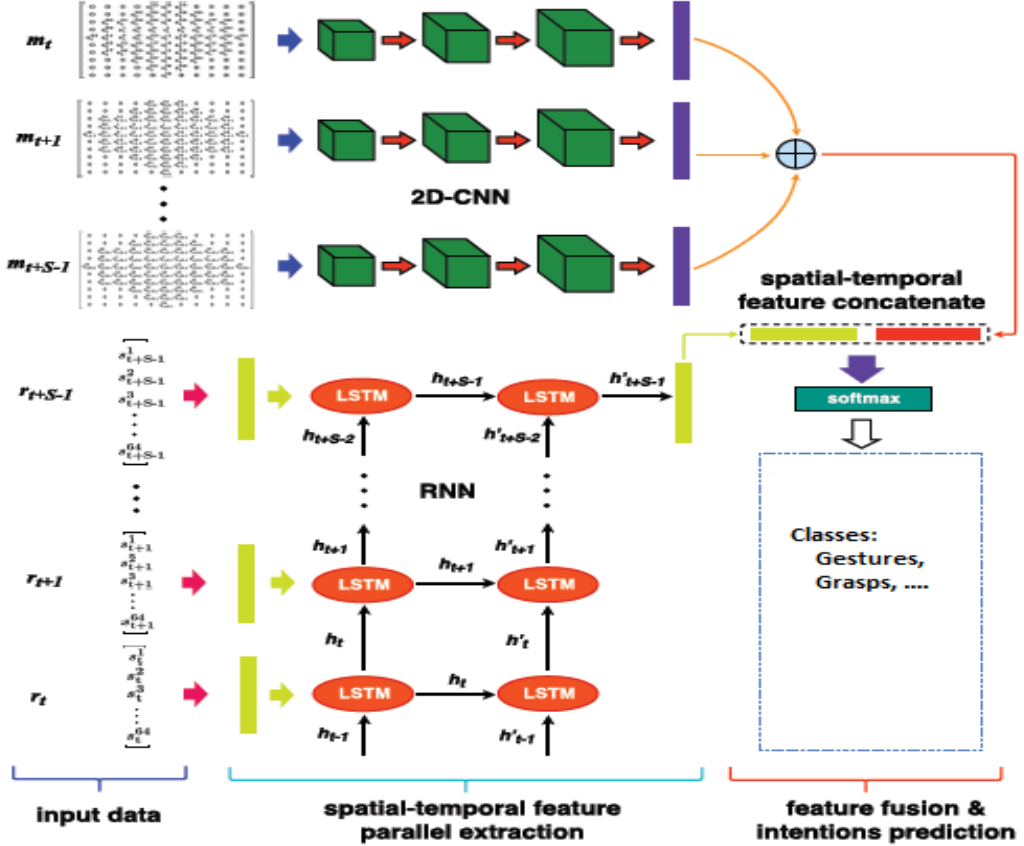


Figure 2.10.3: Parallel convolutional recurrent neural networks [48]

#### Power Spectrum Density Classification with RCNN:

This method analyzes the EEG data as video data [49]. A video consists of sequential images. This method converts at first the EEG data to images with frequency data by applying Fast Fourier Transform (FFT) to the EEG signals to convert the signals from the time to the frequency domain. In this method as in [49], the EEG data is converted to 2D presentation, which matches the channels localization on the head. These channels (electrodes) frequencies are just like pixels in the case of images. The EEG data as in [49] is converted with PSD function to frequency bands (channels). PSD function, calculates the frequency by applying Fast Fourier Transform to the EEG data [49]. Of course the frequency bands here are presented as deep learning layer depth or channels. In the case of images, these channels are R,G,B which stand for Red, Green, and Blue colors. The algorithm as in [49] calculates the frequency bands for Theta, Alpha, and Beta frequency ranges. In this study, there is no specific frequency range in the case of gestures vs. grasps as in 3.1.1, and the case of precision vs. power grasps as in 3.1.2, and 3.1.3. According to that, also three frequency bands has been applied but to cover all the EEG frequency ranges as following [49]:

- 1st frequency band from 0.5 to 49Hz
- 2nd frequency band from 51 to 80Hz
- 3rd frequency band from 80 to 100Hz

Then images are generated given the electrodes locations in 2D space. After that, the images are fed into convolutional layers as in 2.10.4 as following [49]:

- 3 Stacks are used. 1st stack has 4 convolutional layers, 2nd stack has 2 convolutional layers, and 3rd stack has 1 convolutional layer. The used padding is "same".
- Number of kernels in each layer is twice the number in the previous stack.
- Number of used kernels in the 3 stacks where: 31, 62, 124 for the case of 31 electrodes, and 16, 32, 64 for the case of using 16 electrodes.
- Image size in this case is 31 for the case of 31 electrodes and 16 for the case of using 16 electrodes.
- Stacks are separated by maxpool layer with pool size (2,2).
- Then a fully connected layer with dropout=0.5 and 512 units is used.
- Then an LSTM Layer is used with number of units=62 in the 31 electrodes case and 32 for the 16 electrodes case.
- Then a fully connected layer with dropout=0.5 and 248 units for the 31 electrodes case and 124 units for the 16 electrodes case is used.
- Number of time-windows used are 6. One EEG Image for each time-window.

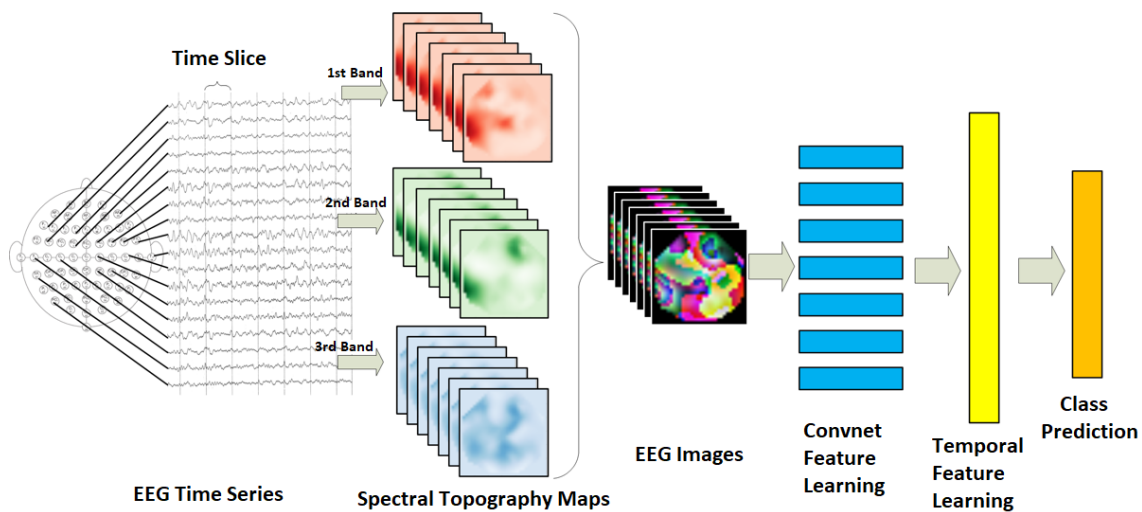


Figure 2.10.4: [49]

- EEG Time-Series Signals are acquired and converted to three frequency bands.
- The extracted frequency bands are used to generate 3-channel (depth) images.
- This sequence of images is then fed into RCNN for learning and classification

### 2.10.2 The Boosting Methods

In this study, many different algorithms are used. Each one achieves different accuracy for different dataset. The goal of using boosting methods is to enhance the accuracy by concatenating different algorithms. The following boosting algorithms will be used for the case of cross-subject classification:

- AdaBoost [140]: It implements sequence of weak-learners. The final prediction is then calculated from all the data by combining the predictions from all weak learners through a max-voting as in 2.10.5. AdaBoost corrects the errors in the classification by giving the data that was misclassified in the previous iteration more weights than the data that was correctly classified.
- GradientBoost [142]: It is the same as AdaBoost, however instead of changing the weights as in AdaBoost, GradientBoost tries to fit the new estimator to the errors which were misclassified by the previous estimator.
- XGBoost [143]: It stands for eXtreme Gradient Boosting. It is a fast GradientBoost algorithm. Instead of sequentially training the model, XGBoost provides the Parallelization of the training using more CPU Cores.

The following boosting methods in cross-subjects classification have been used in this study:

AdaBoost with TS, LogReg, SVC linear-kernel, SVC RBF-kernel estimators (learners). This showed better results than other algorithms.

weighted AdaBoost with the following weights and estimators:

- TS with the weight 0.25
- LogReg with the weight 0.5
- SVC linear-kernel with the weight 0.25.

GradBoost with the following estimators:

- Initial estimator: TS
- LogReg
- SVC with linear-kernel
- SVC with RBF-kernel

GradBoost. Same as the previous one but instead of removing the SVC with RBF-kernel, the TS has been removed and the LogReg has been used as initial estimator.

XGBoost with the following estimators:

- TS
- LogReg

- SVC with linear-kernel
- SVC with RBF-kernel

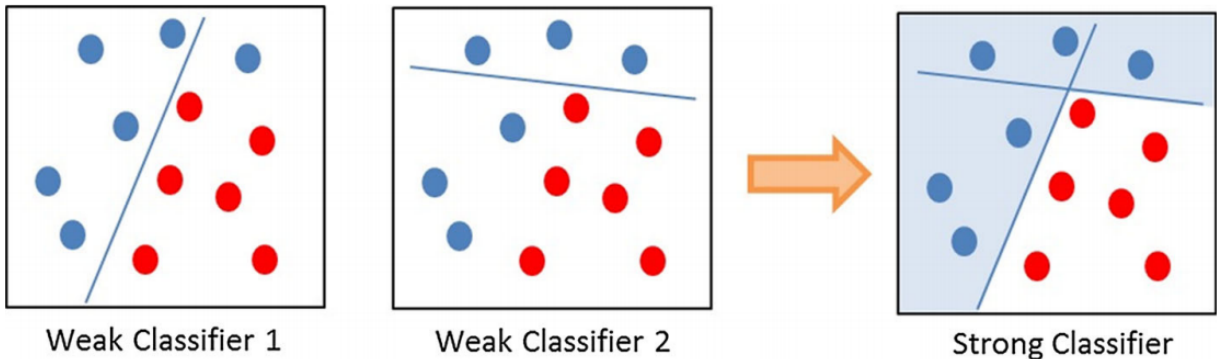


Figure 2.10.5: AdaBoost Method of combining weak learners [141]

## 2.11 Classification using 31 and 16 Channels

In this study, there are 31 electrodes as in actiCAP from Brainvision. The number of the electrodes is  $31 + 1$  reference electrode(Fz) + 1 Ground (GND) electrode. The scalp map and the localization of the electrodes on the head are plotted using the program EEGLAB(Delorme and Makeig, 2004) as in 2.11.1. The classification of EEG data also needed to be tested using a reduced set of electrodes. The reduction of the number of electrodes from 31 to 16 has been made by eliminating the side electrodes which contain more artifacts, and at the same time keeping the electrodes that cover the movement related Brodmann areas as in 1.9.3 and as explained in the brain lobes 1.9.2, and in the Brodmann areas 1.9.3. the most important brodmann areas for this study are 1,2,3,4,5,6,7, and the 8 areas, which can be covered by using 16 electrodes. These areas are the most movement related areas. The 16 EEG electrodes localization on the scalp are plotted in 2.11.2.

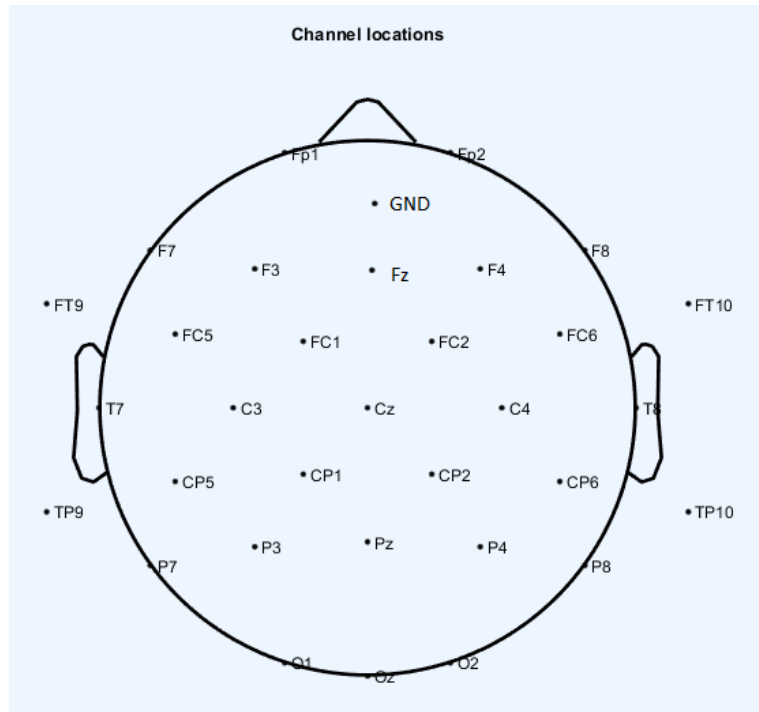


Figure 2.11.1: 31 electrodes localization plotted in EEGLAB(Delorme and Makeig, 2004)

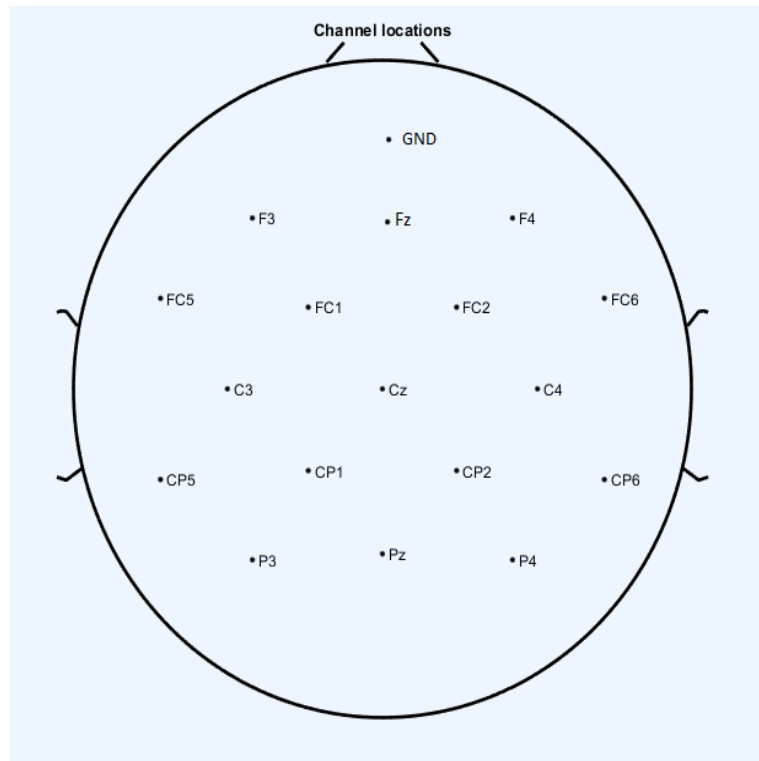


Figure 2.11.2: 16 electrodes localization plotted in EEGLAB(Delorme and Makeig, 2004)

### 3 Results

In this section, the results of filtering, ICA artifacts removal, epoching, binary classification (gestures vs. grasps, precision vs. power grasps), multi-grasps classification, and cross-subjects classification (gestures vs. grasps, power vs. precision grasps) will be plotted and explained.

#### 3.1 Filtering

The average accuracy results using frequency-window approach over all 11 subjects with TS for gestures vs. grasps can be found in 3.1.1. It is clear that the classification accuracy in 3.1.1 is almost the same (about 80%) for all frequency-windows.

The average accuracy results using frequency-window approach over all 11 subjects with TS for precision vs. power grasps in 3.1.2 is also almost the same (about 60%) for all frequency-windows.

In the average accuracy results using frequency-window approach over all 11 subjects for the multi-classification case in 3.1.3, there is classification accuracy increase by increasing the frequency and especially above 66.83Hz. According to the results in 3.1.3, the multi-classification for 20 different grasps will be done not only without band-pass filtering but also for the range (66.83-100)Hz. That is why, multi-classification will be tested for the complete range (0.5-100)Hz and for the range (66.83-100)Hz for S1, S2, and S10, by bandpass filtering the EEG data for the frequency range (66.83-100)Hz.

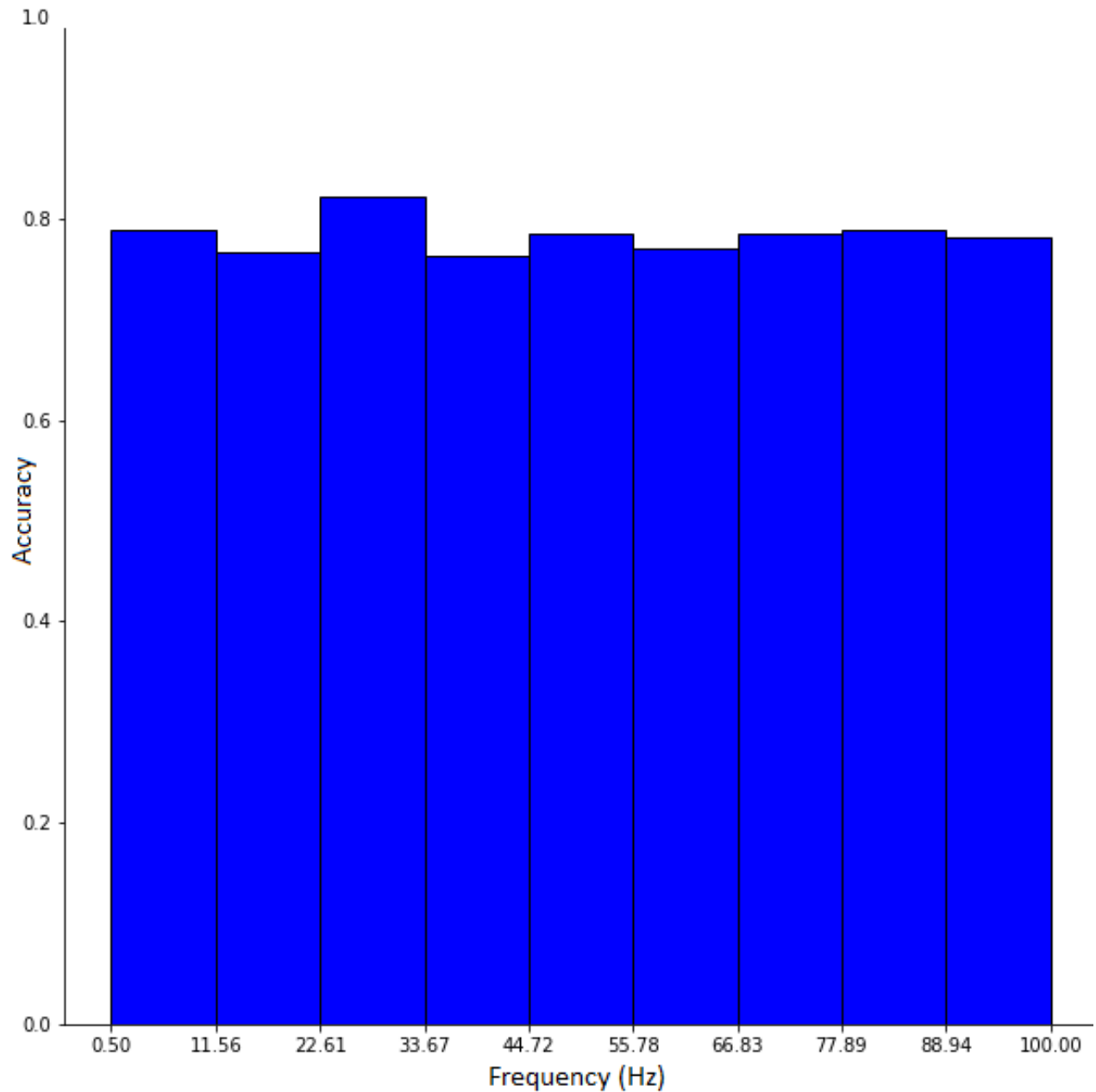


Figure 3.1.1: Average gestures vs. grasps classification results for different frequency-intervals

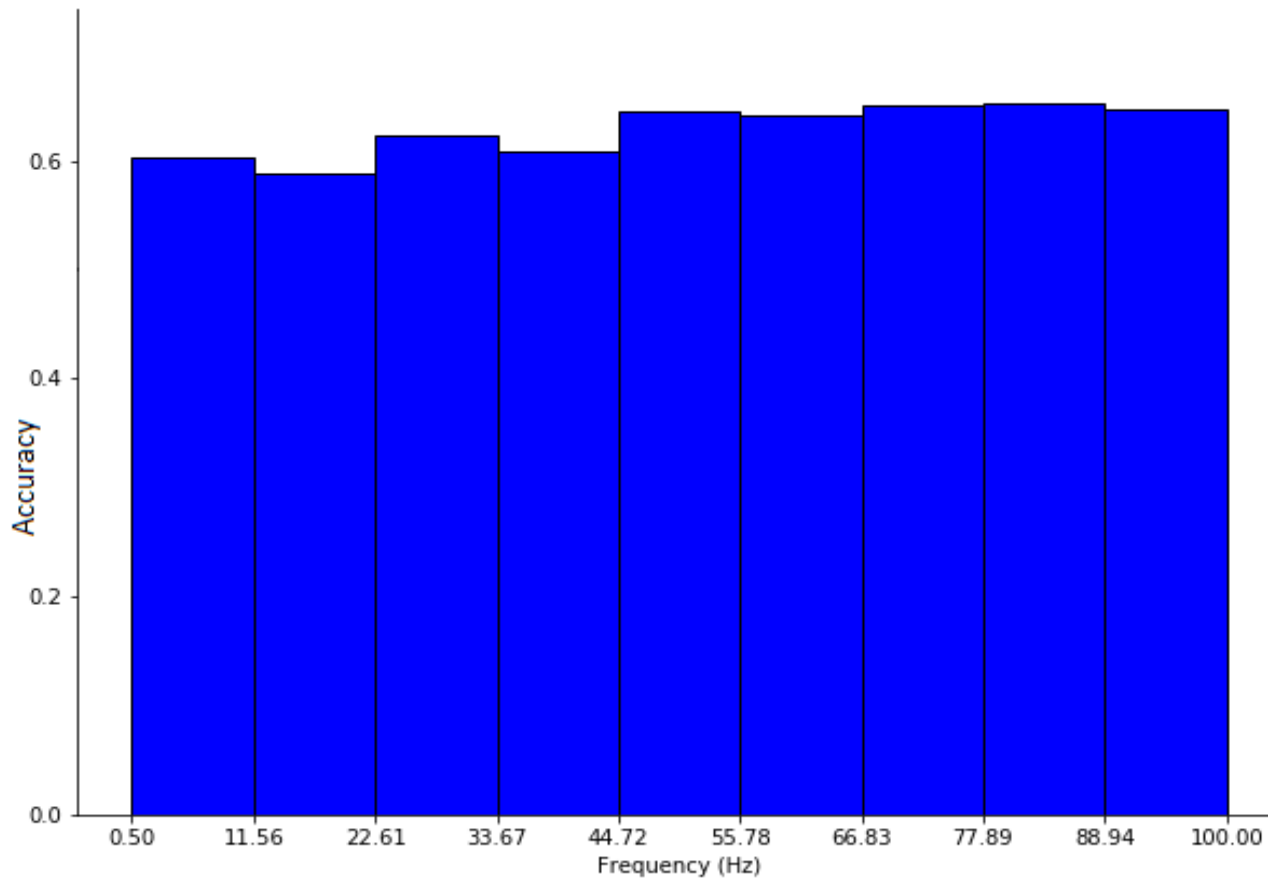


Figure 3.1.2: Average precision vs. power grasps classification results for different frequency-intervals

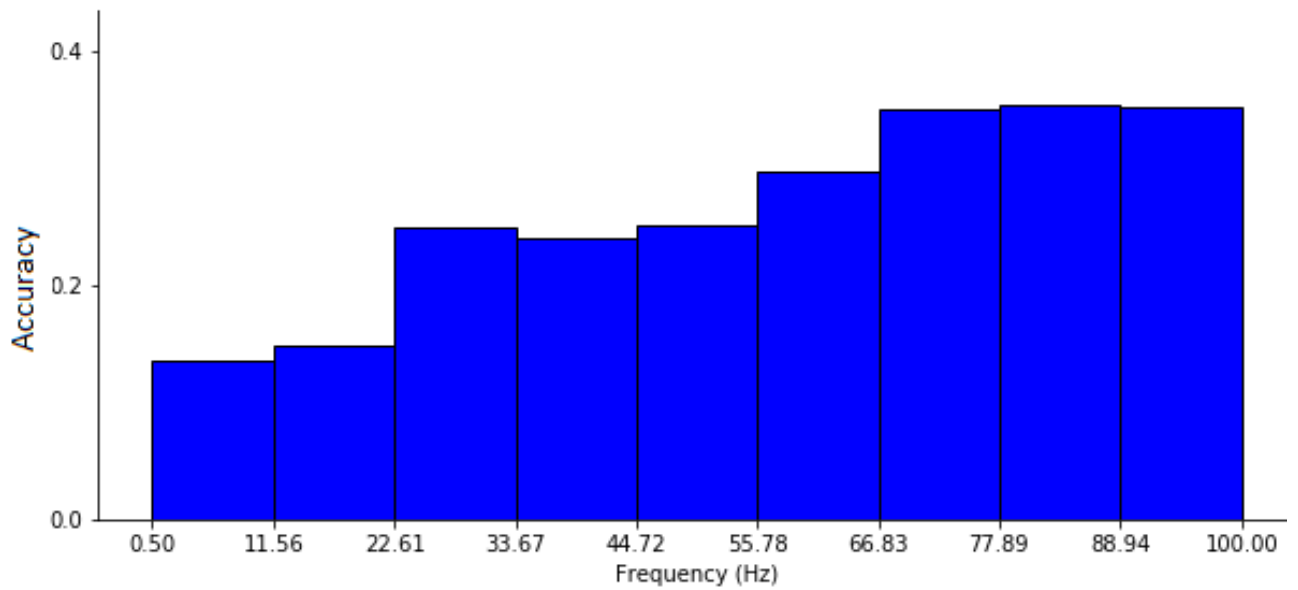


Figure 3.1.3: Average multi-grasps classification results for different frequency-intervals

### 3.2 EEG Artifacts Removal

To remove EEG artifacts, the ICA algorithm in EEGLAB(Delorme and Makeig, 2004) has been used. As an example for this, the ICA components for S1 in 3.2.1 are plotted. In 3.2.1, there are 31 components. The colors of the plotted components range from dark to light blue and from dark to light red. The red color indicates the positivity and the blue color indicates the negativity. The darker the red color in an area is, the more positive concentration the area has. The darker the blue color in an area is, the more negative concentration the area has. Either the dark red color, or the dark blue color over a region on the scalp map indicates that this region is more activated than others. The components in 3.2.1, which have been highlighted in red are manually identified as artifacts and will be removed.

In the first removed ICA component of S1 in 3.2.2, the scalp-map in the upper-left corner shows the activated areas in the brain during the execution of a task. There is a high concentration (dark blue color) in the frontal area near the eyes and hence this is a frontal eye artifact [101]. The continuous data in the upper-right corner shows the continuous EEG data before the epoching (The horizontal axis corresponds to time in milli seconds, and the vertical axis corresponds to the trials, where the blue spots show the eye artifacts). The activity power spectrum in the downside of the plot shows the power of the signal with respect to the frequency. The power of this signal is high while the frequency is low, and then by increasing the frequency, the power of the signal decreases.

In 3.2.3, there is high concentration (dark red color on the right side), and hence this seems to be muscle artifact [101]. Also here, the power of the signal is high while the frequency is low (below about 5Hz).

In 3.2.4, there is also a horizontal eye artifact to the right (the subject looks right). In this artifact, the power of the signal is also high while the frequency is low.

The artifact in 3.2.5 is a bilateral with opposite sign artifact for the eye horizontal eye movement [144]. The power of this signal is also high while the frequency is low.

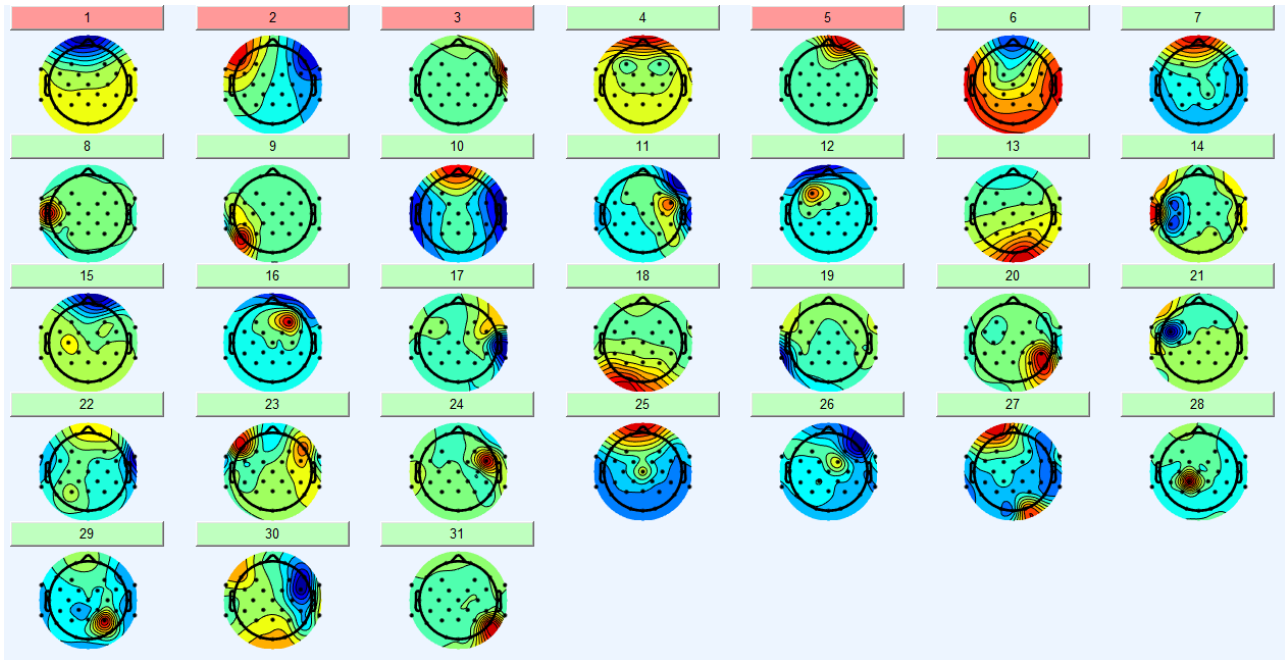


Figure 3.2.1: ICA components of S1 plotted in EEGLAB(Delorme and Makeig, 2004)

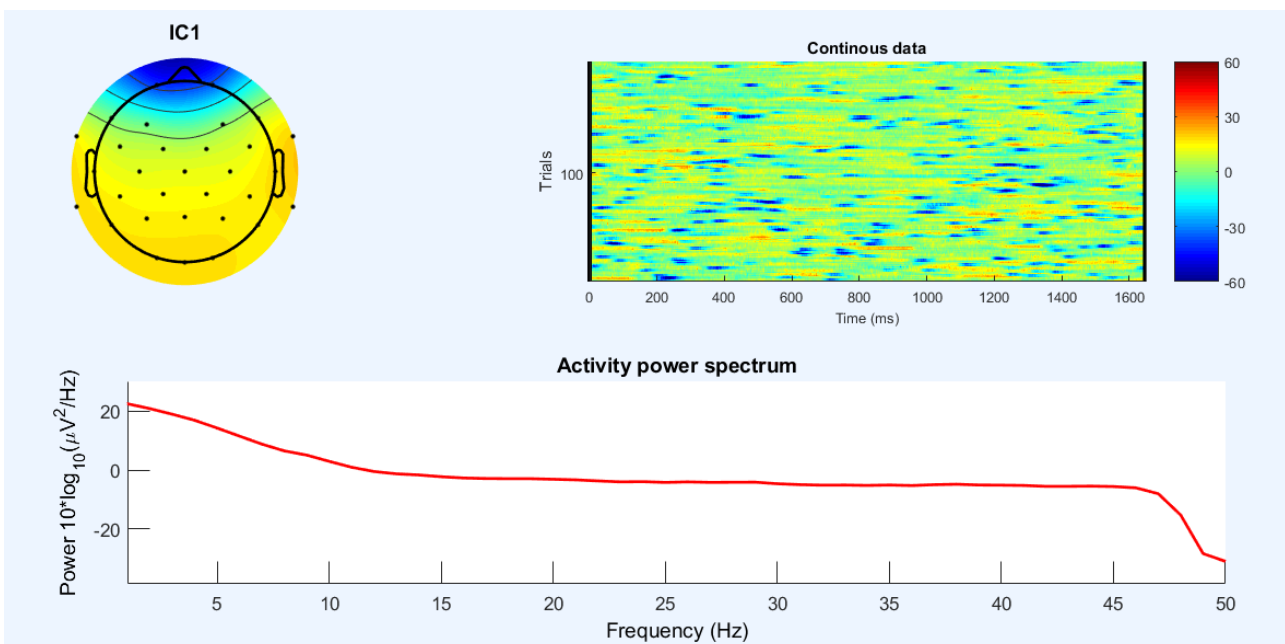


Figure 3.2.2: S1 ICA component as eye artifact plotted in EEGLAB(Delorme and Makeig, 2004)

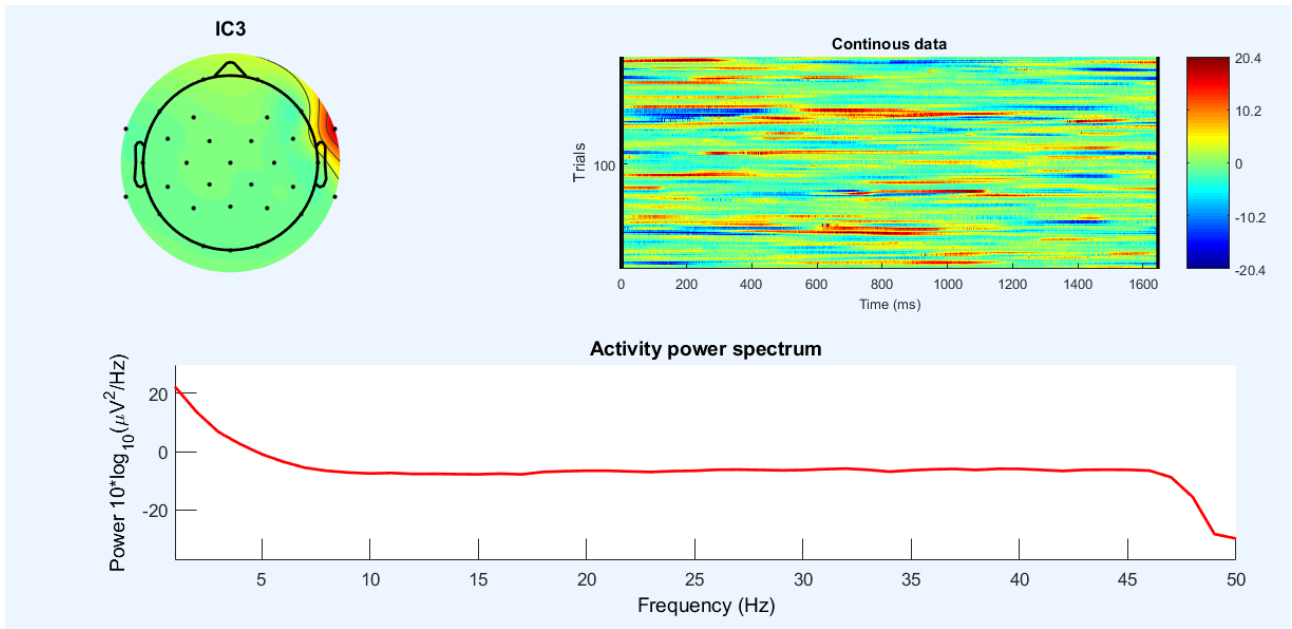


Figure 3.2.3: S1 ICA component muscle artifact plotted in EEGLAB(Delorme and Makeig, 2004)

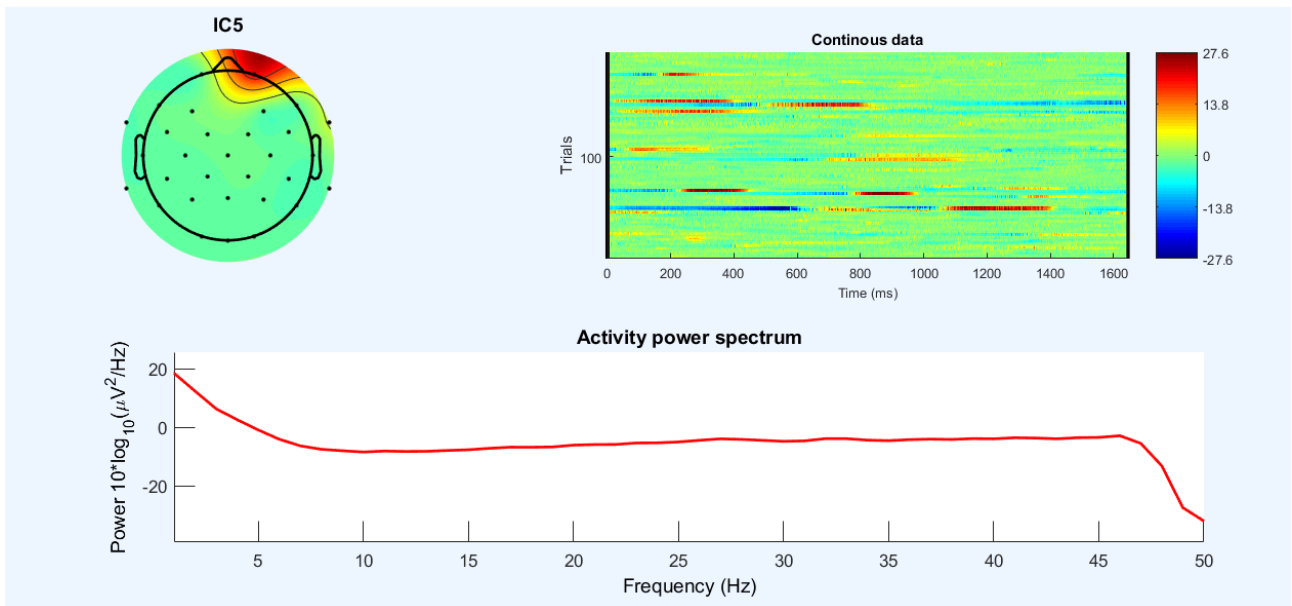


Figure 3.2.4: S1 ICA component as eye artifact plotted in EEGLAB(Delorme and Makeig, 2004)

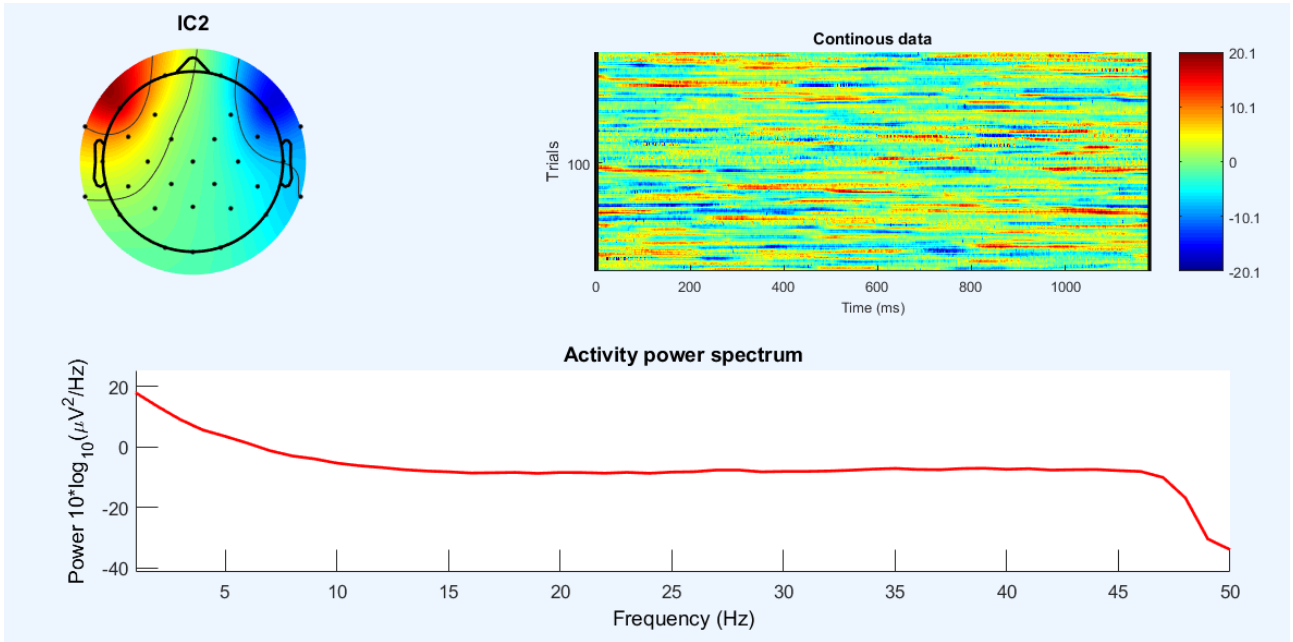


Figure 3.2.5: S1 ICA component as eye artifact plotted in EEGLAB(Delorme and Makeig, 2004)

Another example for the ICA components is the ICA components in S2 as in 3.2.6. There are more motoric components and less artifacts components in S2 as in the 6th, 7th, 9th, 11th, 14th, 20th, 21th, 23th, 24th, 26th, 27th, 28th, 29th, 30th, and 31th Components. The 2nd component in S2 as in 3.2.6 is also bilateral with opposite sign artifacts for the eye horizontal eye movement [144]. All the 4th, 5th, 8th, 10th, 12th, 15th, 16th, 17th, 18th, 19th, 22th, and 25th Components of S2 in 3.2.6 contain (eye, face, muscle, and neck) artifacts.

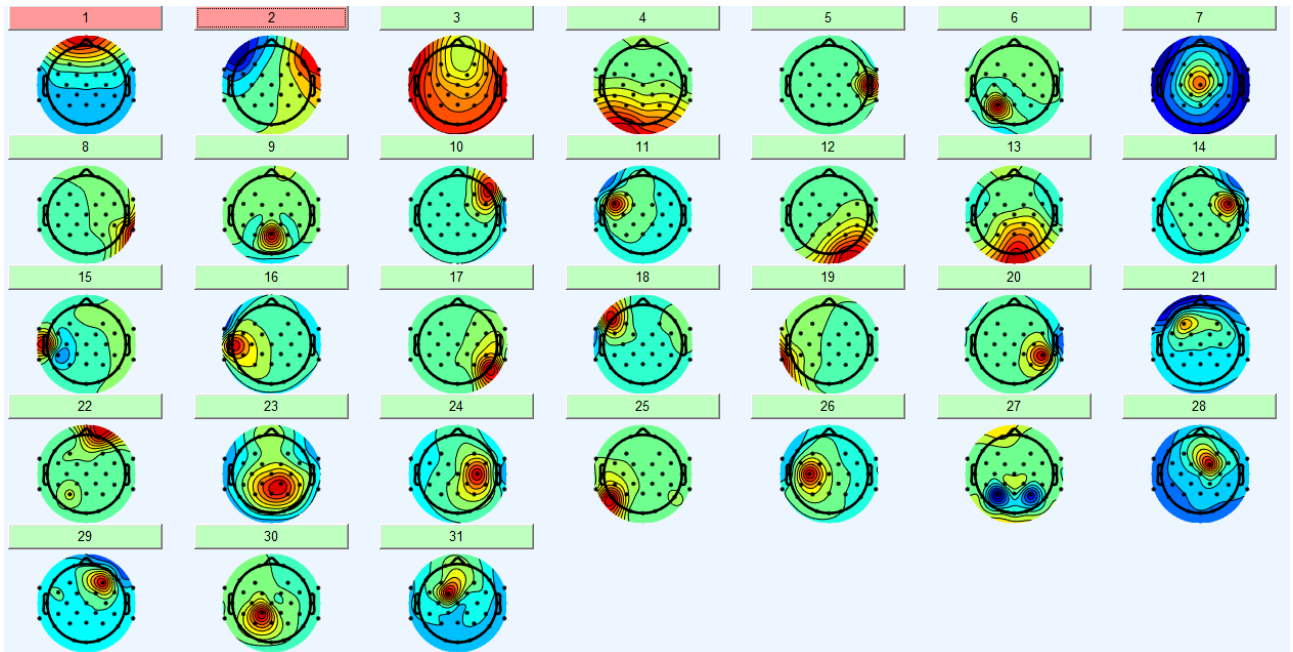


Figure 3.2.6: ICA components for S2 plotted in EEGLAB(Delorme, Makeig, 2004)

### 3.3 Epoching

By using the time-window approach, and to define the suitable epoch, the classification results over all 11 subjects for the gestures vs. grasps using 31 electrodes are found in 3.3.1. This figure 3.3.1 shows the classification accuracy for different time-windows as explained in this study in 2.5. The time windows in 3.3.1 are as following:

- 04-03 Start: The time-window-size is 100ms between 400ms and 300ms before the hand movement start event.
- 03-02 Start: The time-window-size is 100ms between 300ms and 200ms before the hand movement start event.
- 02-01 Start: The time-window-size is 100ms between 200ms and 100ms before the hand movement start event.
- 01-0 Start: The time-window-size is 100ms between 100ms before the start event and the start event of the hand movement.
- Start 0-01: The time-window-size is 100ms between the start event and 100ms after the start event of the hand movement.
- Start 01-02: The time-window-size is 100ms between 100ms and 200ms after the hand movement start event.
- Start 02-03: The time-window-size is 100ms between 200ms and 300ms after the hand movement start event.
- Start 03-04: The time-window-size is 100ms between 300ms and 400ms after the hand movement start event.
- Start 04-05: The time-window-size is 100ms between 400ms and 500ms after the hand movement start event.
- Start 05-06: The time window-size is 100ms between 500ms and 600ms after the hand movement start event.

The classification results in 3.3.1 show, that the highest classification accuracy is in the time-window (04-03 Start) and the time-window (Start 01-02). There is a bit increase in the accuracy time-windows after the (Start 01-02), however the goal in this study is rather to predict the type of the movement and possibly before the subject starts doing a gesture or a grasp. That is why, the epoch size will be chosen to be between 400ms before and 200ms after the start event of the hand movement.

The average classification results over all 11 subjects of gestures vs. grasps by using 16 electrodes in 3.3.2 show also the same as explained in the case of gestures vs. grasps using 31 electrodes, that the highest classification accuracy is in the time-window (04-03 Start) and the time-window (Start 01-02). That is why, the epoch size will be also chosen to be between 400ms before and 200ms after the start event of the hand movement.

The average classification results over all 11 subjects for the precision vs. power grasps are found in 3.3.3. The best classification results can be found in the range between the time-window (04-03 Start) and the time-window (Start 02-03). According to this, the epoch for the case of precision vs. power grasps will be chosen to be between 400ms before and 300ms after the start event of the hand movement.

The average classification results over all 11 subjects for the precision vs. power grasps using 16 electrodes are found in 3.3.4. Here also, the best classification results can be found in the range between the time-window (04-03 Start) and the time-window (Start 02-03). According to this, the epoch for the case of precision vs. power grasps using 16 electrodes will be also chosen to be between 400ms before and 300ms after the start event of the hand movement 3.3.4.

The multi-classification results for S2 are found in 3.3.5. Here, the classification results are the best for the time-window (02-01 Start) and also the time-window (Start 02-03). According to this, the epoch in the multi-classification case for S2 will be chosen to be 200ms before and 300ms after the start event of the hand movement.

The multi-classification results for S10 are found in 3.3.6. Here, the classification results are also the best for the time-window (02-01 Start) and also the time-window (Start 02-03). According to this, the epoch in the multi-classification case for S10 will be chosen to be 200ms before and 300ms after the start event of the hand movement.

The multi-classification results for S1 are found in 3.3.7. Here, the classification results are bad (less than 20% for all time-windows) in comparison with the ones in S2 (more than 45%) and S10 (more than 35%). The multi-classification results of S1 will be analyzed in this study and compared with the multi-classification results from S2 and S10. The epoching will be also taken the same as in S2 and S10 to compare the results correctly. The epoch in the multi-classification case for S1 will be also chosen to be 200ms before and 300ms after the start event of the hand movement.

It is important to mention, that all the other multi-classification results of other subjects in the epoching step were not better than the ones in S10, and that the best multi-classification results in the epoching step were in S2. That is why, in the classification step, only S2, S10, and S1 will be analyzed.

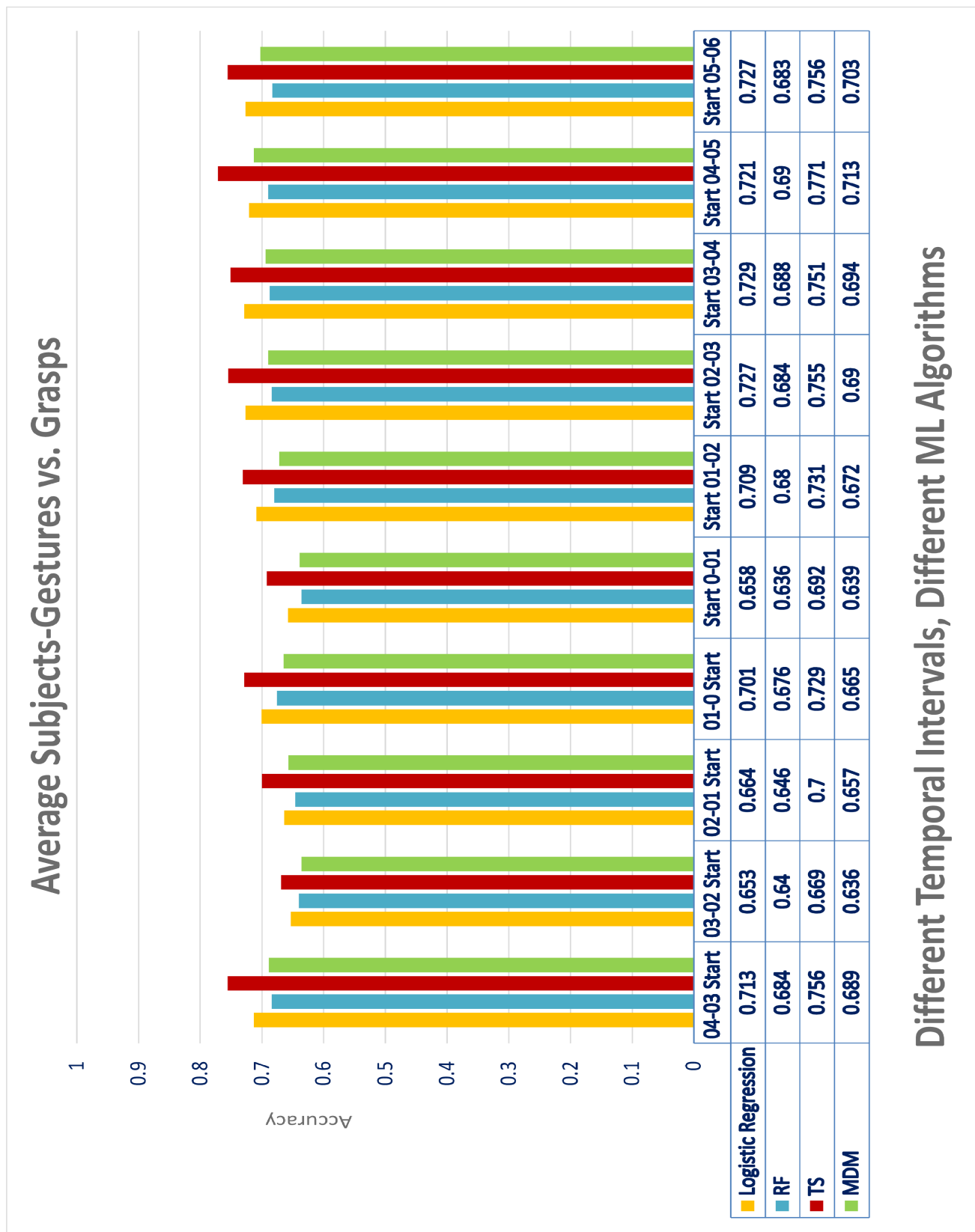


Figure 3.3.1: Average gestures vs. grasps classification results for different time intervals using LogReg, RF, TS, and MDM

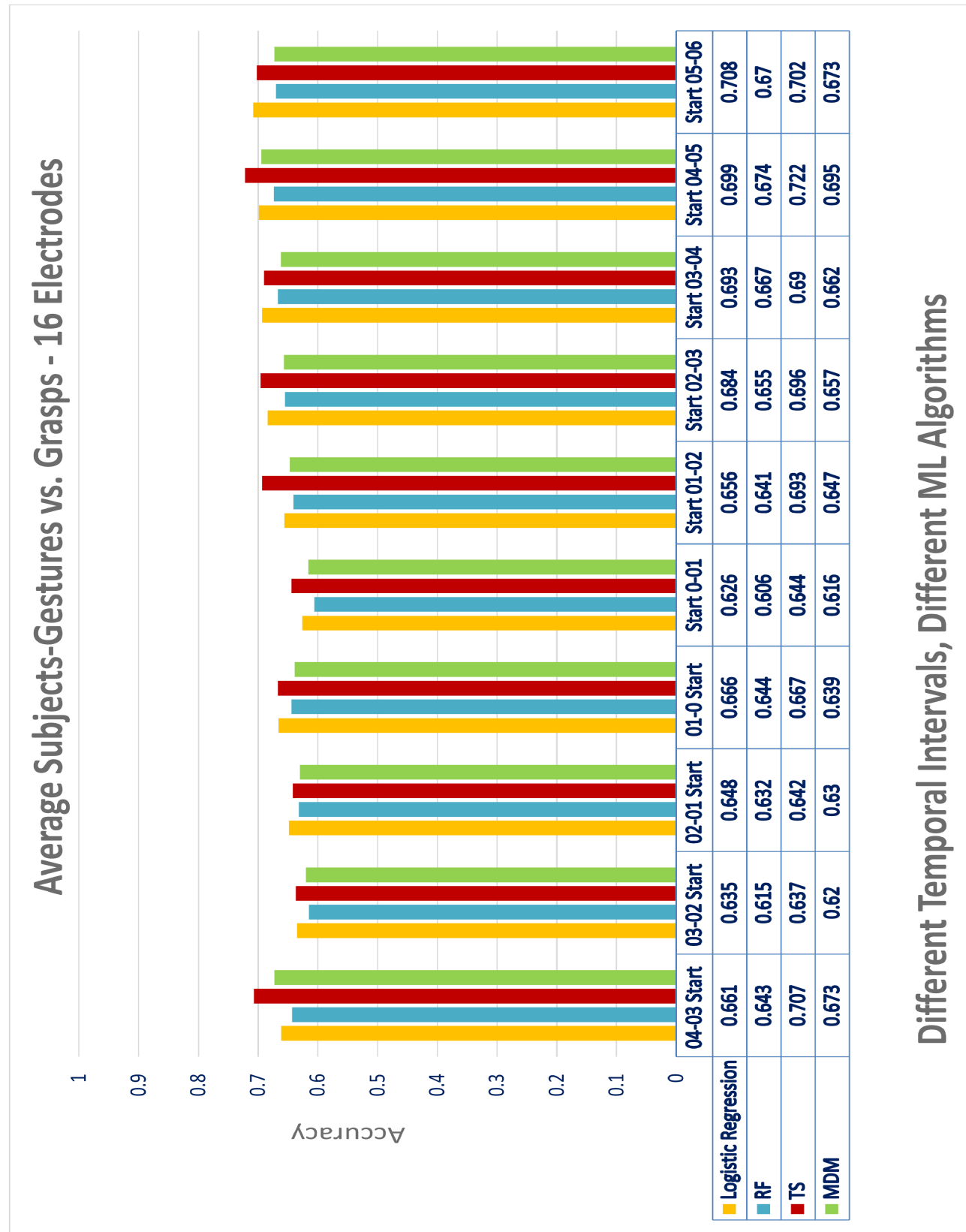


Figure 3.3.2: Average gestures vs. grasps classification results for different time intervals using LogReg, RF, TS, and MDM in the case of using only 16 electrodes



Figure 3.3.3: Average power vs. precision grasps classification results for different time intervals using LogReg, RF, TS, and MDM

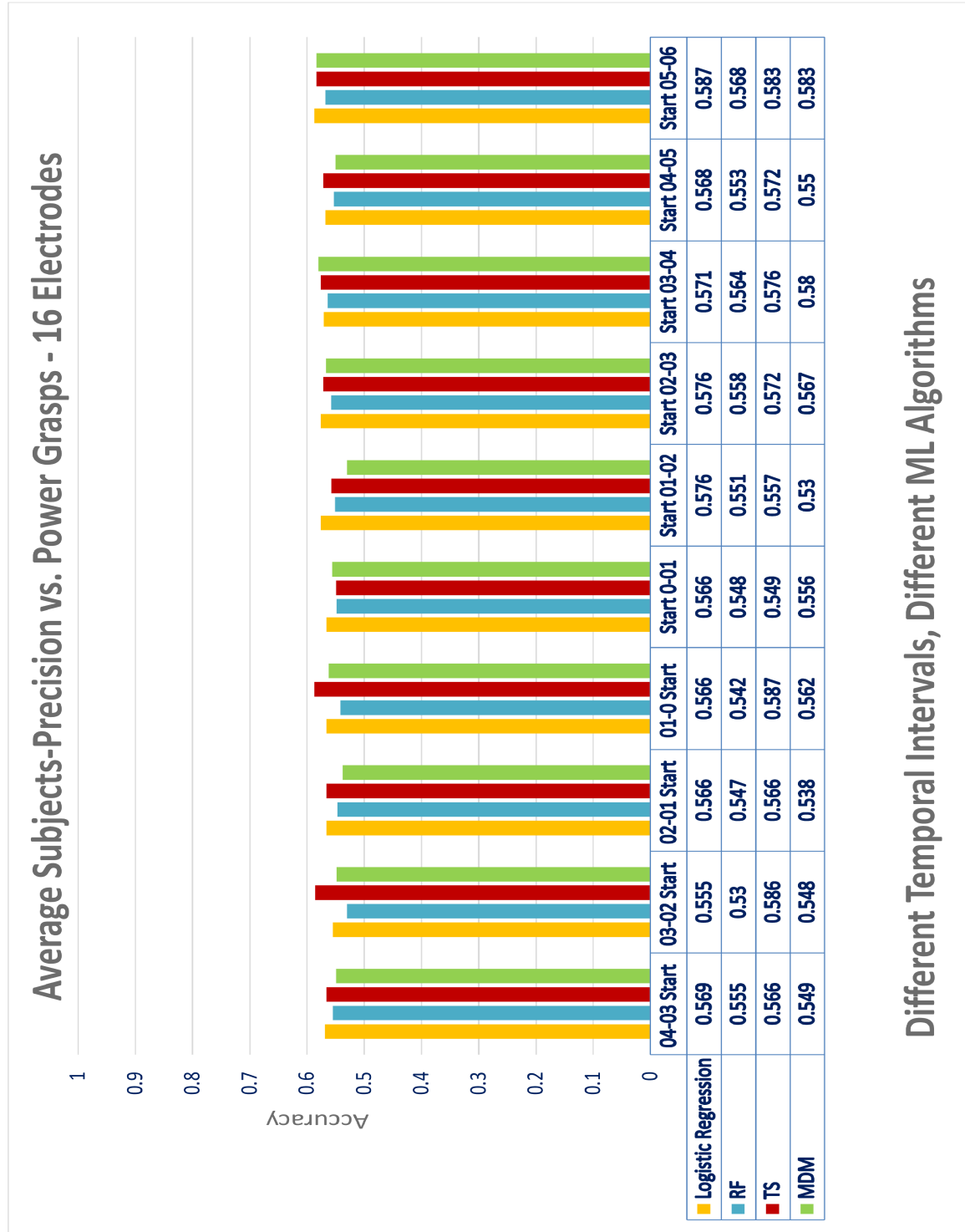


Figure 3.3.4: Average precision vs. power grasps classification results for different time intervals using LogReg, RF, TS, and MDM in the case of using only 16 electrodes

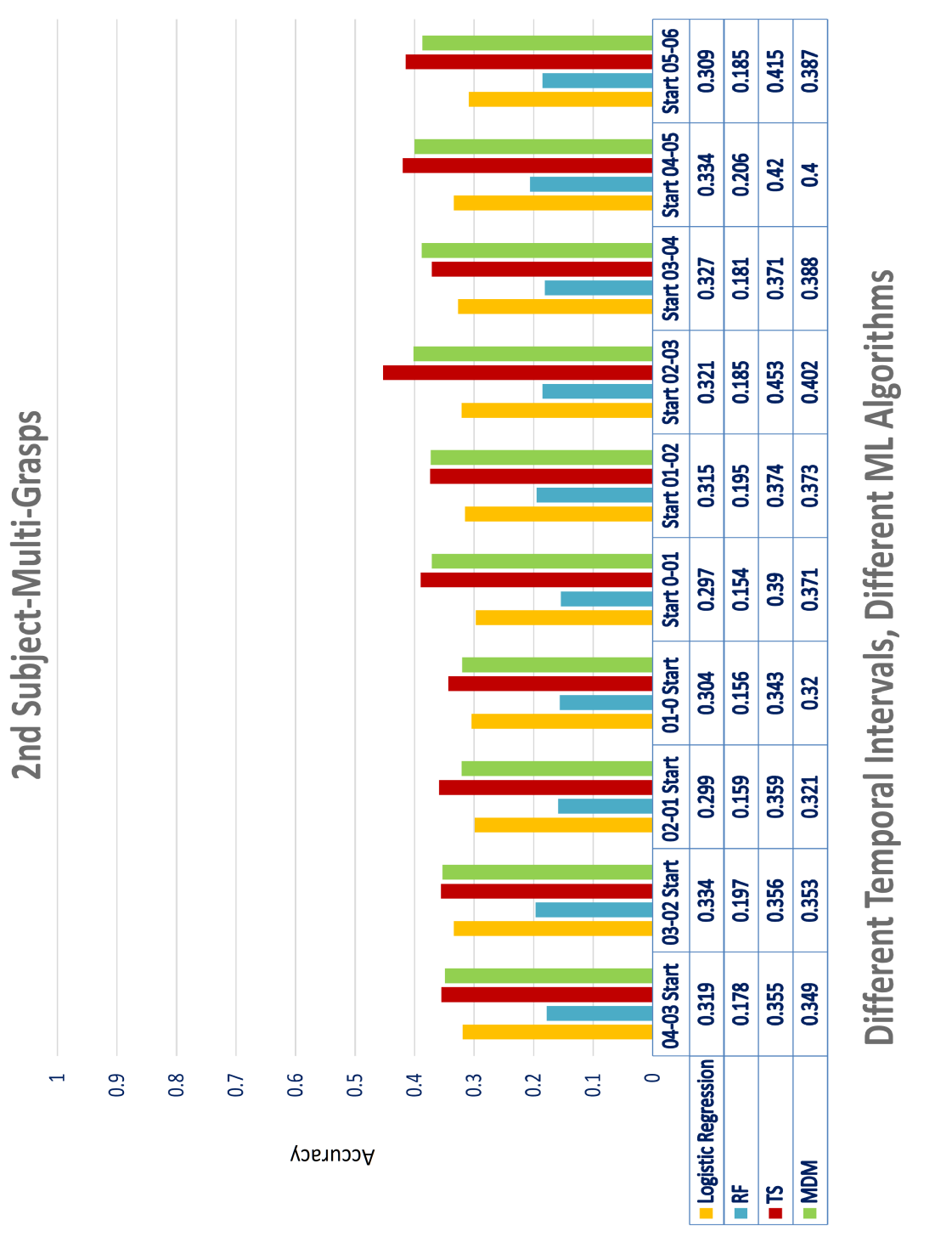


Figure 3.3.5: S2 multi-classification results for different time intervals using LogReg, RF, TS, and MDM

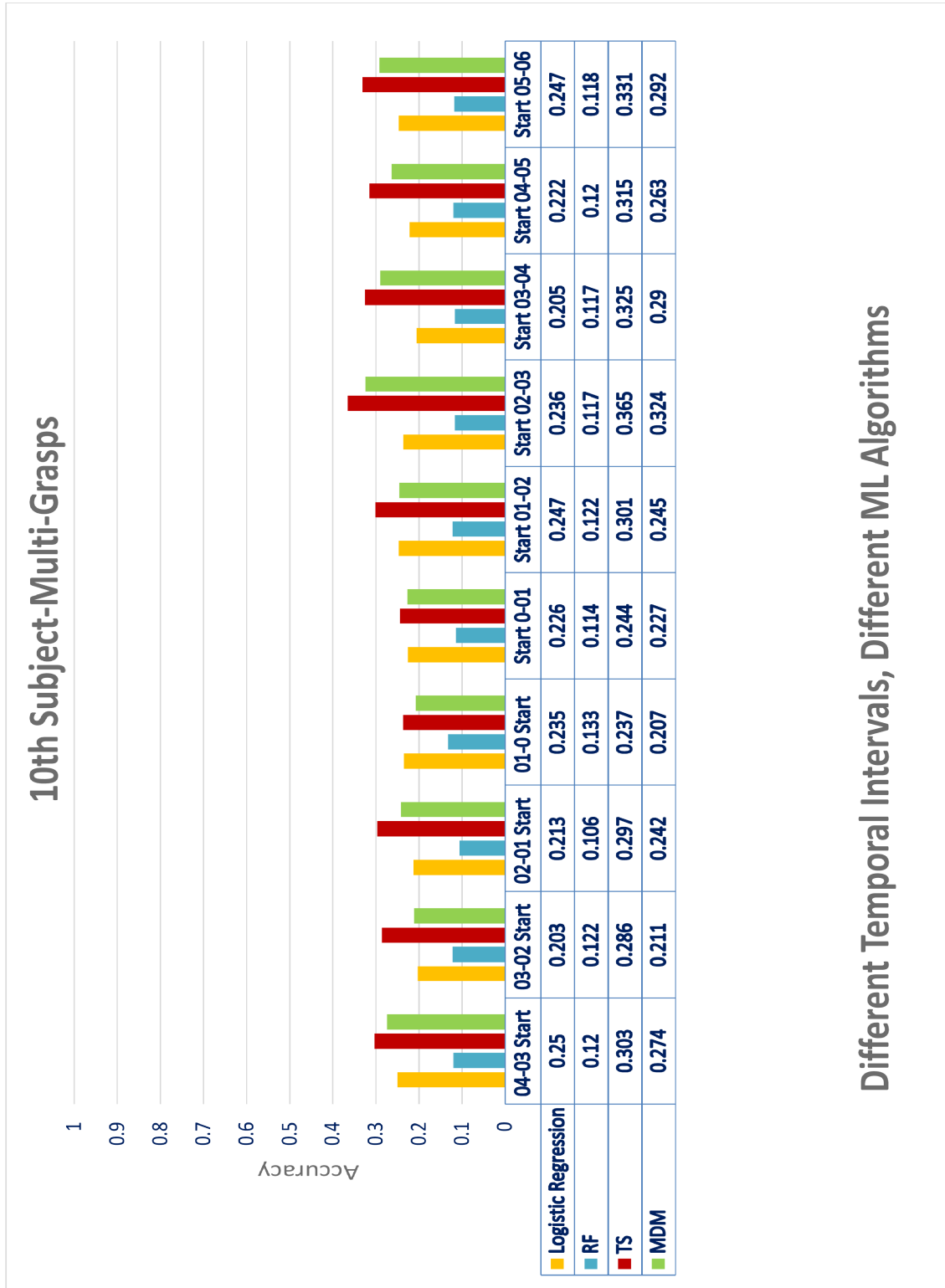
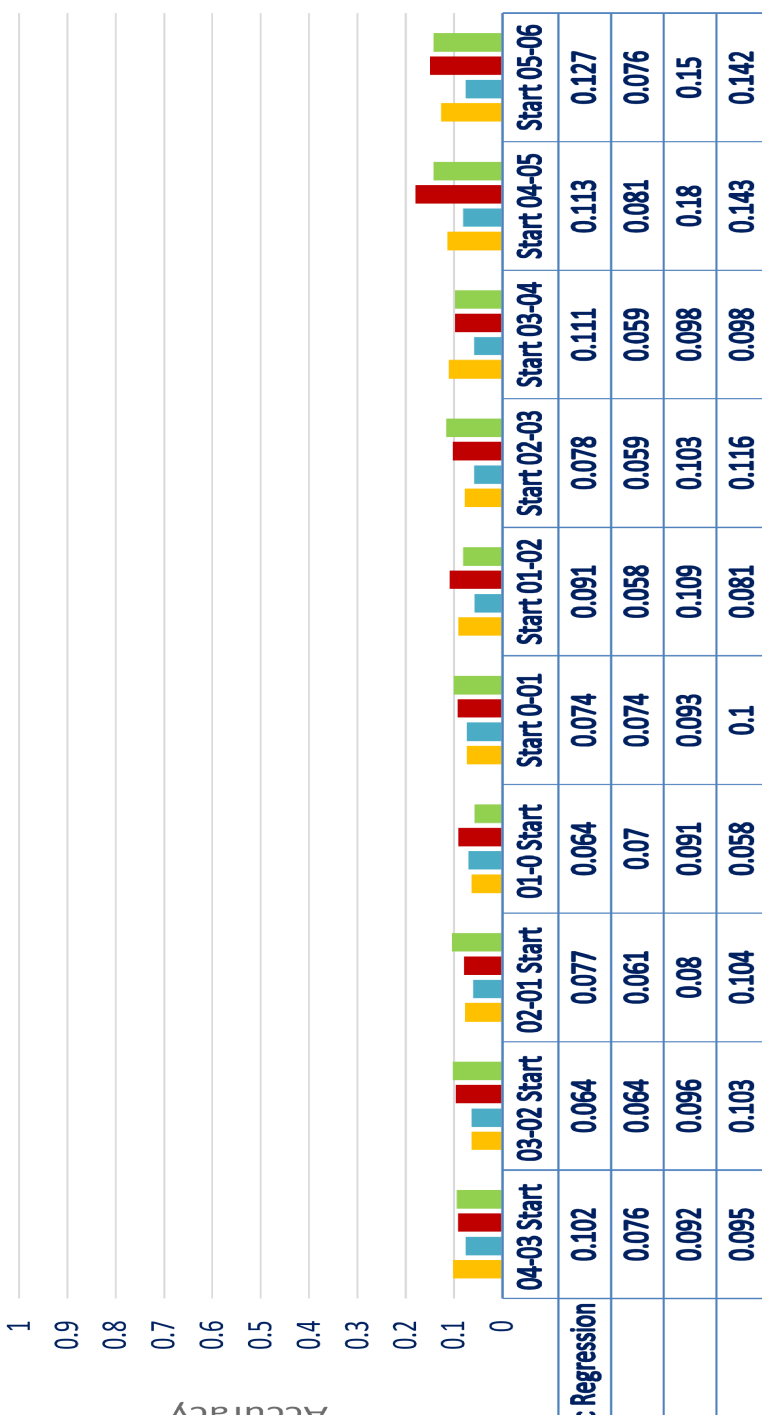


Figure 3.3.6: S10 multi-classification results for different time intervals using LogReg, RF, TS, and MDM

## 1st Subject-Multi-Grasps



Different Temporal Intervals, Different ML Algorithms

Figure 3.3.7: S1 multi-classification results for different time intervals using LogReg, RF, TS, and MDM

## 3.4 Binary Classification of Individual Subjects

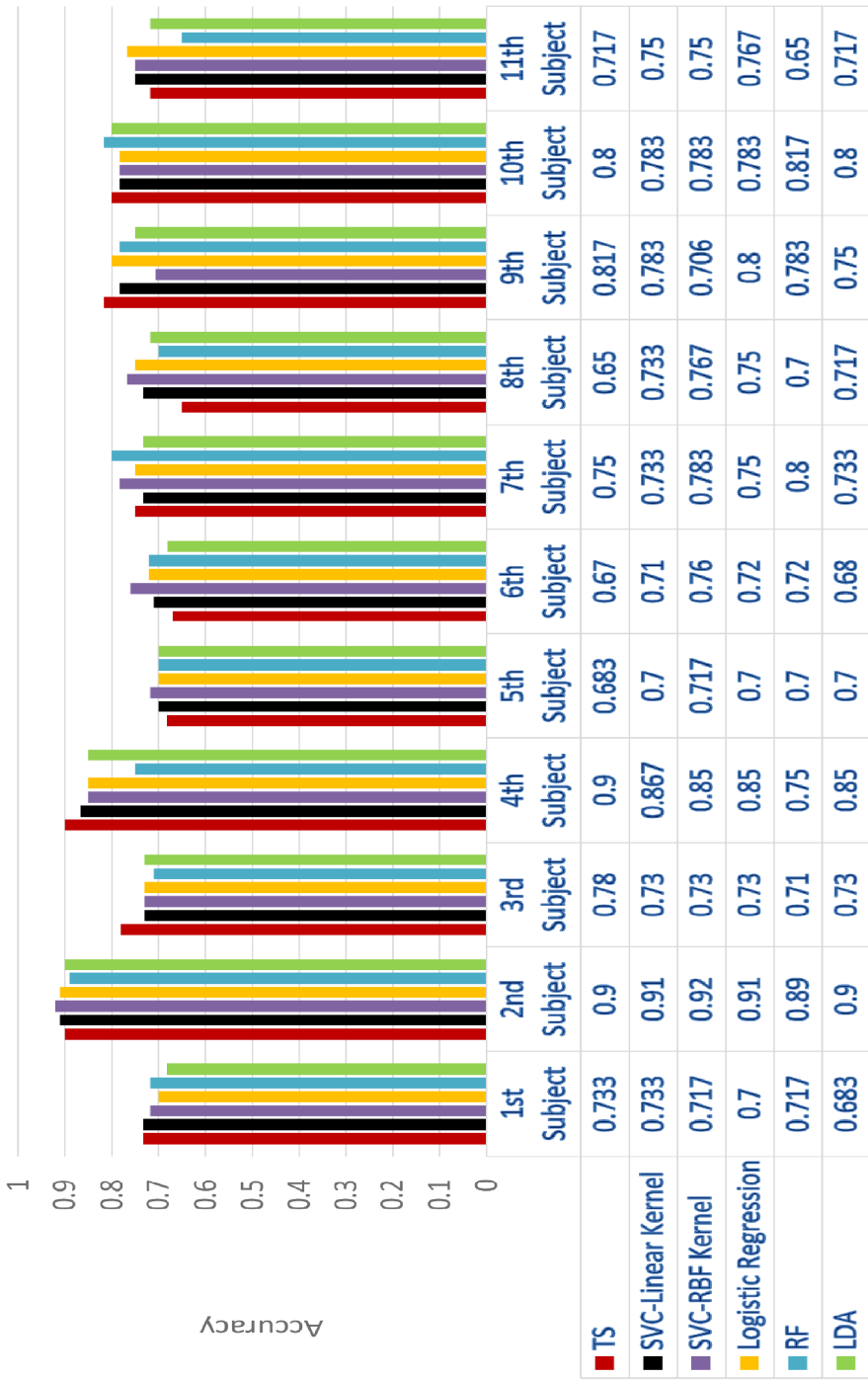
In this section, the classification results by using machine learning methods (CSP, and TS) will be plotted and explained.

### 3.4.1 Classification Results for Gestures vs. Grasps

After defining the best suitable time-interval for the three classification types: gestures vs. grasps (400ms before and 200ms after hand movement start), a new classification has been made on the new time interval for all subjects using 31 and 16 electrodes. In the classification results for the gestures vs. grasps case for all 11 subjects in 3.4.1, the best results are of S2, and S4. The best classification result of S2 is with the classifier SVC with RBF kernel: 92% by using 30 CSP filters, with  $C=1000$ , and  $\gamma=0.001$ . The classification result of S2 using SVC with linear kernel is 91% using 20 CSP filters with  $C=1$ . The classification result of S2 using LogReg is also 91% using 40 CSP filters with  $C=1000$ . The classification with LDA was not as good as the other algorithms almost in all subjects. The classification result with RF in S2 is 89% using 20 CSP filters and 300 estimators.

The classification results for the gestures vs. grasps case using only 16 electrodes for all 11 subjects in 3.4.2. The classification results in 3.4.2 are the best for S2 and S10. The best classification result for S10 is with the classifier TS: 91.7%, and also with the classifier SVC with RBF kernel: 81.7% by using 3 CSP filters, with  $C=1000$ , and  $\gamma=0.001$ . The classification result for the S2 using SVC with RBF kernel is 85% using 10 CSP filters with  $C=1$  and  $\gamma=0.01$ . And also for S2 the SVC with linear kernel achieved: 84% by using 20 CSP filters with  $C=0.1$ . The classification with LDA was here also not as good as the other algorithms almost in all subjects.

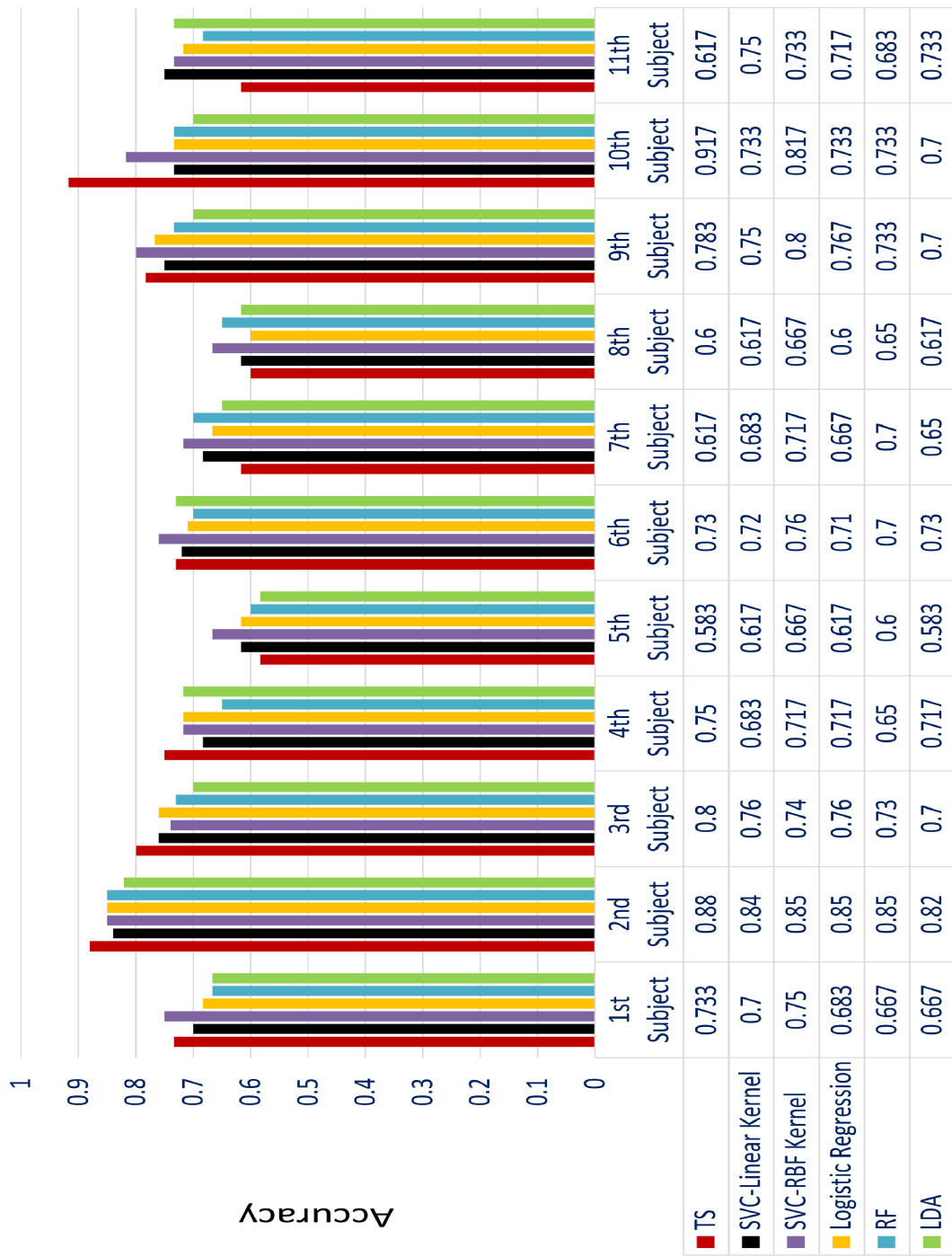
Gestures vs. Grasps Accuracies for all Subjects



Different ML Algorithms for different Subjects

Figure 3.4.1: Comparison between binary classification results (gestures vs. grasps) of individual subjects using TS, SVC with linear kernel, SVC with RBF kernel, LogReg, RF, and LDA

Gestures vs. Grasps for 16 Electrodes



Different ML Algorithms for different Subjects

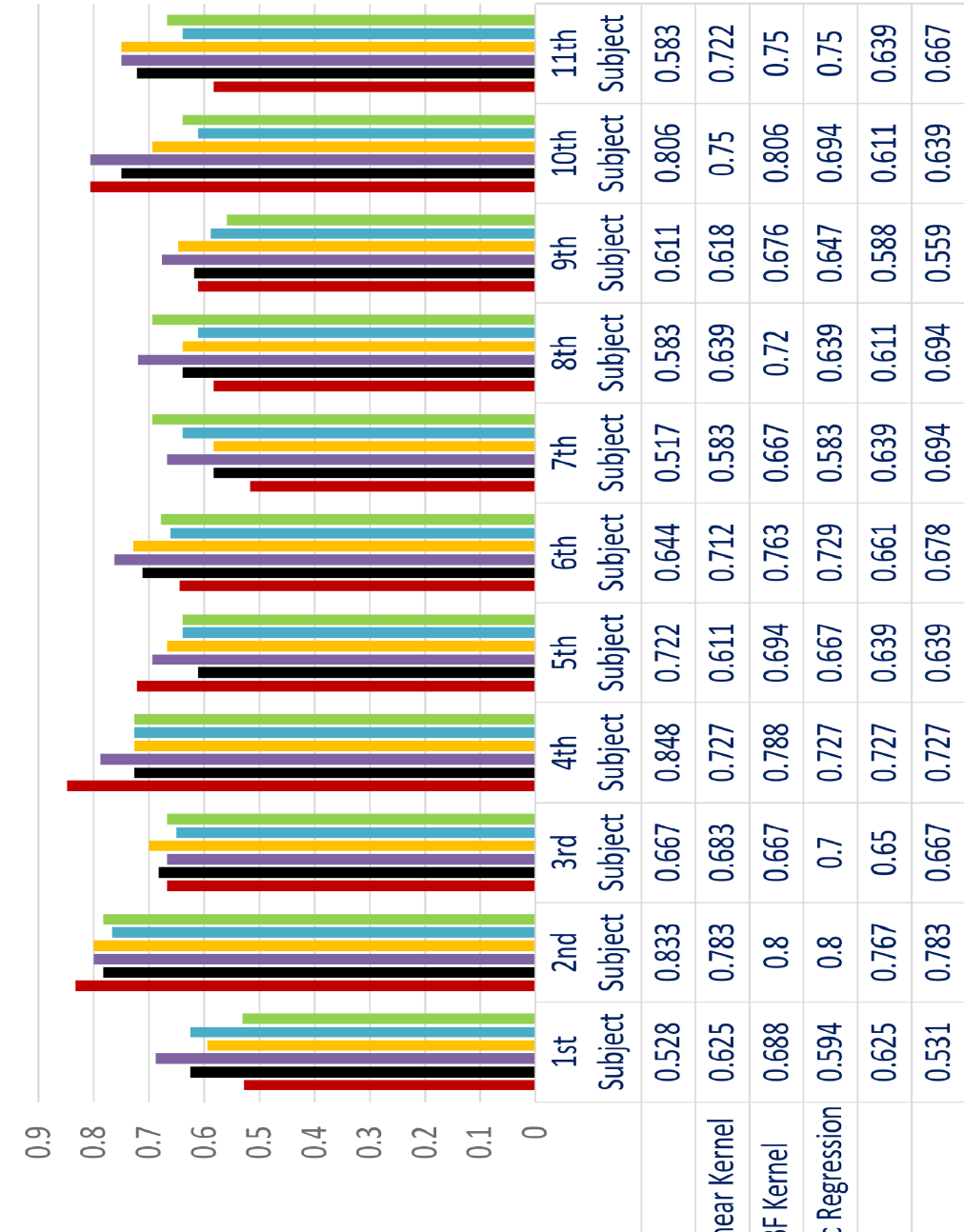
Figure 3.4.2: Comparison between binary classification results (gestures vs. grasps) of individual subjects using TS, SVC with linear kernel, SVC with RBF kernel, LogReg, RF, and LDA in the case of using only 16 electrodes

### 3.4.2 Classification Results for Precision vs. Power Grasps

The classification results for the precision vs. power grasps case for all 11 subjects in 3.4.3. The classification results in 3.4.3 are the best for S2, S4, and S10. The best classification result for S2 is with the classifier TS: 83.3%, and also with the classifier SVC with RBF kernel: 80% by using 20 CSP filters, with  $C=100$ , and  $\gamma=0.1$ , and also with LogReg classifier: 80% using 30 CSP filters with  $C=1$ . The best classification result for S4 is with the TS classifier: 84.8%. SVC with RBF kernel in S4 could achieve: 78.8% using 10 CSP filters with  $C=10^{+8}$  and  $\gamma=10^{-8}$ . In S10, TS could achieve the best classification results: 80.6%, and also SVC with RBF kernel for S10 could achieve: 80.6% using 40 CSP filters with  $C=10^{+8}$  and  $\gamma=10^{-8}$ .

The classification results for the precision vs. power grasps using only 16 electrodes for all 11 subjects in 3.4.4. The classification results in 3.4.4 are the best for S2, S4, and S10. The best classification result for S2 is also with the classifier TS: 83.3%. The best classification result for S4 is with SVC with linear kernel: 75.8% using 10 CSP filters with  $C=10^{-1}$ . In S10, SVC with RBF kernel could achieve the best classification result: 83.3% using 20 CSP filters with  $C=10^{+8}$  and  $\gamma=10^{-7}$ .

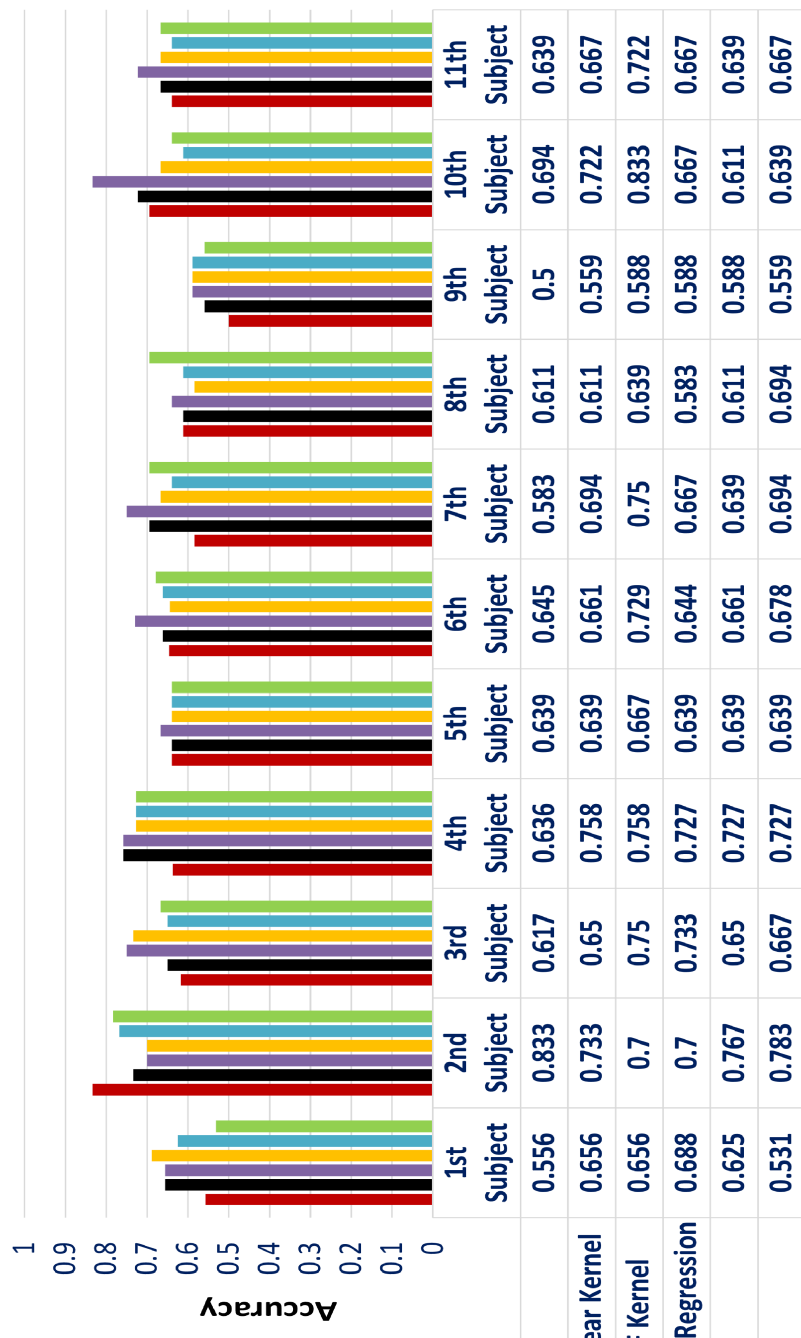
### Precision vs. Power Grasps Binary Classification



Different ML Algorithms for different Subjects

Figure 3.4.3: Comparison between binary classification results (precision vs. power grasps) of individual subjects using TS, SVC with linear kernel, SVC with RBF kernel, LogReg, RF, and LDA

Precision vs. Power Grasps Binary Classification for 16 Electrodes



Different ML Algorithms for different Subjects

Figure 3.4.4: Comparison between binary classification results (precision vs. power grasps) of individual subjects using TS, SVC with linear kernel, SVC with RBF kernel, LogReg, and LDA using only 16 electrodes

### 3.4.3 Comparison between ML Algorithms

For the case of gestures vs. grasps, the classification results comparison between ML algorithms for the case of gestures vs. grasps for individual subjects is plotted in 3.4.5. These classification results are calculated by taking the average over all 11 subjects for every algorithm to evaluate the performance of it. The classification results are almost the same for TS, SVC with linear kernel, SVC with RBF kernel, and also LogReg. The classification accuracies in RF, and LDA were a bit worse than the others. Also, using 16 instead of 31 electrodes caused a drop in the classification accuracy in all algorithms.

For the case of precision vs. power grasps, the classification comparison between ML algorithms for the case of precision vs. power grasps for individual subjects is plotted in 3.4.6. These classification results are calculated by taking the average over all 11 subjects for every algorithm (TS, SVC with RBF kernel, SVC with linear kernel, LogReg, RF, and also LDA) to evaluate the performance of it over all subjects. In the classification results for the case of precision vs. power grasps, the SVC with RBF kernel could clearly outperform the other algorithms with accuracy: 72.9% (31 electrodes) and 70.8% (16 electrodes). The classification accuracies in RF, and LDA were the worst. Also, using 16 instead of 31 electrodes caused a drop in the classification accuracy in all algorithms.

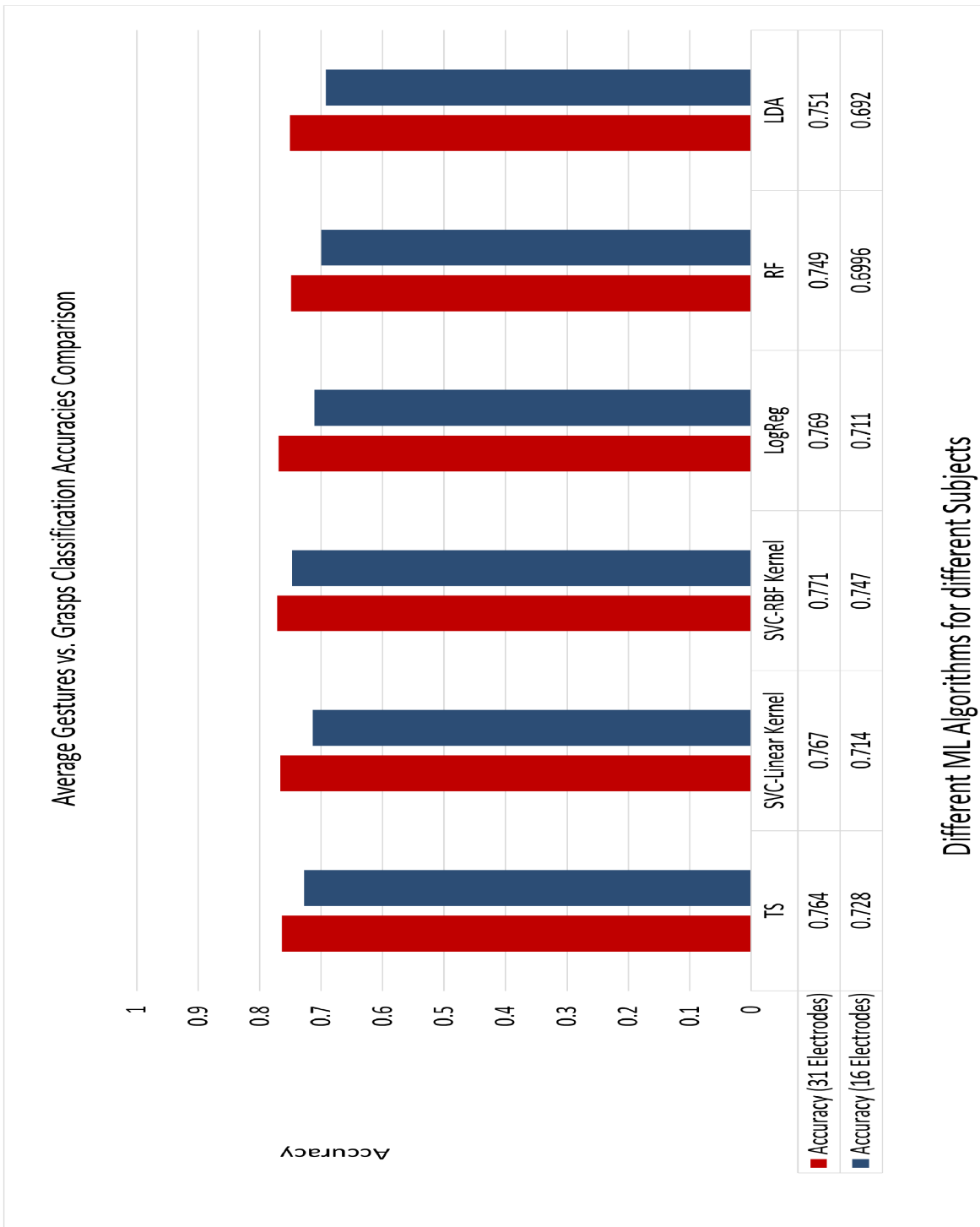


Figure 3.4.5: Comparison between different ML algorithms classification results (gestures vs. grasps) using 31-16 electrodes

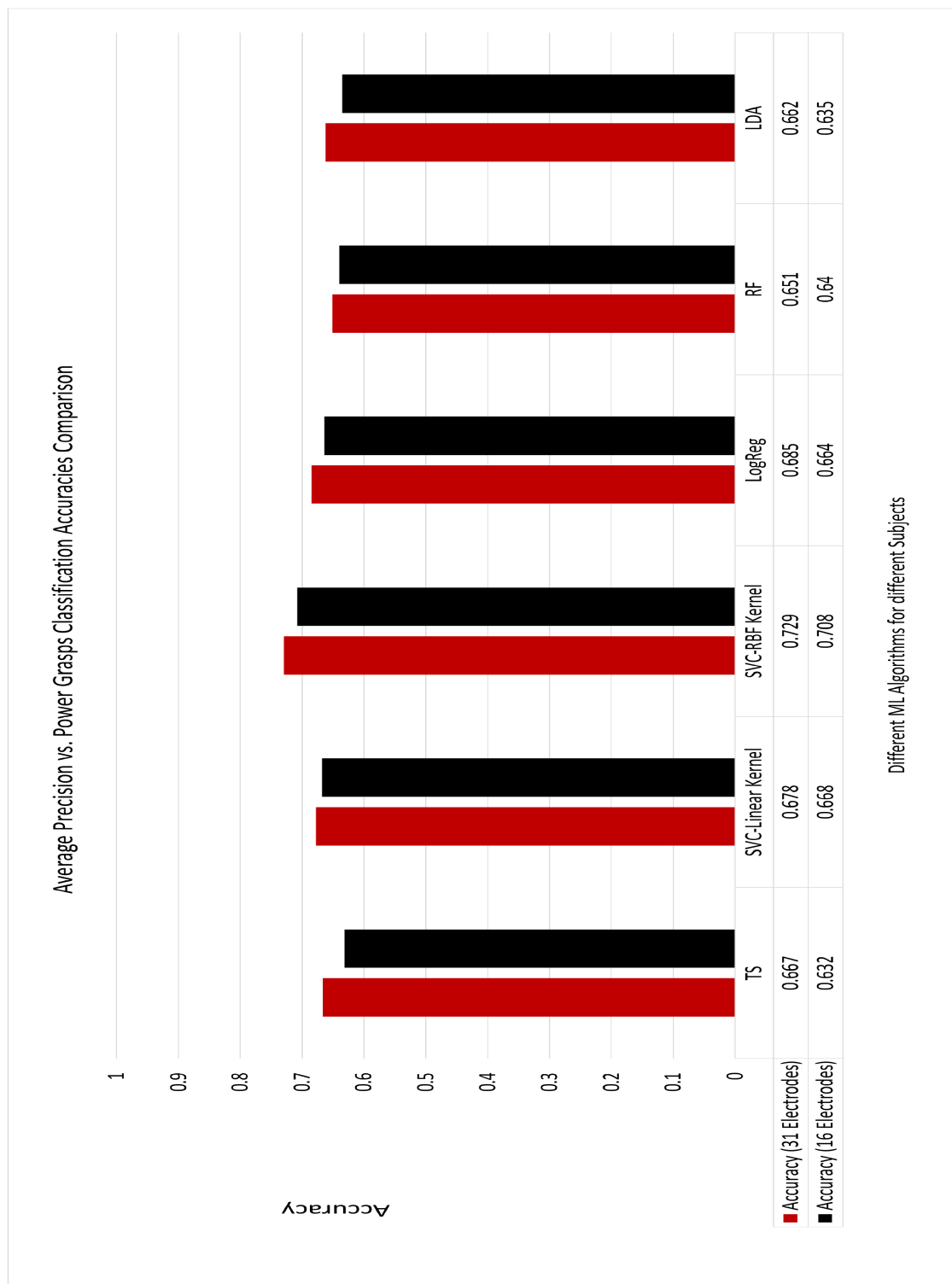


Figure 3.4.6: Comparison between different ML algorithms classification results (precision vs. power grasps) using 31-16 electrodes

### 3.4.4 Common Spatial Pattern

The spatial patterns on the brain of S2 and the change of frequency for two different conditions: gestures, and grasps are shown in 3.4.7. In 3.4.7 on the left side, the scalp map with the regions, that correspond to both conditions (gestures, grasps). Blue corresponds to gestures and red corresponds to grasps. On the right in 3.4.7, the frequency changes for both conditions are plotted. On the right side of the plot, generally the power of the EEG signals in the case of gestures is higher than the case of the grasps.

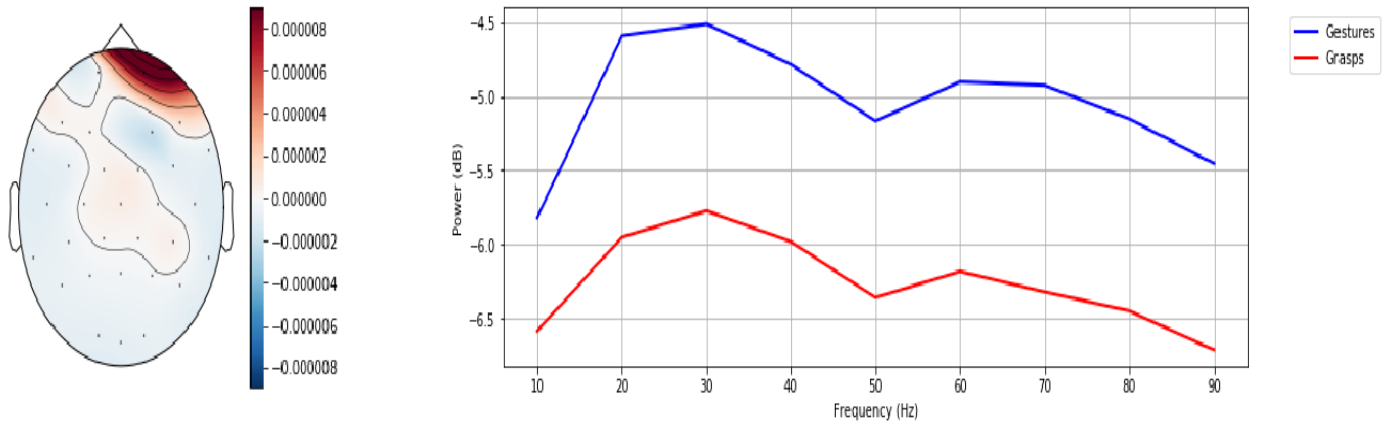


Figure 3.4.7: S2 spatial Patterns Gestures vs. Grasps

The spatial patterns on the brain of S2 and the change of frequency for two different conditions: precision, and power grasps are shown in 3.4.8. On the left side, the scalp map with the regions that correspond to both conditions (precision grasps, and power grasps). Blue corresponds to precision and red corresponds to power grasps. On the right side in 3.4.8, the frequency changes for both conditions are plotted. The regions in red color which correspond to the power grasps are more located on the back of the head, whereas for the precision grasps, the regions in blue color are more located on the left hemisphere and the front of the head. On the right side of the plot, generally the power of the EEG signals in the case of power Grasps is higher than the case of the precision grasps.

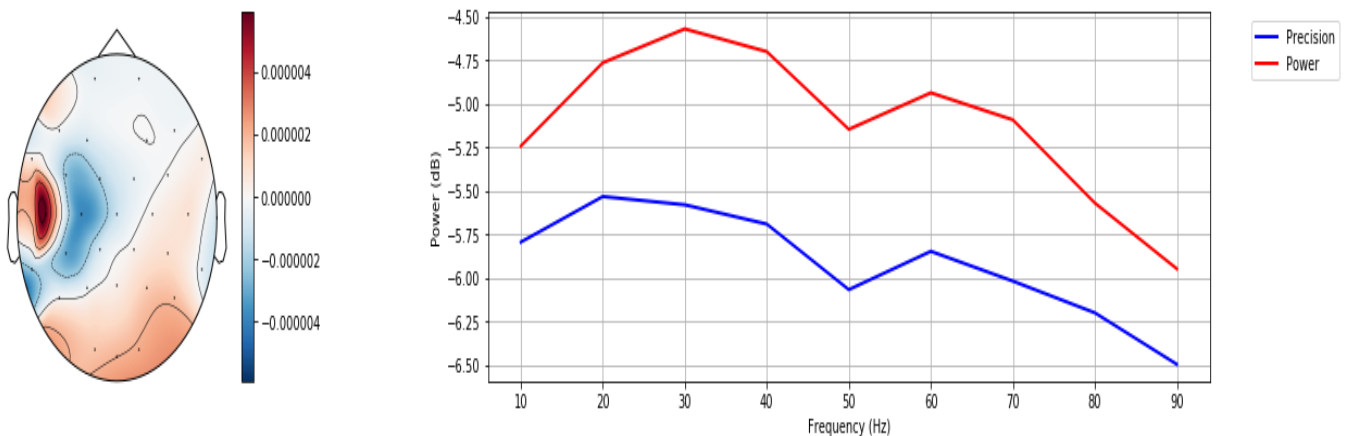


Figure 3.4.8: S2 spatial patterns of precision vs. power grasps

### 3.4.5 Covariance Matrices for Gestures vs. Grasps

In the plotted covariance matrix of S2 for the gestures task in 3.4.9, the covariance between electrodes is shown. The darker the cell is, the higher the covariance between electrodes exists. The main diagonal has lighter squares in comparison with the others. This is because the main diagonal shows the covariance between the same electrodes, and hence the covariance cells should be lighter. Also. There is a strong covariance along FC1, FC2 and also along F4, F3, Cz electrodes.

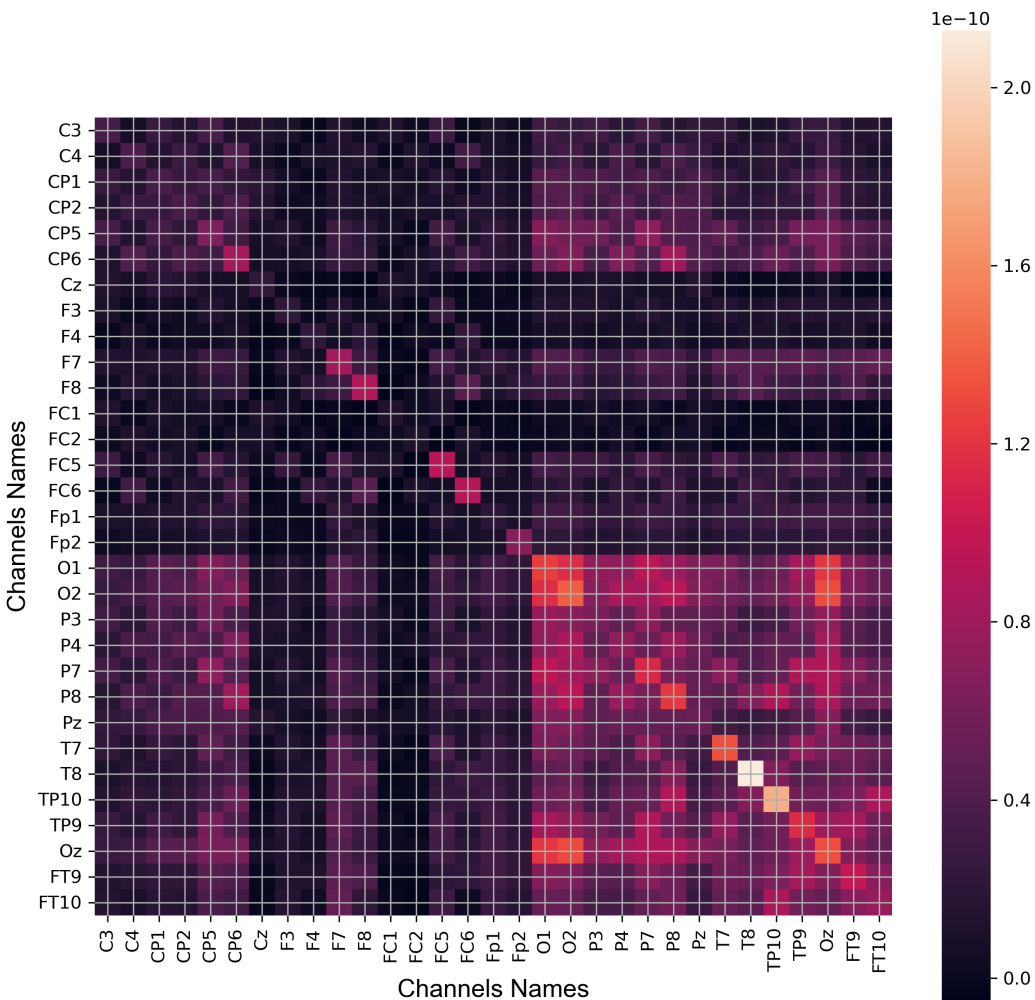


Figure 3.4.9: S2 mean covariance matrix in gestures using pyRiemann package [127]

In the plotted covariance matrix of S2 for the grasps task in 3.4.10, there are more covariances along FC1, FC2 and F4, F3, Cz electrodes. However generally the channels are lighter and especially in the right down side. And also the covariance is less in the cells O1-Pz, O1-P8, O1-P7, O1-P4, O1-P3, O1-O2 and the same for O2.

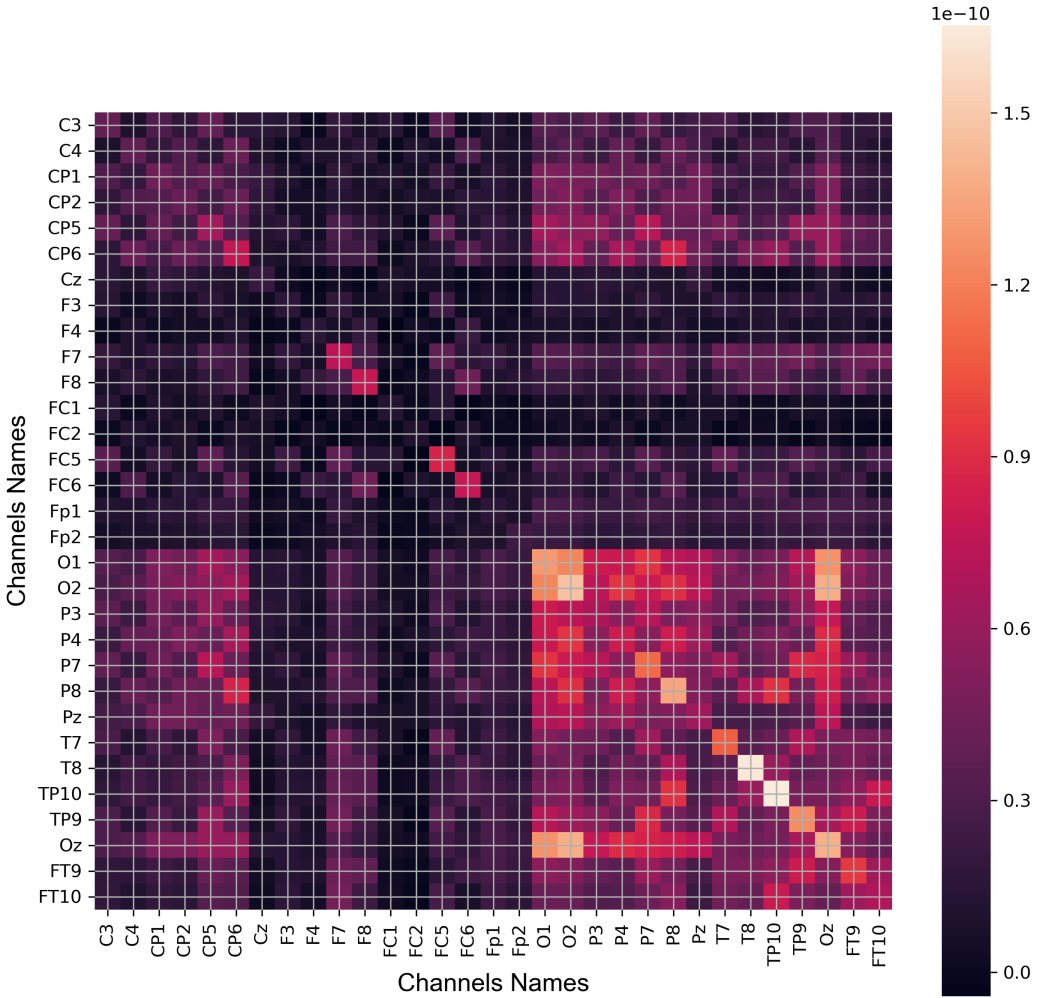


Figure 3.4.10: S2 mean covariance matrix in grasps using pyRiemann package [127]

## 3.5 Multi-Grasps Classification

In this section, the multi-grasps classification results, the confusion matrices, and the covariance matrices for different grasps will be plotted and explained.

### 3.5.1 Multi-Grasps Classification Results

In this study, it has been found, that only S2, and S10 have acceptable multi-classification results as in 3.3.5, and 3.3.6. That is why, only the multi-classification of S2 and S10 will be analyzed and plotted. To make a comparison between the good and the bad classification results, the results of S1 will be also plotted and explained. The multi-classification results using TS for 20 different grasps are: S2: 58% by using 31 electrodes, S2: 29% by using 16 electrodes, S10: 37%

by using 31 electrodes, S10: 17% by using 16 electrodes, S1: 10% by using 31 electrodes, and S1: 12% by using 16 electrodes. According to 3.1.3, and the discussion made in this study in 3.1, the multi-classification-results by bandpass filtering the EEG data for the range (66.83-100)Hz are: S2: 56% (a bit lower) by using 31 electrodes, S2: 29% by using 16 electrodes, S10: 42% (a bit higher) by using 31 electrodes, S10: 17% by using 16 electrodes, S1: 10% by using 31 electrodes, and S1: 12% by using 16 electrodes. Since the classification results by bandpass filtering (66.83-100)Hz the EEG data for S2, S10, and S1 are generally not better than the results by taking the complete frequency range (0-100)Hz, the analysis of the results (confusion matrices, and classification reports) will only be done for the frequency range (0-100)Hz. Also the SVC with RBF kernel was also tested to classify between 20 different grasps of S2 and could surprisingly achieve high results of 57% using GridSearch algorithm with cross validation [111] by applying 20 CSP filters, with  $C=10$  and  $\gamma=0.1$ . Also the SVC with linear kernel was also used to classify between 20 different grasps of S2 and could also achieve: 57% using GridSearchCV [111] using 40 CSP filters, with  $C=1$ . This proves the fact that not only TS, but also CSP methods are suitable for multi-classification [104]. At the end, to test if the CSP methods can outperform TS in the case of multi-classification by using GridSearchCV, the SVC with RBF kernel and the SVC with linear kernel were tested on another subject S1 (31 electrodes) but could not achieve better results, as they only could achieve the same classification accuracy of 10%. That is why for further analysis of the multi-classification, only TS will be used.

### 3.5.2 Confusion Matrices and Classification Reports

The confusion matrix of 20 grasps classification for S2 in 3.5.1 shows where the classifier exactly makes errors. The confusion matrix shows the matching between the predicted Labels (the classes that have been predicted by the TS algorithm from the EEG patterns) and the true labels (the actual labels). From the confusion matrix of S2 in 3.5.1, errors in the confusion matrices are any cells that are located outside the main diagonal. Errors in the confusion matrices indicate that the algorithm has predicted a label when it should be another label (class). Since S2 achieved high classification results as in 3.3.5, the confusion matrix for S2 has a clear main diagonal represented as blue squares along it. These blue squares show exactly the correct matching between true and predicted labels. The darker these squares are, the higher the classification accuracy they have. Any squares out of this main diagonal identify that the classifier made an error. The darker the square outside the main diagonal is, the larger the error the classifier makes. In the classification report of S2 in 3.5.1 of S2, the 20 grasps classification results with TS are listed. Three different classification parameters (Precision, Recall, and F1-Score) are given for every class. These parameters are explained in this study in 2.9.1. "Support" in the classification report of S2 in 3.5.1 means the number of trials in every class. In the last line, the average over all classes of the Precision, Recall, and F1-Score is calculated. According to the confusion matrix of S2 in 3.5.1, the TS achieves a classification accuracy over 20 classes of 58%. Micro average F1-Score here is a measure of the accuracy.

According to the classification report 3.5.1 of S2 in the case of multi-grasps, the best F1-Scores for individual classes of S2 are the Glass: 62%, the Phone: 89%, the Book: 91%, the SmallCup: 77%, the Bat: 71%, the PenDraw: 60%, the DoorKnb: 91%, and the BottleCap: 67%

classes. This is also visible in the confusion matrix of S2 as in 3.5.1, where all the Glass, Phone, Book, SmallCup, Bat, PenDraw, DoorKnb, and the BottleCap are found on the main diagonal as dark cells.

The micro average of precision, recall, and f1-score of S2 in 3.5.1 is the same but it was not the same for individual tasks. In some tasks, the precision (exactness) was high (100%) as in Cap while the f1-score was not (57%) also the recall in Bat was 100% while the f1-score was 71%. The best classes in the classification report of S2 in 3.5.1 are the classes who have the highest precision, recall, and f1-score and they are: Phone, Book, and DoorKnb.

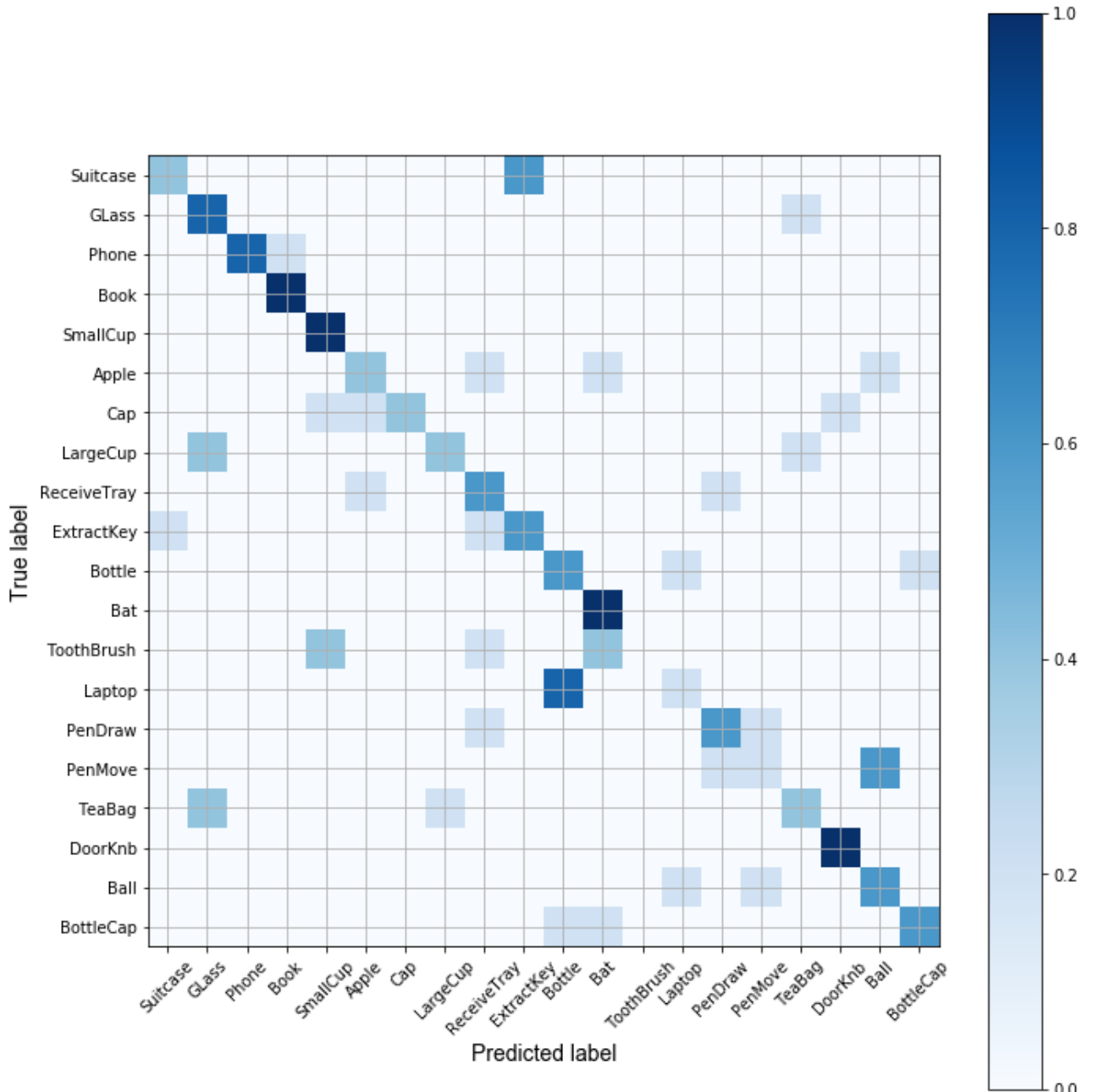


Figure 3.5.1: S2 normalized confusion matrix for 20 grasps

From the confusion matrix of S2 by measuring from only 16 electrodes in 3.5.2, it is clear,

Task	Precision	Recall	F1-Score	Support
Suitcase	0.67	0.4	0.5	5
Glass	0.5	0.8	0.62	5
Phone	1	0.8	0.89	5
Book	0.83	1	0.91	5
SmallCup	0.62	1	0.77	5
Apple	0.5	0.4	0.44	5
Cap	1	0.4	0.57	5
LargeCup	0.67	0.4	0.5	5
ReceiveTray	0.43	0.6	0.5	5
ExtractKey	0.5	0.6	0.55	5
Bottle	0.38	0.6	0.46	5
Bat	0.56	1	0.71	5
Toothbrush	0	0	0	5
Laptop	0.33	0.2	0.25	5
PenDraw	0.6	0.6	0.6	5
PenMove	0.33	0.2	0.25	5
TeaBag	0.5	0.4	0.44	5
DoorKnb	0.83	1	0.91	5
Ball	0.43	0.6	0.5	5
BottleCap	0.75	0.6	0.67	5
micro avg	0.58	0.58	0.58	100

Table 3.5.1: S2 Classification report for 20 grasps

that in the case of only measuring from 16 electrodes there are more errors. These new errors are due to the missing neuro information which resulted from the missing electrodes.

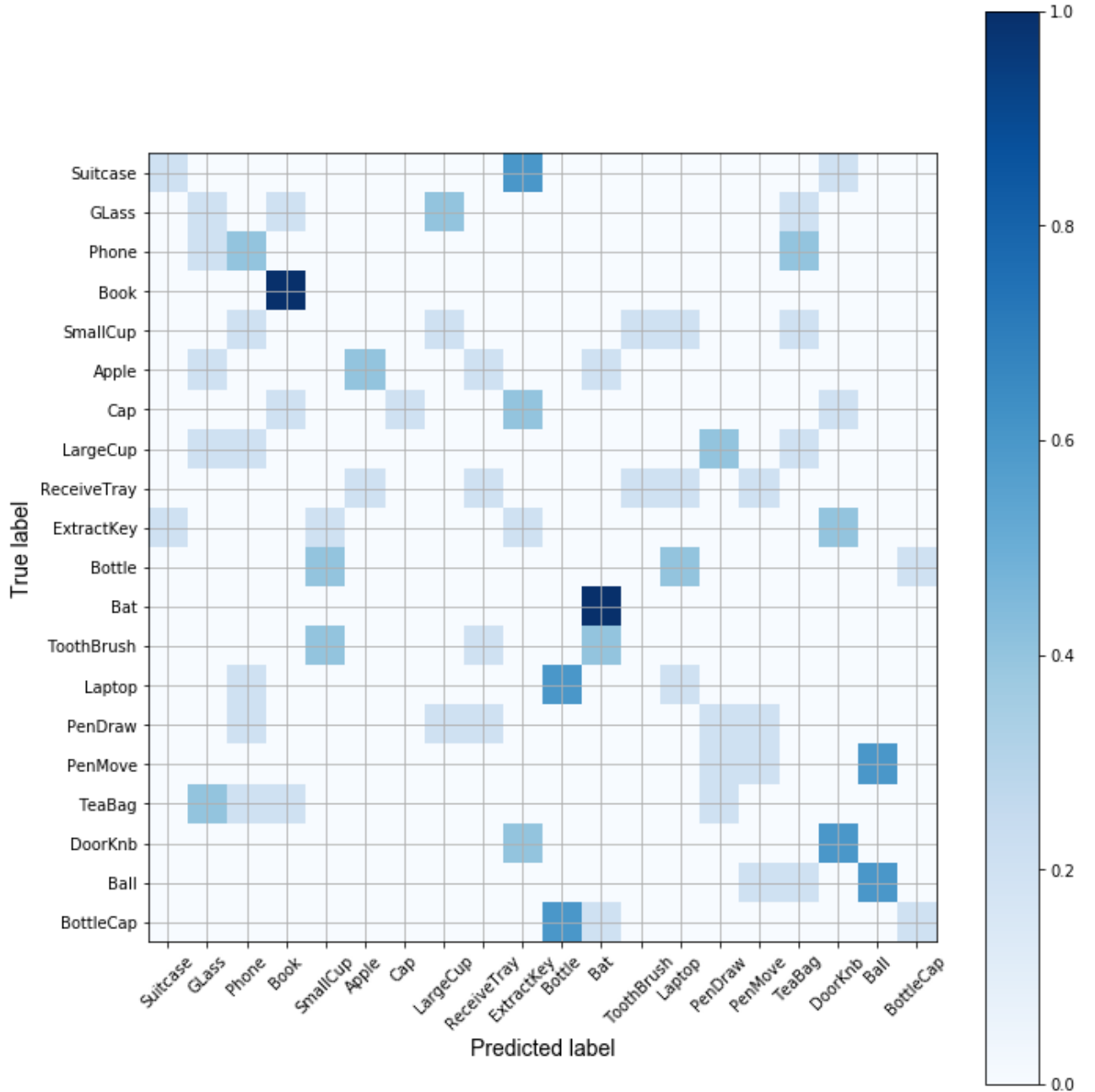


Figure 3.5.2: S2 16-electrodes normalized confusion matrix for 20 grasps

In the classification report of S2 using only 16 electrodes in 3.5.2, the micro average f1-score over all classes in this case dropped to the half: 29%. The micro average of precision, recall, and f1-score are also the same. The best classes which have the best precision, recall, and f1-score are: Book, Bat, and Ball.

According to the classification report of S10 in 3.5.3, the best classes (which have the best f1-score, recall, and precision) for S10 are: Laptop, DoorKnob, TeaBag, ReceiveTray, and Cap

Task	Precision	Recall	F1-Score	Support
Suitcase	0.5	0.2	0.29	5
Glass	0.17	0.2	0.18	5
Phone	0.29	0.4	0.33	5
Book	0.62	1	0.77	5
SmallCup	0	0	0	5
Apple	0.67	0.4	0.5	5
Cap	1	0.2	0.33	5
LargeCup	0	0	0	5
ReceiveTray	0.25	0.2	0.22	5
ExtractKey	0.12	0.2	0.15	5
Bottle	0	0	0	5
Bat	0.56	1	0.71	5
Toothbrush	0	0	0	5
Laptop	0.2	0.2	0.2	5
PenDraw	0.2	0.2	0.2	5
PenMove	0.25	0.2	0.22	5
TeaBag	0	0	0	5
DoorKnb	0.43	0.6	0.5	5
Ball	0.5	0.6	0.55	5
BottleCap	0.5	0.2	0.29	5
micro avg	0.29	0.29	0.29	100

Table 3.5.2: S2 Classification report for 20 grasps using 16 electrodes

classes. This is also visible in the confusion matrix of S10 in 3.5.3. Here also the micro average of precision, recall, and f1-score is the same: 37%.

In the classification report of S10 in the case of measuring only from 16 electrodes in 3.5.4, the micro average f1-score drops down to the half: 17%. Also only ExtractKey class could achieve reasonable results f1-score: 57%, recall: 57%, and precision: 50%. Here also the micro average of precision, recall, and f1-score is the same: 17%. The confusion matrix of S10 in the case of measuring only from 16 electrodes in 3.5.4 shows many squares out of the main diagonal. ExtractKey is dark blue in the main diagonal. Phone is also dark blue but it could not achieve high f1-score (only 44%) as in the classification report in S10 in 3.5.4, also the algorithm in this case failed totally to predict the SmallCup, Apple, Cap, LargeCup, Bottle, Bat, Toothbrush, PenDraw, PenMove, TeaBag, Ball, and BottleCap.

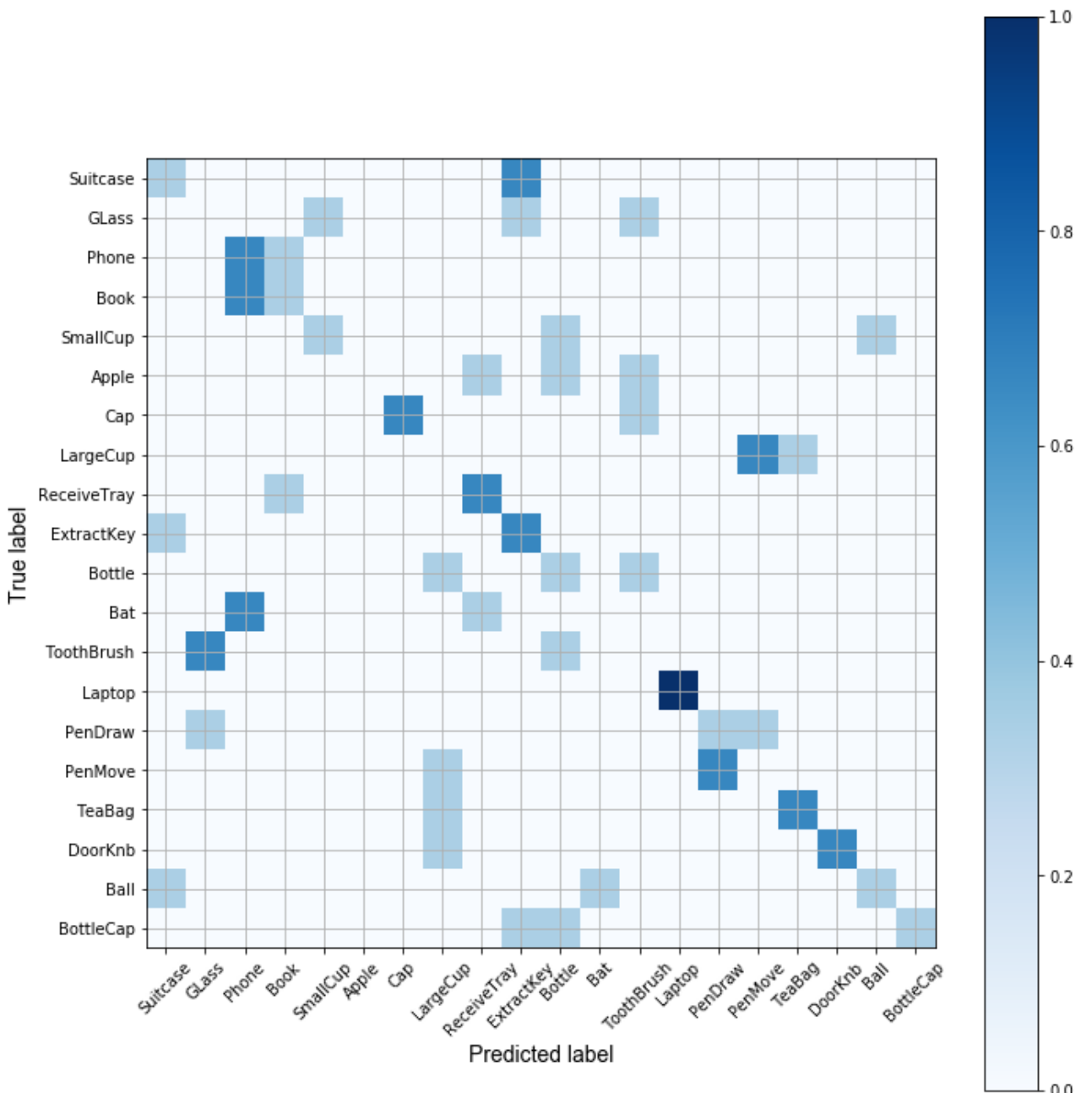


Figure 3.5.3: S10 normalized confusion matrix for 20 grasps

	Precision	Recall	F1-Score	Support
Suitcase	0.33	0.33	0.33	3
Glass	0	0	0	3
Phone	0.33	0.67	0.44	3
Book	0.33	0.33	0.33	3
SmallCup	0.5	0.33	0.4	3
Apple	0	0	0	3
Cap	1	0.67	0.8	3
LargeCup	0	0	0	3
ReceiveTray	0.5	0.67	0.57	3
ExtractKey	0.33	0.67	0.44	3
Bottle	0.2	0.33	0.25	3
Bat	0	0	0	3
Toothbrush	0	0	0	3
Laptop	1	1	1	3
PenDraw	0.33	0.33	0.33	3
PenMove	0	0	0	3
TeaBag	0.67	0.67	0.67	3
DoorKnb	1	0.67	0.8	3
Ball	0.5	0.33	0.4	3
BottleCap	1	0.33	0.5	3
micro avg	0.37	0.37	0.37	60

Table 3.5.3: S10 Classification report for 20 grasps

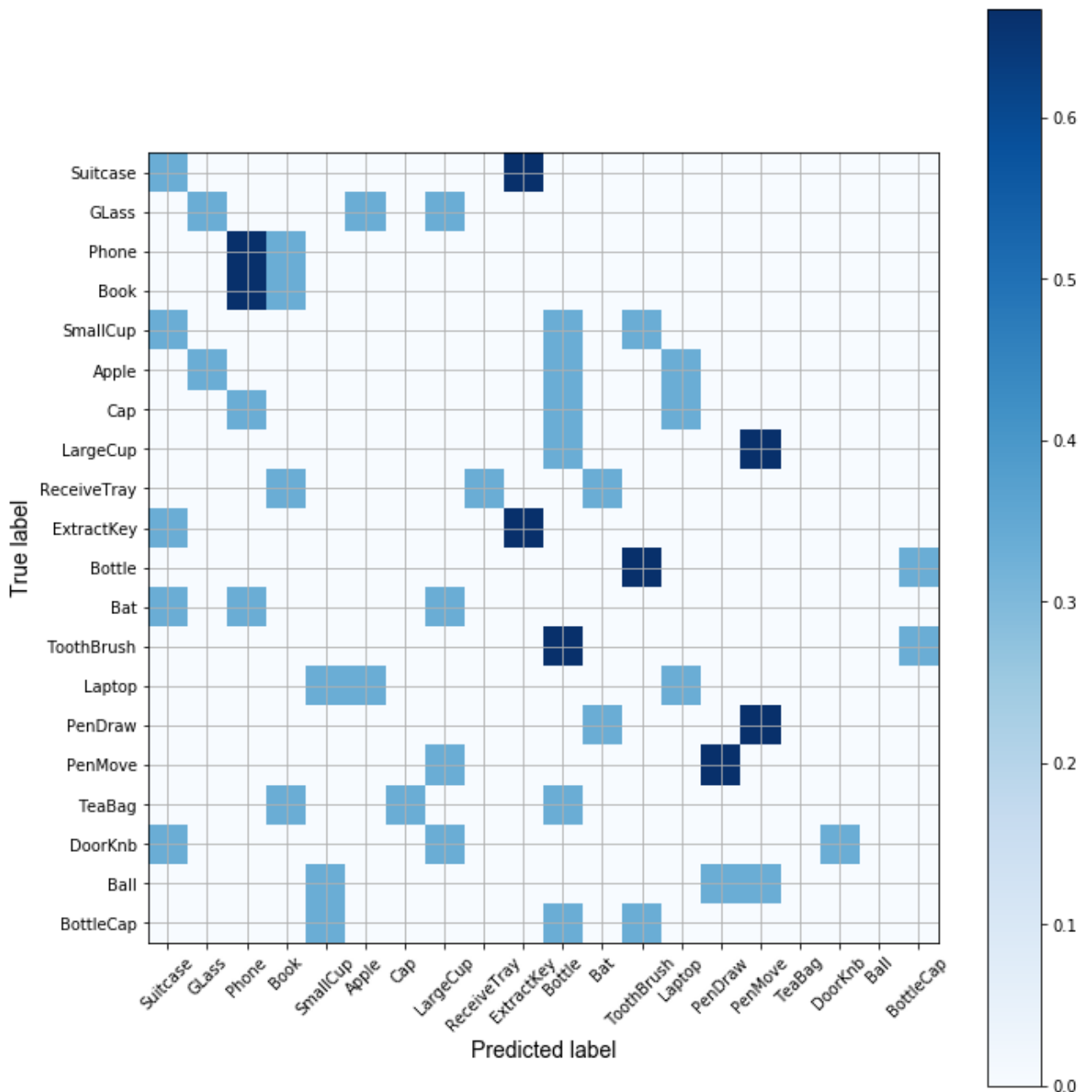


Figure 3.5.4: S10 16-electrodes normalized confusion matrix for 20 grasps

Although the confusion matrix of S1 in 3.5.5 describes 20 grasps classification for a subject with 31 electrodes measurement, there is a lot of dispersion in it and there is no clear main diagonal at all. According to the classification report of S1 in 3.5.5, the best class is DoorKnob with f1-score: 67%, recall: 67%, and precision: 67%. The micro average of the precision, recall, and f1-score is the same: 10%.

The confusion matrix of S1 in the case of measuring only from 16 electrodes in 3.5.6 has also a lot of dispersion. According to the classification report 3.5.6 of S1 by measuring only from 16 electrodes, the best class here is also DoorKnob with the same f1-score: 67%, recall: 67%, and precision: 67%. The micro average of the precision, recall, and f1-score is the same: 12%.

	Precision	Recall	F1-Score	Support
Suitcase	0.2	0.33	0.25	3
Glass	0.5	0.33	0.4	3
Phone	0.33	0.67	0.44	3
Book	0.25	0.33	0.29	3
SmallCup	0	0	0	3
Apple	0	0	0	3
Cap	0	0	0	3
LargeCup	0	0	0	3
ReceiveTray	1	0.33	0.5	3
ExtractKey	0.5	0.67	0.57	3
Bottle	0	0	0	3
Bat	0	0	0	3
Toothbrush	0	0	0	3
Laptop	0.33	0.33	0.33	3
PenDraw	0	0	0	3
PenMove	0	0	0	3
TeaBag	0	0	0	3
DoorKnb	1	0.33	0.5	3
Ball	0	0	0	3
BottleCap	0	0	0	3
micro avg	0.17	0.17	0.17	60

Table 3.5.4: S10 Classification report for 20 grasps using 16 electrodes

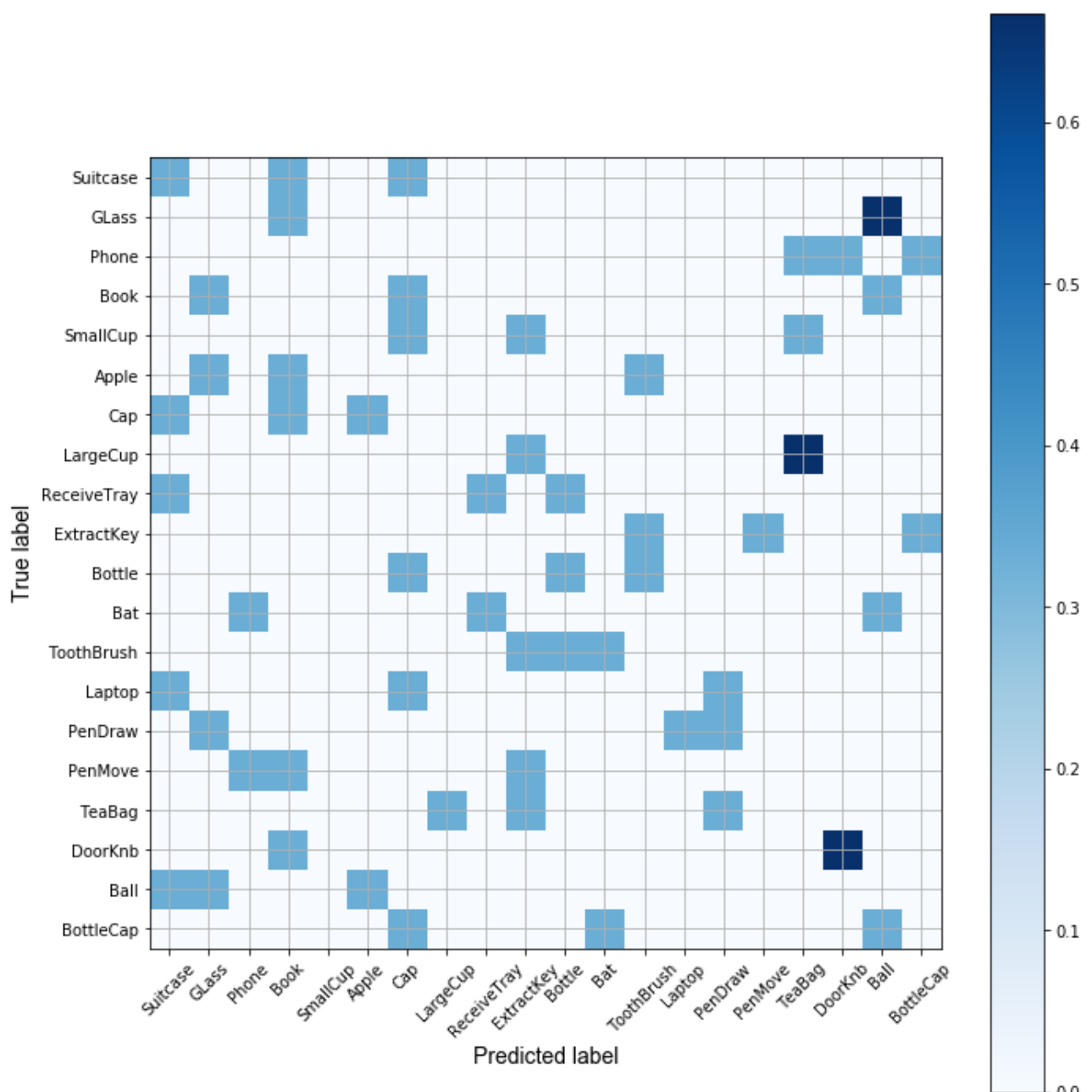


Figure 3.5.5: S1 normalized confusion matrix for 20 grasps

	Precision	Recall	F1-Score	Support
Suitcase	0.2	0.33	0.25	3
Glass	0	0	0	3
Phone	0	0	0	3
Book	0	0	0	3
SmallCup	0	0	0	3
Apple	0	0	0	3
Cap	0	0	0	3
LargeCup	0	0	0	3
ReceiveTray	0.5	0.33	0.4	3
ExtractKey	0	0	0	3
Bottle	0.33	0.33	0.33	3
Bat	0	0	0	3
Toothbrush	0	0	0	3
Laptop	0	0	0	3
PenDraw	0.33	0.33	0.33	3
PenMove	0	0	0	3
TeaBag	0	0	0	3
DoorKnb	0.67	0.67	0.67	3
Ball	0	0	0	3
BottleCap	0	0	0	3
micro avg	0.1	0.1	0.1	60

Table 3.5.5: S1 Classification report for 20 grasps

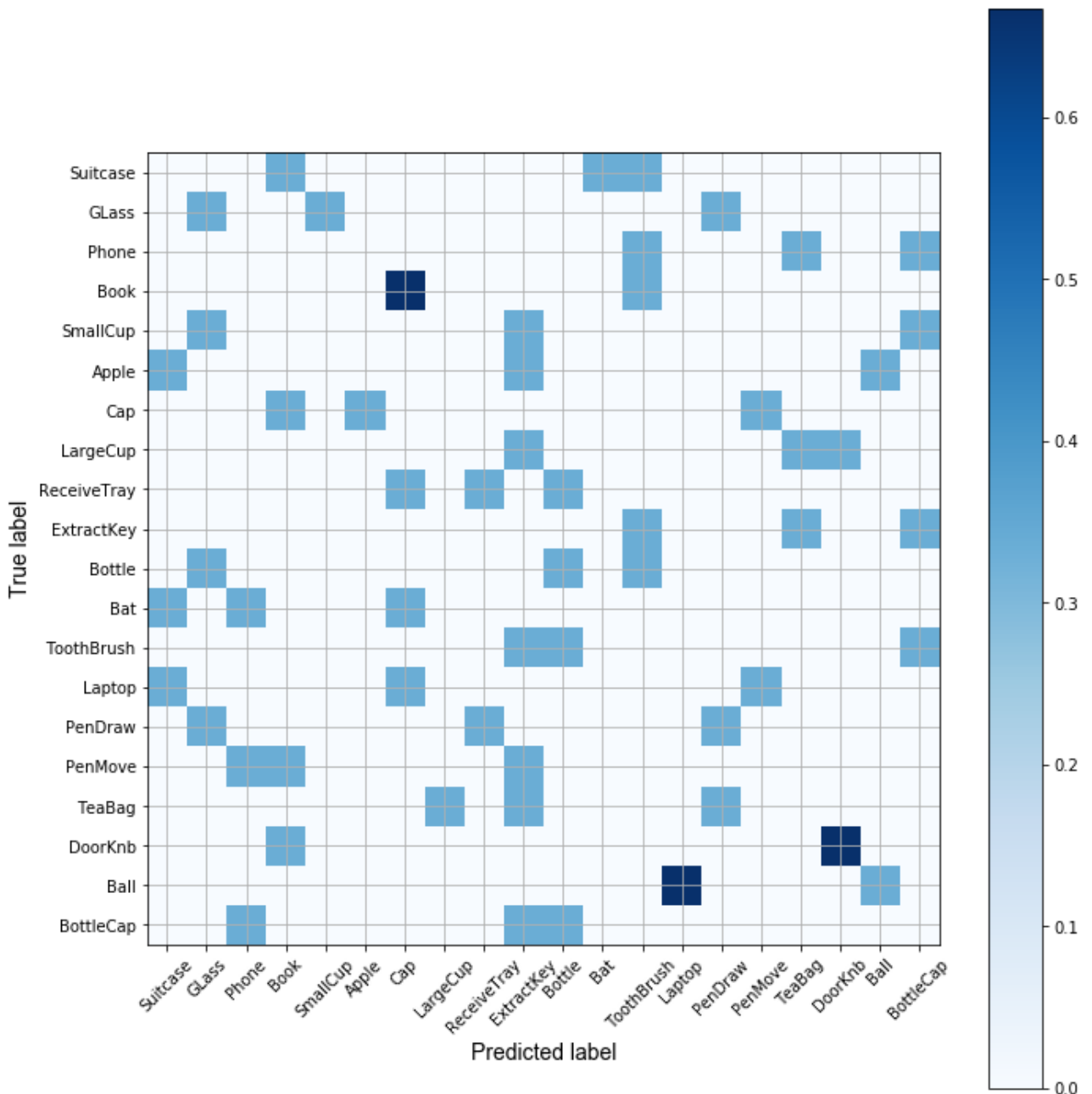


Figure 3.5.6: S1 16-electrodes normalized confusion matrix for 20 grasps

### 3.5.3 Covariance Matrices for different Grasps

In the plotted covariance matrix of the S2 for the Suitcase task as in 3.5.7, there is covariance between the FC1, FC2, Cz, F3, F4 and other electrodes. There is also covariance between the Fp1, and Fp2 and the other electrodes. However since the Fp1, and Fp2 contain eye artifacts, then this covariance might not be task-relevant. Although the eye artifacts has been removed using the ICA algorithm, there are still here eye artifacts. Also there is less covariance in the down-right area.

	Precision	Recall	F1-Score	Support
Suitcase	0	0	0	3
Glass	0.25	0.33	0.29	3
Phone	0	0	0	3
Book	0	0	0	3
SmallCup	0	0	0	3
Apple	0	0	0	3
Cap	0	0	0	3
LargeCup	0	0	0	3
ReceiveTray	0.5	0.33	0.4	3
ExtractKey	0	0	0	3
Bottle	0.25	0.33	0.29	3
Bat	0	0	0	3
Toothbrush	0	0	0	3
Laptop	0	0	0	3
PenDraw	0.33	0.33	0.33	3
PenMove	0	0	0	3
TeaBag	0	0	0	3
DoorKnb	0.67	0.67	0.67	3
Ball	0.5	0.33	0.4	3
BottleCap	0	0	0	3
micro avg	0.12	0.12	0.12	60

Table 3.5.6: S1 Classification report for 20 grasps using 16 electrodes

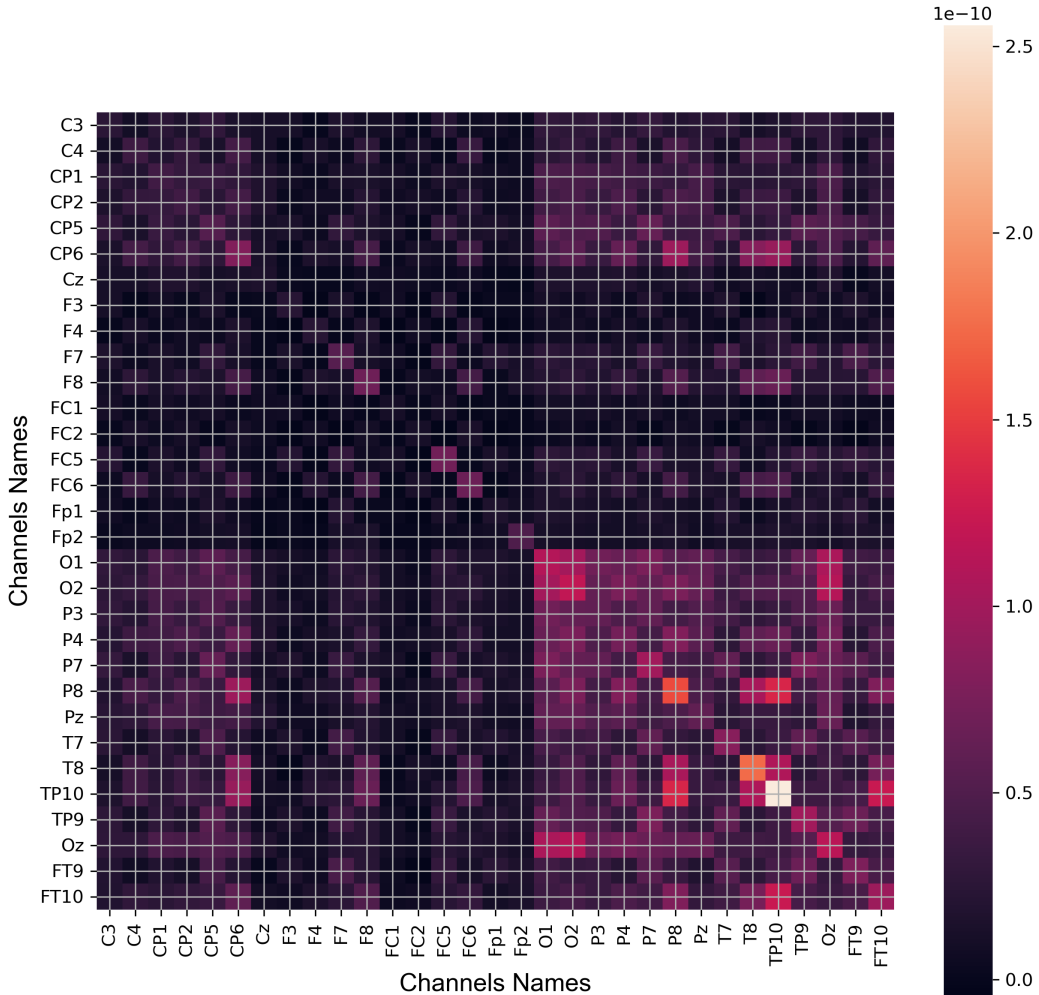


Figure 3.5.7: S2 mean covariance matrix for the Suitcase task using pyRiemann package [127]

In the plotted covariance matrix of S2 for the SmallCup task as in 3.5.8, there is clearly lighter covariance cells in this task in comparison with the Suitcase task as in 3.5.7. The same rule here also applies that there are more covariances along the Fp1, Fp2, FC2, FC1, F4, F3, Cz electrodes.

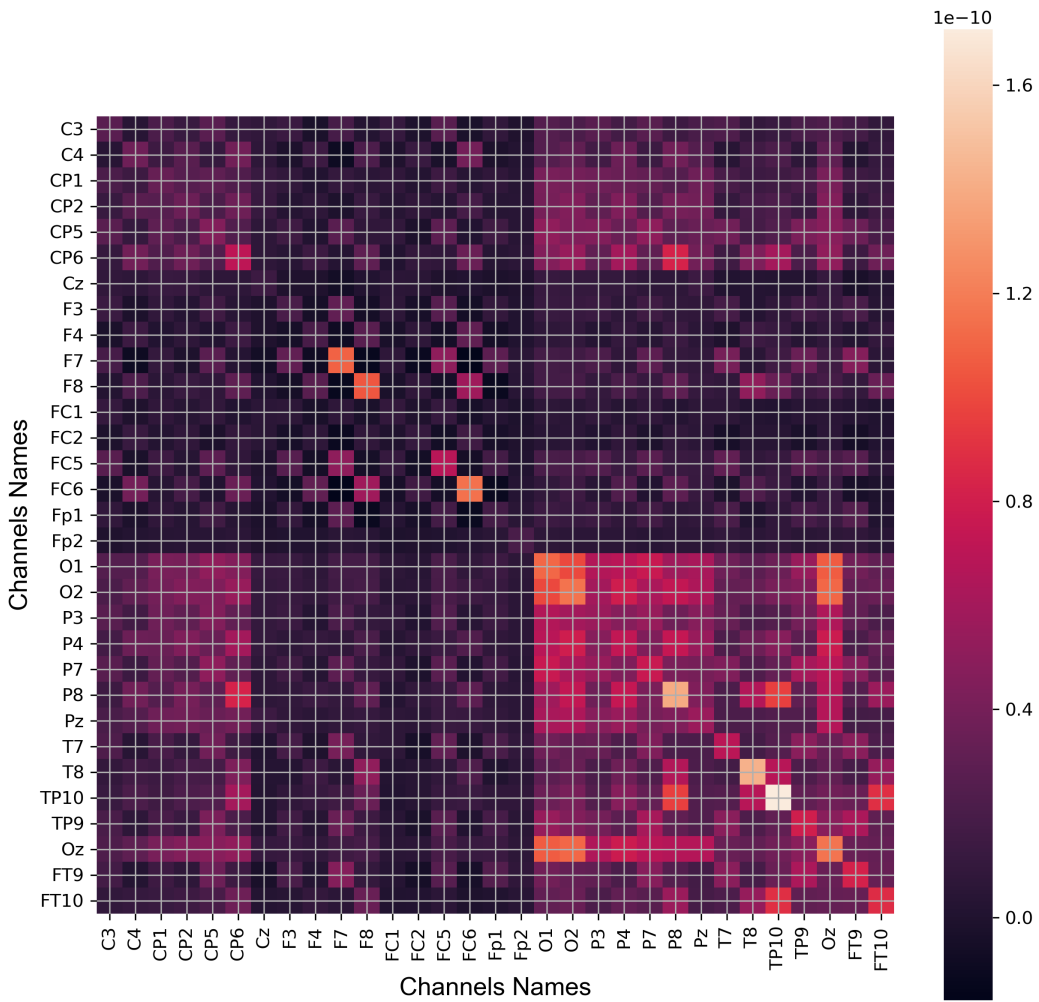


Figure 3.5.8: S2 mean covariance matrix for the SmallCup task using pyRiemann package [127]

In the plotted covariance matrix of the S2 for the ExtractKey task in 3.5.9, there are clearly darker cells between Pz, and FT10, FT9, TP9, TP10, T8, T7 electrodes.

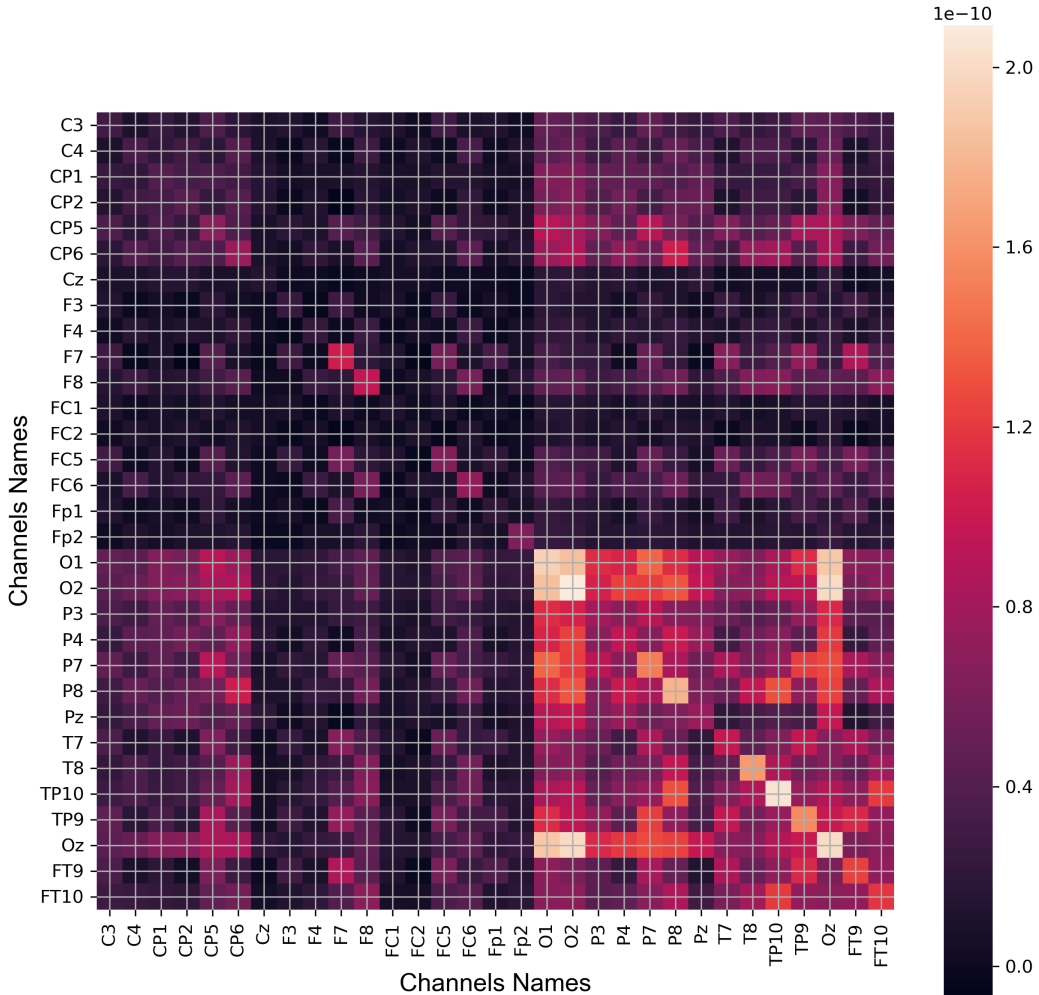


Figure 3.5.9: S2 mean covariance matrix for the ExtractKey task using pyRiemann package [127]

## 3.6 Cross-Subjects Classification

The cross-subjects classification in this study is made for gestures vs. grasps and precision vs. power grasps.

### 3.6.1 Cross-Subjects Gestures vs. Grasps Classification

To test if it is possible to transfer the trained model of gestures vs. grasps from subject to another, different ML, ML with boosting, and DL methods were used in this study. As in the figure 3.6.1, the classification accuracy results are for both 31 electrodes (left side of the graph) and 16 electrodes (right of the graph) and using different ML, ML boosting, and DL

algorithms. The best classification results in this diagram could not be more than 60%. The number of all trials from all subjects is equal in both gestures and grasps classes. This means that 60% is 10% more than the chance level: 50%. The classification results are for cross-subjects: gestures vs. grasps by measuring from 31, and 16 electrodes are approximately the same with a small difference. ML boosting methods were the best and could help ML algorithms to get slightly better classification results. The best ML boosting method result is the Gradboost with (TS, LogReg, SVC with linear kernel): 59.8% (31 electrodes), and 58.7% (16 electrodes). Also Gradboost with (TS, LogReg, SVC with linear kernel, and SVC with RBF kernel) achieved 58% (31 electrodes) and 59.3% (16 electrodes). And also XGB with (TS, LogReg, SVC with linear kernel, and SVC with RBF kernel) could achieve 56.7% (31 electrodes) and 58.5% (16 electrodes). TS achieved only 53.8% (31 electrodes) and 50.2% (16 electrodes). SVC with linear kernel could achieve 53.7% (31 electrodes) using 30 CSP filters with  $C=1000$ , and 54.2% (16 electrodes) using 20 CSP filters with  $C=10000$ . SVC with RBF kernel achieved: 56.8% (31 electrodes) using 30 CSP filters, with  $C=100$ , and  $\gamma=10^{-6}$ , and 54% (16 electrodes) using 10 CSP filters with  $C=10000$  and  $\gamma=0.001$ . LogReg achieved 53.7% (31 electrodes) using 20 CSP filters, with  $C=0.1$ , and 54.2% (16 electrodes) using 20 CSP filters with  $C=1$ . LDA could achieve 54.5% (31 electrodes) using 30 CSP filters, and 54.2% (16 electrodes) using 10 CSP filters. RF also could not achieve better than 54% (31 electrodes) using 10 CSP filters and 300 estimators (decision trees), and 52.2% (16 electrodes) using 30 CSP filters and only 150 estimators. DL methods could not achieve the desired classification results. In the figure 3.6.2, the classification result of the PSD RCNN is: 50.2% (31 electrodes), and 50.6% (16 electrodes). The classification result of the Parallel RCNN: 52.5% (31 electrodes), and 53.3% (16 electrodes). The classification result of Cascade RCNN: 52.2% (31 electrodes), and 55% (16 electrodes).

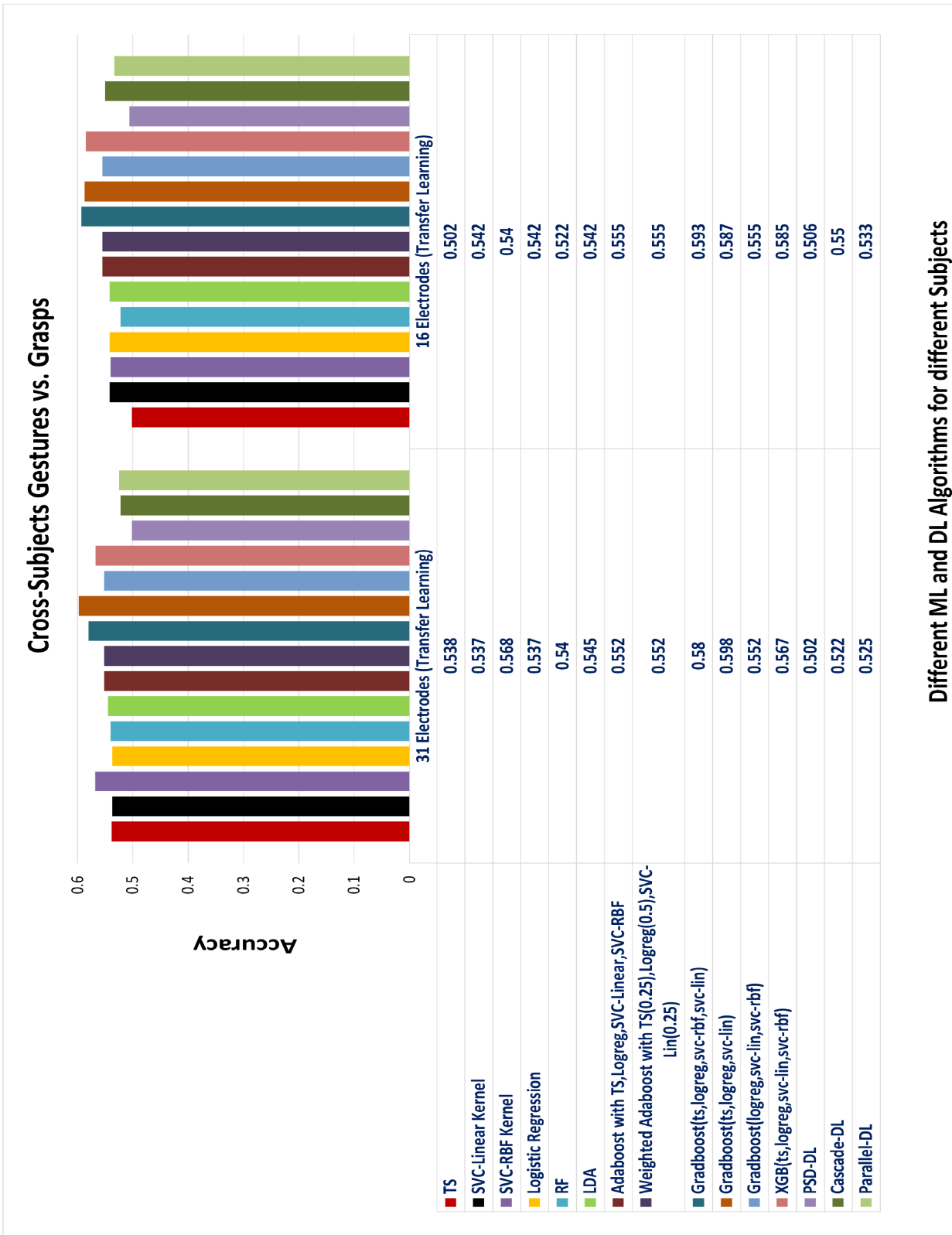


Figure 3.6.1: Comparison between cross-subject classification methods for the gestures vs. grasps case using 31 and 16 electrodes

### 3.6.2 Cross-Subjects Classification for Precision vs. Power Grasps

To test if it is possible to transfer the trained model of precision vs. power grasps from subject to another, different machine learning, machine learning with boosting, and deep learning methods were used. In the figure 3.6.2, the classification accuracy results are plotted by measuring from 31 and 16 electrodes and using different ML and DL algorithms. Generally the best classification results in this diagram could not be better than 60%. The number of the labels is equal in both classes: precision and power grasps, and hence 60% is 10% is more than the chance level: 50%. The classification results are almost the same with a small difference. It is clear from the results in 3.6.2, that the deep learning methods are not better than other ML and ML boosting methods. The classification result of the PSD Recurrent Convolutional Neural Networks is: 50% (31 electrodes), and 54% (16 electrodes). The classification result of the Parallel RCNN: 51% (31 electrodes), and 50% (16 electrodes). The classification result of Cascade RCNN: 57% (31 electrodes), and 55% (16 electrodes). ML boosting method helped ML algorithms to get better classification result but not in all types and not in all combinations. The best ML boosting method result is the Gradboost with (TS, LogReg, SVC with linear kernel): 59% (31 electrodes), and 58% (16 electrodes). By applying Grid Search algorithm, the SVC with linear kernel could achieve 59% (31 electrodes) using 20 CSP filters with  $C=10000$ , and 56% (16 electrodes) using 10 CSP filters with  $C=10000$ . By applying Grid Search algorithm, the SVC with RBF kernel achieved: 59% (31 electrodes) using 30 CSP filters, with  $C=1$ , and  $\gamma=0.01$ , and 58.6% (16 electrodes) using 3 CSP filters with  $C=10000$  and  $\gamma=0.001$ . By applying Grid Search algorithm, LogReg achieved 58% (31 electrodes) using 20 CSP filters, with  $C=100$ , and 57% (16 electrodes) using 20 CSP filters with  $C=10$ . By applying Grid Search algorithm, LDA could achieve 58% (31 electrodes) using 20 CSP filters, and 57% (16 electrodes) using 6 CSP filters. By applying Grid Search algorithm, RF also could not achieve better than 54% (31 electrodes) using 10 CSP filters and 300 estimators (decision trees), and 58% (16 electrodes) using 30 CSP filters and only 150 estimators.

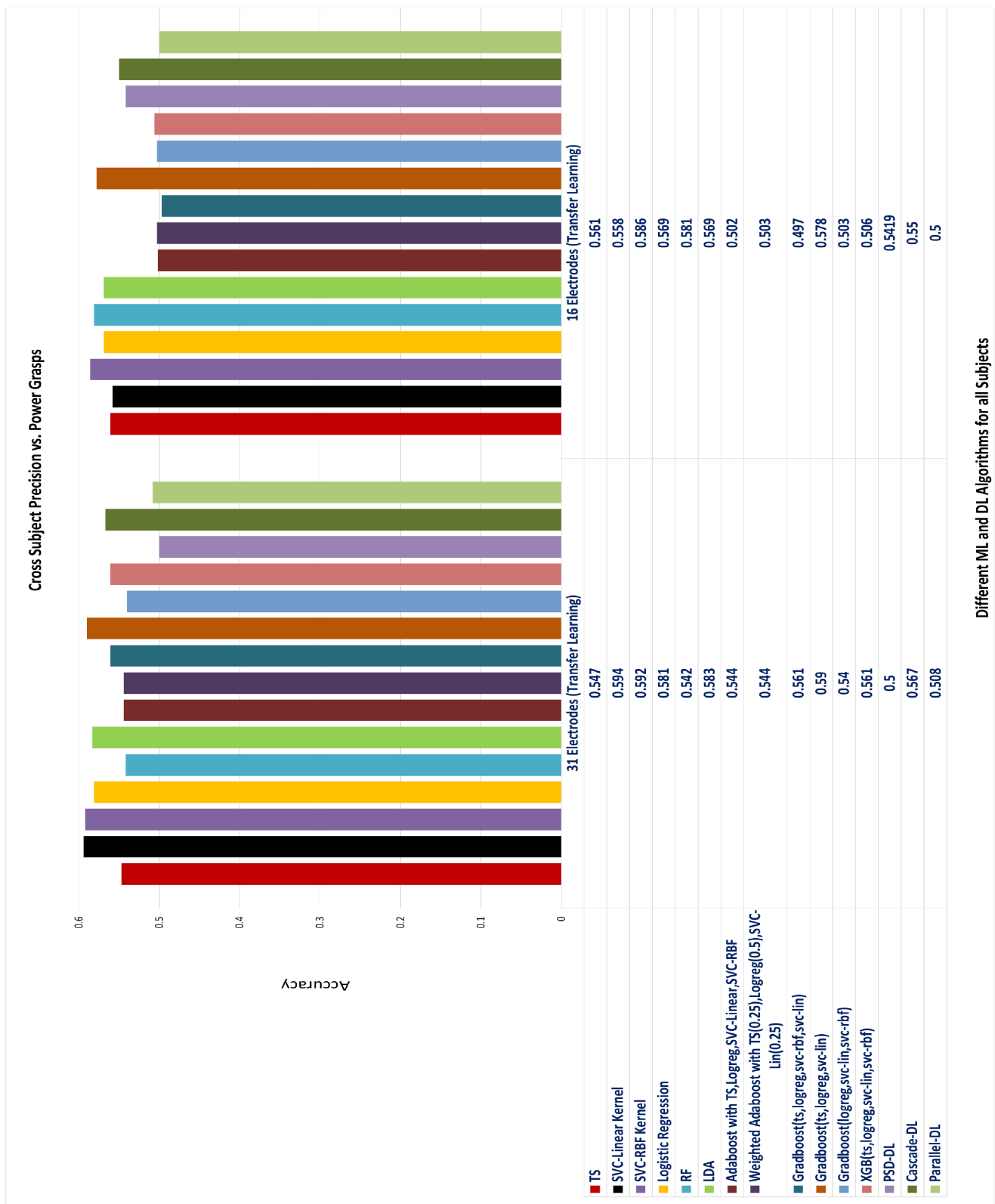


Figure 3.6.2: Comparison between cross-subject classification methods for the precision vs. power grasps case using 31 and 16 electrodes

## 4 Discussion

Main Hypothesis: Machine Learning classified EEG-signals should be sufficiently usable to differentiate between different tasks and grasps of the hand: The possibility of using non-invasive EEG signals to differentiate between gestures and grasps types of hand movements:

The classification results for gestures vs. grasps 3.4.1 show, that it is possible to classify between gestures and grasps. It is important also to mention, that the classification results were good for all subjects (above 70% for all 11 subjects). The achieved results in this study were also a bit similar to a study made to detect the grasp intention during the hand movement [44], where accuracy rates greater than 70% across 4 subjects and 400 trials for each subject could be reached. In this study, only 60 or 100 trials (30 or 50 trials per class) for each subject are available.

The possibility of using non-invasive EEG signals to differentiate between two most known types of grasps: precision and power grasps. In this study, Binary classification between precision and power grasps wasn't as good as the binary classification between gestures and grasps, but could achieve classification results of more than 65% for all subjects as in 3.4.3. The best achieved results in this study for the binary classification between precision and power grasps were less than [45], where an average of 75.90 % accuracy over 10 subjects when classifying between precision and power types of grasps using 64 electrodes and 200 trials for each grasp type could be achieved. In this study, only (6x3) or (6x5) trials for each grasp type (precision or power grasp) were available.

The possibility of using non-invasive EEG signals to differentiate between different 20 grasps types. In this study, the multi-classification results using the TS algorithm of the S2 and S10 were the best. 58% Accuracy as in 3.5.1 S2 of 20 different grasps with only 5 trials for each class is a very good result. The best classification results are in [46], where the study was made on 4 subjects, and could classify between 9 different power grasp classes with the best classification result of one subject: 48% and between 7 different precision grasp classes with the best classification result of another subject: 40%. Unfortunately all the other subjects in this study except the 10th one: 37% as in 3.5.3 could not achieve acceptable results in the case of multi-classification.

The EEG-based machine learning and deep learning classifiers can be transferred from a study cohort to another single subject with a sufficient accuracy: The possibility of cross-subject binary classification for both gestures vs. grasps and precision vs. power grasps using transfer learning from subject to another, by training on 9 subjects and testing on the tenth one. The classification results in the case of cross-subjects classification using the boosting methods were not better than 60 % in 3.6.1 for the case of gestures vs. grasps binary classification and also were not better than 60% as in 3.6.2 for the case of precision vs. power grasps binary classification. Deep learning methods in this study could not achieve higher classification results than the boosting, and the CSP methods for both the gestures vs. grasps case as in 3.6.1 and the precision vs. power grasps case as in 3.6.2. This might be due to the fact, that deep learning needs big and very clean data. Unfortunately, this is not the case in this study. According to the classification using PSD RCNN in [49], an average classification result of 91.1% over 13 subjects to classify between 4 classes using 64 electrodes, and 2670 samples could be achieved. Also, according to

the classification using cascade/parallel RCNN as in [48], in both parallel and cascade methods, 98.3% classification accuracy over 108 subjects to classify between 5 classes using 64 electrodes, and 3,145,160 EEG records could be achieved.

The possibility of using only 16 instead of 31 channels: Using 16 electrodes instead of 31 electrodes, caused generally a drop of the classification accuracy as in the case of Gestures vs. Grasps binary classification in 3.4.5, and the case of Precision vs. Power Grasps binary classification in 3.4.6. However in the case of the binary classification, this drop is acceptable. In some cases for some subjects, like the 10th subject in the case of binary classification between Gestures and Grasps, the classification accuracy using 16 was about 10% better than the classification accuracy using 31 electrodes. On the other hand, in the case of multi-classification, removing electrodes caused in a high drop in the classification accuracy as in the 2nd subject in 3.5.2, where the classification accuracy dropped from 58% to 29%, and also in the 10th subject in 3.5.4, where the classification accuracy dropped from 37% to 17%. This might be due to the fact that for different grasps more regions in the brain are activated and hence there is a need for more electrodes. In [51], only 4 out of 62 electrodes to classify between 3 different types of arm movements (close, open arm, and close hand) were used, and best classification result of 91% using only 4 electrodes could be achieved. In [50], only 8 electrodes out of 64 electrodes to classify between left and right hand movement were used, and best classification result of 97% could be achieved. Lastly, in [52], the classification results of 3 classes using 61, 25, 15, and 5 electrodes were compared, and an average accuracy over 15 subjects: 66.9% using 61 electrodes, 64.2% using 25 electrodes, 59.8% using 15 electrodes, and 54.0% using 5 electrodes could be achieved.

## 4.1 Comparison between Machine Learning methods

LogReg algorithm was not the best of the CSP methods but could outperform the RF and the LDA methods in both gestures vs. grasps classification for individual subjects 3.4.5, and precision vs. power grasps for individual subjects in 3.4.3. By comparing the best result of LogReg in S2 for gestures vs. grasps: 91% with the best result achieved in Kaggle competition by Alexandre Barachant [107]: 97.1%, it is clear, that the results in [107] were better. However both results are above 90%.

RF could achieve almost the same classification accuracy as LDA in both gestures vs. grasps 3.4.5, and precision vs. power grasps 3.4.6 case. This was not the same in [118] as the RF could outperform the LDA by classifying between the right hand and the feet using CSP features.

SVC with RBF kernel could outperform the SVC with linear kernel in both gestures vs. grasps classifiers' comparison in 3.4.5 and precision vs. power grasps classifiers' comparison in 3.4.6. This is similar to a study made in [113], where the SVC with RBF kernel also could outperform the SVC with linear kernel. The SVC with RBF kernel in this study could achieve the best result in S2: 92% in the case of gestures vs. grasps classification as in 3.4.1. This result is also the same as the best classification result in [112] using CSP to classify between imagined hand and foot movement.

TS method was one of the best algorithms in the binary case: gestures vs. grasps classification in 3.4.5 and binary case: precision vs. power grasps classification in 3.4.6, and it could achieve

the best classification results in the multi-classification case as in S2 in 3.3.5 and for S10 in 3.3.6.

## 4.2 Comparison between Machine Learning and Deep Learning Methods

Machine learning methods with CSP and machine learning with TS have shown that they are the best fit for the EEG data classification. Deep learning methods could not achieve high results in comparison with CSP, TS methods as in the cross-subjects classification for gestures vs. grasps in 3.6.1, and the precision vs. power grasps in 3.6.2. Since there is no big data for individual subjects in this study, the deep learning methods are only used in the case of cross-subjects classification by training on 9 subjects and testing on the 10th one. However also in this type of classification, the machine learning methods with CSP and the TS and the boosting methods were better than the DL methods as in the cross-subjects: gestures vs. grasps classification in 3.6.1, and cross-subjects classification: precision vs. power grasps in 3.6.2.

## 4.3 Comparison according to the Gender, and the Age of the Subject

In this study, the best subjects (S2, S4, and S10) were men. This is in the case of binary classification of gestures vs. grasps as in 3.4.1, and precision vs. power grasps in 3.4.3. However in this study, there are only 3 females and 8 males, and there are also many males who gave bad classification results. Also, S2, S4, S10 are older than 50 years. S2 is 53 years old, S4 is 58 years old, and S10 is 72 years old. Although S11 is male and 70 years old, he could not achieve high results comparing with the S2, S4, and S10.

## 4.4 Common Spatial Pattern

Common Spatial Pattern of S2:

In the common spatial pattern of S2 in the case of gestures vs. grasps in 3.4.7, during the grasps, there is more concentration in the frontal area (red color). This concentration might be eye artifacts, that has been falsely detected as a pattern while the subject is moving his hand to grasp. This case is similar to the one in the Kaggle competition of Alexandre Barachant [107], where the eye artifacts also influenced the spatial pattern in "subject 5", when classifying during and after the hand movement. It is also important to mention, that in this study the spatial patterns were not the same for all subjects. This might be the reason why the cross-subjects classification did not achieve higher than 60% classification results.

## 4.5 Confusion Matrices

EEG Data Multi-Classification Confusion Matrix:

In the confusion matrix of S2 for the multi-classification case in 3.5.1, it is clear, that the algorithm is correctly predicting many grasps from the main diagonal. There are of course errors. Some of these errors can be interpreted as following:

- The error resulted from falsely predicting True Label: Bottle as Predicted Label: Bottle-Cap. In both cases, the subject moves his/her both hands: one to hold the bottle and

the other to open the bottle cap, and hence this might be the reason why the algorithm is making an error because in both cases the subject is moving his hand to grasp the bottle.

- The error resulted from falsely predicting True Label: LargeCup as Predicted Label: Glass. Both the LargeCup and the Glass are of the type: Power Grasp. The difference between them is that the Glass is grasped from the side, whereas the large cup is grasped from the top as in the picture in 2.1.3.
- The error resulted from falsely predicting True Label: Apple as Predicted Label: Ball. Both tasks here are very similar. Also the same grasping type (power spherical grasp as in 2.1.1) and the same position.
- The error resulted from falsely predicting True Label: LargeCup as Predicted Label: TeaBag. Here, the tea bag is located inside the large cup with the tea bag's holder outside the large cup. This error depends on the way the subject holds the tea bag's holder.
- The error resulted from falsely predicting True Label: Toothbrush as in picture 23 in 2.1.3 as Predicted Label: Bat as in picture 22 in 2.1.3. Here, grasping the toothbrush tends to be more precision grasp, whereas grasping the tennis bat tends to be more power grasp. However both are of type palm grasp with abducted thumb as in 2.1.1.
- The error resulted from falsely predicting True Label: Cap as in picture 17 in 2.1.3 as Predicted Label: DoorKnb as in picture 28 in 2.1.3. Both types of grasps are similar: sphere grasp as in 2.1.1.

Although the classification results by using 16 electrodes in S2 dropped down to the half as in the classification report of S2 in 3.5.2 and the confusion matrix of S2 using 16 electrodes gets worse than before as in 3.5.2, the following can be noticed:

- The error resulted from predicting True Label: Phone as Predicted Label: Book. Interestingly this error is no more found in the case of only 16 electrodes. Also the error resulted from falsely predicting True Label: Cap as Predicted Label: SmallCup is no more found in the case of 16 electrodes. This might be due to the fact, that the electrodes which are no more used in the case of 16 electrodes, contain many artifacts (eye artifacts, and muscle artifacts) and these electrodes were responsible for these errors.

In the confusion matrix of S10 in 3.5.3, the following errors can be noticed:

- The error resulted from falsely predicting True Label: Bottle as Predicted Label: LargeCup. Both of these types of grasps are power grasps with the same hand grasp type.
- The error resulted from falsely predicting True Label: Bat as Predicted Label: Phone. Both types of grasps are power grasps with abducted thumb.
- The error resulted from falsely predicting True Label: PenDraw as Predicted Label: PenMove. The same pen is grasped in both tasks. In the first case, the pen is grasped and then a line is drawn. In the second case, the pen is grasped and moved to another place.

- The error resulted from falsely predicting True Label: TeaBag as Predicted Label: LargeCup. The tea bag is located inside the large cup, and hence both are in the same position. The subject here makes an error by holding the tea bag in a similar way as holding the large cup.

Although the classification results of S10 by measuring from 16 electrodes dropped down to the half as in 3.5.4, and the confusion matrix of S10 for the case of 16 electrodes gets worse than before as in 3.5.4, the following can be noticed:

- From the confusion matrix of S10 3.5.4, the error resulted from predicting True Label: Glass as Predicted Label: SmallCup. Interestingly this error is no more found in the case of only using 16 electrodes. Also the error resulted from predicting True Label: LargeCup as Predicted Label: TeaBag is no more found in the case of 16 electrodes. This might be due to the fact, that the electrodes which have been taken out in the case of 16 electrodes contain many artifacts (eye artifacts, and muscle artifacts) and these electrodes were responsible for these errors.

## 5 Conclusion, Limitations, and Future Outlook

In this section, firstly the conclusion will be deduced, then the limitations in this study will be explained. Lastly in the future outlook, new methods, and suggestions will be discussed.

### 5.1 Conclusion

The classification results in this study could prove the hypothesis, that the EEG data is able to classify between gestures, and grasps and between precision, and power grasps for all subjects. Removing side electrodes could not enhance the classification accuracy. In fact it caused a drop in the classification accuracy for all cases. It is true that side electrodes contain artifacts, however they also contain many neuro information. For the multi-classification case, good classification results could be only achieved in S2, and partially in S10 using TS. TS was the best method to classify between 20 grasps: 58%, but it was not the only one. SVC with RBF kernel and SVC with linear kernel were tested with GridSearchCV (grid search with cross validation) [111] and gave almost the same classification accuracy: 57%. Cross-subject classification could not reach better than 60% accuracy, this might be due to the fact that there is a high variance of EEG data between different subjects in this study.

### 5.2 Limitations

In this study, there are limitations in the EEG data, specifically in the electrodes types, the electrodes number, and the number of trials. The electrodes in this study contain many artifacts as in the ICA components in S1 in Figure 3.2.1. There is a study in [145], where the Electrooculography (EOG) electrode has been used to remove eye artifacts. This electrode is placed near the eye to capture the eye movement artifacts to be then used to eliminate eye artifacts from other electrodes. The second limitation in this study is the number of electrodes. 31 electrodes

can capture the brain signals correctly, however to increase the spatial resolution in 1.4.1, the number of electrodes can be increased [146].

The third and most important limitation in this study is the number of trials. Machine learning and especially deep learning algorithms need big data [139]. In all of the other similar studies, there are more trials as in [44], where the intention of grasp during reaching movements from EEG data was detected using 400 trials for each of 4 subjects. Also in [45], the classification was made between precision and power grasps using 200 trials for each grasp type. And also using the deep learning methods as in [49], the number of EEG samples used was 2670 samples to classify between 4 classes using 64 electrodes. And lastly according to the classification using cascade/parallel recurrent convolutional neural networks as in [48], in both parallel and cascade methods, 3,145,160 EEG records were used to achieve 98.3% classification accuracy of 5 classes using 64 electrodes.

### 5.3 Future Outlook

There are many areas of research in the neuroprosthetics industry. One of them is the ability to sense touch. As in [147], Professor. Bensmaia said: "When you grasp an object, you have all this information about the object - its size, its shape, its texture, if it is moving across the skin,". From his talk, it is clear that the touch sensors signals which come from the hand to the brain are very useful to detect the kind of grasp which should be done at the right moment. Sensory feedback is very important to increase the dexterity of the prosthetic hand [147].

Another approach is integrating the machine vision into the prosthetic hand as in [148], Kianoush Nazarpour, bioengineer said: "Think of a blind man with a walking stick. Does that stick restore his sight? No. But the simple sensory feedback he obtains by tapping it in learned ways allows his brain to reach a relatively sophisticated impression of his surroundings". The camera can be placed near the wrist towards the fingers so that, when the subject moves the hand to grasp something the machine vision algorithm identifies the best fingers position to grasp the object [148].

It is also possible to use measured EEG database from different hand movements to teach machine learning algorithms to be then used for new prosthetics as in [149].

It is even possible to let the neuroprosthetics learn from the patient itself [150]. Since there is difference in EEG signals from subject to subject [47], it might be better to teach the neuroprosthetics on different EEG signals from the same subject while performing different hand movements.

## References

- [1] Teruya TH Killeen JD Ballard JL Abou-Zamzam AM, Jr. *Major lower extremity amputation in an academic vascular center.* Ann Vasc Surg, 2003.
- [2] Lazaro-Martinez JL Quintana-Marrero Y Maynar-Moliner M Rabellino M et al Aragon-Sanchez J, Garcia-Rojas A. *Epidemiology of diabetes-related lower extremity amputations in Gran Canaria, Canary Islands (Spain).* Diabetes Res Clin Pract., 2009.
- [3] Rosamond Madden Alana Officer Aleksandra Posarac-Katherine Seelman Tom Shakespeare Sándor Sipos Mark Swanson Maya Thomas Zhuoying Qiu Sally Hartley, Venus Ilagan. *World Report On Disability.* World Health Organization and World Bank, 2011.
- [4] Ellen J.; Ephraim Patti L.; Travison-Thomas G.; Brookmeyer Ron (March 2008). Ziegler-Graham, Kathryn; MacKenzie. *Estimating the Prevalence of Limb Loss in the United States: 2005 to 2050.* Archives of Physical Medicine and Rehabilitation, 2008.
- [5] Adığüzel E Uran A Sarısoy G-Goktepe AS Tan AK Durmus D, Safaz I. *The relationship between prosthesis use, phantom pain and psychiatric symptoms in male traumatic limb amputees.* Compr Psychiatry., 2015.
- [6] Adığüzel E Uran A Sarısoy G-Goktepe AS Tan AK Durmus D, Safaz I. *Anxiety and depression following traumatic limb amputation: a systematic review.* Injury., 2014.
- [7] Parkes CM. *Components of the reaction to loss of a lamb, spouse or home.* J Psychosom Res., 1972.
- [8] Roberto Barone Rocco Antonio Romeo-Alberto Dellacasa Bellingegni Rinaldo Sacchetti Angelo Davalli Giovanni Di Pino Federico Ranieri Vincenzo Di Lazzaro Eugenio Guglielmelli Loredana Zollo Anna Lisa Ciancio, Francesca Cordella. *Control of Prosthetic Hands via the Peripheral Nervous System.* frontiers in Neuroscience, 2016.
- [9] I A Kapandji. *The Physiology of the Joints.* Edinburgh : Churchill Livingstone, 1982-1987, 2007.
- [10] Rinaldo Sacchetti Angelo Davalli Andrea Giovanni Cutti Eugenio Guglielmelli Francesca Cordella, Anna Lisa Ciancio and Loredana Zollo. *Literature Review on Needs of Upper Limb Prostheses Users.* frontiers in Neuroscience, 2016.
- [11] Parker PA Scott RN1. *Myoelectric prostheses: state of the art.* Jouranl of Medical engineering and technology, 1988.
- [12] Battyeet et al. *The use of myo-electric currents in the operation of prostheses.* J Bone Joint Surg Br., 1955.
- [13] POPOV B. *THE BIO-ELECTRICALLY CONTROLLED PROSTHESIS.* J Bone Joint Surg Br, 1965.

- [14] Kyberd PJ Losier YG Parker PA Fougner A, Stavdahl O. *Control of upper limb prostheses: terminology and proportional myoelectric control-a review*. IEEE Trans Neural Syst Rehabil Eng., 2012.
- [15] Chau T Biddiss E. *Upper-limb prosthetics: critical factors in device abandonment*. Am J Phys Med Rehabil, 2007.
- [16] Witteveen H in 't Veld RH Hermens H Stramigioli S Rietman H Veltink P Misra S Peerdeeman B, Boere D. *Myoelectric forearm prostheses: state of the art from a user-centered perspective*. J Rehabil Res Dev, 2011.
- [17] Head J. *The Effect of Socket Movement and Electrode Contact on Myoelectric Prosthetic Control during Daily Living Activities*. Ph.D. thesis, Salford: University of Salford., 2014.
- [18] Kelly B Davis A Chestek CA Gates DH Engdahl SM, Christie BP. *Surveying the interest of individuals with upper limb loss in novel prosthetic control techniques*. J Neuroeng Rehabil., 2015.
- [19] Kashman N Weber K Mathiowetz V, Volland G. *Adult norms for the Box and Block Test of manual dexterity*. Am J Occup Ther., 1985.
- [20] Le V Mitchell A Muniz S Vollmer MA Oxford Grice K, Vogel KA. *Adult norms for a commercially available Nine Hole Peg Test for finger dexterity*. Am J Occup Ther, 2003.
- [21] Heckathorne C. W. Farrell T. R., Weir R. F. *The effect of controller delay on box and block test performance*, in *MyoElectric Controls/Powered Prosthetics Symposium*. Fredericton, NB., 2005.
- [22] Gasson M. Tjerks T. Metcalf C. Chappell P. H. et al Kyberd P. J., Murgia A. *Case studies to demonstrate the range of applications of the Southampton hand assessment procedure*. J. Occup. Ther., 2009.
- [23] Schabowsky CN Holley RJ Monroe B Lum PS Metzger AJ, Dromerick AW. *Feedforward control strategies of subjects with transradial amputation in planar reaching*. J Rehabil Res Dev, 2010.
- [24] Bongers RM Bouwsema H, van der Sluis CK. *Changes in performance over time while learning to use a myoelectric prosthesis*. J Neuroeng Rehabil., 2014.
- [25] Moin Uddin Atique. *Cost-effective Myoelectric Prosthetic Hand*. Journal of Prosthetics and Orthotics, 2018.
- [26] Lipschutz RD et al. Kuiken TA, Dumanian GA. *The use of targeted muscle reinnervation for improved myoelectric prosthesis control in a bilateral shoulder disarticulation amputee*. Prosthet Orthot Int, 2004.
- [27] Todd A Kuiken Gregory A Dumanian Jennifer E Cheesborough, Lauren H Smith. *Targeted Muscle Reinnervation and Advanced Prosthetic Arms*. Seminars in plastic surgery, 2015.

- [28] Hutchinson DT Horch KW. Dhillon GS1, Lawrence SM. *Residual function in peripheral nerve stumps of amputees: implications for neural control of artificial limbs.* J Hand Surg Am, 2004.
- [29] Lipschutz RD Lock BA Stubblefield K Marasco PD Zhou P Dumanian GA Kuiken TA, Miller LA. *Targeted reinnervation for enhanced prosthetic arm function in a woman with a proximal amputation: a case study.* Lancet., 2007.
- [30] E. Spellerberg. *Improvement in artificial arms.* 1965.
- [31] Edoardo Farnioli Alessandro Serio Cristina Piazza Manuel G Catalano, Giorgio Grioli and Antonio Bicchi. *Adaptive synergies for the design and control of the Pisa/IIT softhand.* The International Journal of Robotics Research, 2014.
- [32] Chaitanya Kanodia Jill D Crisman and Ibrahim Zeid. *Graspar: A flexible, easily controllable robotic hand.* IEEE Robotics and Automation Magazine, 1996.
- [33] Frederic Pelletier Clement Gosselin and Thierry Laliberte. *An anthropomorphic underactuated robotic hand with 15 dofs and a single actuator.* IEEE International Conference on Robotics and Automation (ICRA), 2008.
- [34] N.T. Ulrich. *Methods and apparatus for mechanically intelligent grasping.* US Patent: No. 4957320, 1990.
- [35] Kristin Zhao Manuel Catalano Ryan Breighner Amanda Theuer Karen Andrews Giorgio Grioli Marco Santello Sasha B. Godfrey, Matteo Bianchi and Antonio Bicchi. *The SoftHand pro: translation from robotic hand to prosthetic prototype, in Converging Clinical and Engineering Research on Neurorehabilitation II. Biosystems and Biorobotics.* Springer International Publishing AG, 2017.
- [36] Jain Pimenta Neto Boege Grioli et al Fani, Bianchi. *Assessment of myoelectric controller performance and kinematic behavior of a novel soft synergy inspired robotic hand for prosthetic applications.* Front Neurorobot, 2016.
- [37] Emanuel Todorov Zhe Xu, Vikash Kumar. *A low-cost and modular, 20-DOF anthropomorphic robotic hand: design, actuation and modeling.* 13th IEEE-RAS International Conference on Humanoid Robots (Humanoids), 2013.
- [38] Emmanuel Olivi. *Coupling of numerical methods for the forward problem in Magneto- and ElectroEncephalography.* Université Nice Sophia Antipolis, 2011.
- [39] Matthew S. Fifer Matthew S. Johannes Kapil D. Katyal Matthew P. Para Robert Armiger William S. Anderson Nitish V. Thakor Brock A. Wester Nathan E. Crone Guy Hotson, David P McMullen. *Individual Finger Control of the Modular Prosthetic Limb using High-Density Electrocorticography in a Human Subject.* J Neural Eng. Author manuscript; available in PMC, 2017.

- [40] B.C. Burke S. Vanhatalo W.J. Freeman, M.D. Holmes. *Spatial spectra of scalp EEG and EMG from awake humans*. Clin. Neurophysiol., 2003.
- [41] J.R. Wolpaw J.G. Ojemann D.W. Moran E.C. Leuthardt, G. Schalk. *A brain-computer interface using electrocorticographic signals in humans*. Neural Eng., 2004.
- [42] J.E. Huggins S.P. Levine L.A. Schuh G. Pfurtscheller, B. Graimann. *Spatiotemporal patterns of beta desynchronization and gamma synchronization in corticographic data during self-paced movement*. Clin. Neurophysiol., 2003.
- [43] Shain W et al. *Controlling cellular reactive responses around neural prosthetic devices using peripheral and local intervention strategies*. IEEE Trans. Neural Syst. Rehabil. Eng., 2003.
- [44] Robert Leeb Luca Randazzo, Ricardo Chavarriaga. *Detecting intention to grasp during reaching movements from EEG*. 37th Annual International Conference of the IEEE Engineering in Medicine and Biology Society (EMBC), 2015.
- [45] R. Chavarriaga J.d.R. Millán I. Iturrate, R. Leeb. *Decoding of two hand grasping types from EEG*. Published by Verlag der TU Graz, Graz University of Technology, sponsored by g.tec medical engineering GmbH, 2016.
- [46] Yoshihiko Nakamura Uchiyama Emiko, Wataru Takano. *Multi-class grasping classifiers using EEG data and a common spatial pattern filter*. Advanced Robotics, 2017.
- [47] Chen J. H. Lin Y. P., Duann J. R. and T. P. Jung. *Electroencephalographic dynamics of musical emotion perception revealed by independent spectral components*. Neuroreport, 2010.
- [48] Dalin Zhang, Lina Yao, Sen Wang, Weitong Chen, and Robert Boots. *Cascade and Parallel Convolutional Recurrent Neural Networks on EEG-Based Intention Recognition for Brain Computer Interface*. AAAI Publications, Thirty-Second AAAI Conference on Artificial Intelligence, 2018.
- [49] Pouya Bashivan, Irina Rish, and Mohammed Yeasin. *Learning Representations From EEG With Deep Recurrent-Convolutional Neural Networks*. Published as a conference paper at ICLR, 2016.
- [50] Aya Samaha Mohammad H. Alomari and Jordan Khaled AlKamha Applied Science University Amman. *Automated Classification of L/R Hand Movement EEG Signals using Advanced Feature Extraction and Machine Learning*. International Journal of Advanced Computer Science and Applications, 2013.
- [51] Salah M.El-sayed Howida A.Shedeed, Mohamed F.Issa. *Brain EEG Signal Processing For Controlling a Robotic Arm*. 8th International Conference on Computer Engineering and Systems (ICCES), 2013.

- [52] Joana Pereira-Andreea Ioana Sburlea Andreas Schwarz, Patrick Ofner and Gernot R Müller-Putz. *Decoding natural reach-and-grasp actions from human EEG*. J. Neural Eng., 2018.
- [53] Suzana Herculano-Houzel. *The Human Brain in Numbers: A Linearly Scaled-up Primate Brain*. frontiers in Human Neuroscience, 2009.
- [54] Mihail Bota and Larry W. Swanson. *The neuron classification problem*. brainresrev, 2007.
- [55] D Fitzpatrick-LC Katz AS LaMantia JO McNamara D Purves, GJ Augustine and SMWilliams. *Neuroscience*. Sunderland.MA, 2003.
- [56] Freedman M Chayer C1. *Frontal lobe functions*. Curr Neurol Neurosci Rep, 2001.
- [57] Forshing Lui Letitia Pirau. *Frontal Lobe Syndrome*. StatPearls Publishing, 2018.
- [58] W. Penfield and Rasmussen. *The cerebral cortex of a man: A clinical study of localization of function*. New York: Macmillan, 1950.
- [59] U Frith SJ Blakemore. *The Learning Brain*. Blackwell Publishing, 2005.
- [60] Anthony Singhal Jody C.Culham, Cristiana Cavina-Pratesi. *The role of parietal cortex in visuomotor control: What have we learned from neuroimaging?* Neuropsychologia, 2005.
- [61] Luppino G. Fogassi L. *Motor functions of the parietal lobe*. Current Opinion in Neurobiology, 2005.
- [62] Schwartz J. Kandel, J. and Jessell. *Principles of Neural Science. 3rd edition*. Elsevier. New York, 1991.
- [63] Beatrice Paradiso Enrico Grandi Sergio Balbi Enrico Granieri Enzo Colarusso Franco Chioffi Carlo Efisio Marras Alessandro De Benedictis, Hugues Duffau and Silvio Sarubbo. *Anatomo-functional study of the temporo-parieto-occipital region: dissection, tractographic and brain mapping evidence from a neurosurgical perspective*. Journal of Anatomy, 2014.
- [64] Schwartz J. Kandel, J. and Jessell. *Principles of Neural Science. 3rd edition*. Elsevier. New York, 1991.
- [65] *Cognitive Psychology: Mind and Brain*. New Jersey: Prentice Hall, 2007.
- [66] *Cognitive Psychology: Mind and Brain*. New Jersey: Prentice Hall, 2007.
- [67] Miller T. D. Gorgoraptis N. Caine D. Schott J. M. Butler C. Pertzov, Y. and M. Husain. *Binding deficits in memory following medial temporal lobe damage in patients with voltage-gated potassium channel complex antibody-associated limbic encephalitis*. Brain: A Journal of Neurology, 2013.
- [68] Patrick Hof Goran Simic. *In Search of the Definitive Brodmann's Map of Cortical Areas in Human*. Journal of Comparative Neurology, 2015.

- [69] W.A. Gray S. Ionta L.A. M.R. Borich, S.M. Brodie. *Understanding the role of the primary somatosensory cortex: Opportunities for rehabilitation.* Neuropsychologia, 2015.
- [70] Klaus wilhelm. *How the Brain moves us.* MAX PLANCK INSTITUTE FOR HUMAN COGNITIVE AND BRAIN SCIENCE in Leipzig, 2007.
- [71] Nagib Abbas Seha M. Abo-ZahhadSabah M. Ahmed Sherif. *A New EEG Acquisition Protocol for Biometric Identification Using Eye Blinking Signals.* International Journal of Intelligent Systems Technologies and Applications, 2015.
- [72] Shanaya Sidhu. *Brain Waves: What are we looking for exactly?* Crux Ucla. Neurotech Organization, 2019.
- [73] Michael Taylor, Eric; Rutter. *Child and adolescent psychiatry.* Oxford Malden, MA : Blackwell Science, 4th ed edition, 2002.
- [74] Rajendra Acharya U Choo Min Lim D. Puthankattil Subha, Paul K. Joseph. *EEG Signal Analysis: A Survey.* J Med Syst, 2010.
- [75] Gurvit H Keskin YH Emre M Kirmizi-Alsan E, Bayraktaroglu Z and Demiralp T. *Comparative analysis of event-related potentials during Go/NoGo and CPT: Decomposition of electrophysiological markers of response inhibition and sustained attention.* Brain Research, 2006.
- [76] C. L. Ehlers and D. J. Kupfer. *Sleep: Do Young Adult Men and Women Age Differently?* J Sleep Res., 1997.
- [77] Robert P. Vertes. *Hippocampal theta rhythm: a tag for short-term memory.* HIPPOCAMPUS, 2005.
- [78] Diego Mateos José Luis Pérez-Velázquez Jaime Gómez-Ramírez, Shelagh Freedman and Taufik Valiante. *Eyes closed or Eyes open? Exploring the alpha desynchronization hypothesis in resting state functional connectivity networks with intracranial EEG.* BioRxiv, 2017.
- [79] Palva J.M. Palva S. *New vistas for a-frequency band oscillations.* Trends in Neuroscience, 2007.
- [80] Penfield W Jasper H. *Electrocorticograms in man: effect of voluntary movement upon the electrical activity of the precentral gyrus.* Arch Psychiatr Zeitschr Neurol, 1949.
- [81] Bjorg Elisabeth Kilavik Manuel Zaepffel, Romain Trachel and Thomas Brochier. *Modulations of EEG Beta Power during Planning and Execution of Grasping Movements.* PLoS One, 2013.
- [82] Geiss KR Baumeister J, Barthel T and Weiss M. *Influence of phosphatidylserine on cognitive performance and cortical activity after induced stress.* Nutritional Neuroscience, 2008.

- [83] Bressler SL Ding M Zhang Y, Chen Y. *Response preparation and inhibition: the role of the cortical sensorimotor beta rhythm*. Neuroscience, 2008.
- [84] SN Baker. *Oscillatory interactions between sensorimotor cortex and the periphery*. Current Opinion in Neurobiology, 2008.
- [85] Doyle Di Lazzaro Cioni Brown Lalo, Gilbertson. *Phasic increases in cortical beta activity are associated with alterations in sensory processing in the human*. Experimentation Cerebrale, 2006.
- [86] Cornwell Zoe M. Kisley Michael A. *Gamma and beta neural activity evoked during a sensory gating paradigm: Effects of auditory, somatosensory and cross-modal stimulation*. Clinical Neurophysiology, 2006.
- [87] da Silva F.L. Niedermeyer E. *Electroencephalography: Basic Principles, Clinical Applications, and Related Fields*. Lippincott Williams and Wilkins., 2004.
- [88] L. Shupea E. Lettiche G.A. Ojemann F. Aokia, E.E. Fetza. *Increased gamma-range activity in human sensorimotor cortex during performance of visuomotor tasks*. Clinical Neurophysiology, 1999.
- [89] Gordon B Lesser RP Crone NE, Miglioretti DL. *Functional mapping of human sensorimotor cortex with electrocorticographic spectral analysis. II. Event-related synchronization in the gamma band*. Brain. Volume: 121. Issue: 12. Pages: 2301-2315, 1995.
- [90] Muthukumaraswamy SD. *Functional properties of human primary motor cortex gamma oscillations*. J Neurophysiol, 2010.
- [91] Raykhan Khassenova Huseyin Atakan Varol Artur Saudabayev, Zhanibek Rysbek. *Human grasping database for activities of daily living with depth, color and kinematic data streams*. Naturereresearch Journal, 2018.
- [92] Kara Morgan-Short Darren Tanner and Steven J. Luck. *How inappropriate high-pass filters can produce artifactual effects and incorrect conclusions in ERP studies of language and cognition*. Psychophysiology, 2015.
- [93] Henrik Flyvbjerg Johannes Müller Gerking, Gert Pfurtscheller. *Designing optimal spatial filters for single-trial EEG classification in a movement task*. Clinical Neurophysiology Volume 110, Issue 5, 1999.
- [94] J. M. Gerking H. Ramoser and G. Pfurtscheller. *Optimal Spatial filtering of single trial EEG during imagined hand movement*. IEEE Trans. Rehab. Eng, 2000.
- [95] M. Abo-ZahhadSabah M. AhmedSherif Nagib Abbas Seha. *A New EEG Acquisition Protocol for Biometric Identification Using Eye Blinking Signals*. International Journal of Intelligent Systems Technologies and Applications, 2015.

- [96] M. Abo-ZahhadSabah M. AhmedSherif Nagib Abbas Seha. *A New EEG Acquisition Protocol for Biometric Identification Using Eye Blinking Signals*. International Journal of Intelligent Systems Technologies and Applications, 2015.
- [97] Zhe Sage Chen. *The Cocktail Party Problem*. Neural Computation, 2005.
- [98] Humphries C. Lee T. W.-McKeown M. J. Iragui V. Jung T-p, Makeig S. and Sejnowski T. J. *Removing Electroencephalographic Artifacts by Blind Source Separation*. Psychophysiology, 2000.
- [99] Christopher J James and Christian W Hesse. *Independent component analysis for biomedical signals*. Physiol. Meas. 26 R15, 2005.
- [100] Paweł Górski Izabela Rejer. *Independent Component Analysis for EEG Data Preprocessing - Algorithms Comparison*. 12th International Conference on Information Systems and Industrial Management (CISIM), 2013.
- [101] Arnaud Delorme and Scott Makeig. *EEGLAB Tutorial-Chapter 09: Decomposing Data using ICA*. Swartz Center for Computational Neuroscience, 2018.
- [102] Sejnowski TJ Lee TW1, Girolami M. *Independent component analysis using an extended infomax algorithm for mixed subgaussian and supergaussian sources*. Neural Comput, 1999.
- [103] Tim Welsh. *It feels instantaneous, but how long does it really take to think a thought*. The Conversation, 2015.
- [104] Moritz Grosse-Wentrup and Martin Buss. *Multiclass common spatial patterns and information theoretic feature extraction*. IEEE Transactions on Biomedical Engineering, 2008.
- [105] Xiaorong Gao Yijun Wang, Shangkai Gao. *Common Spatial Pattern Method for Channel Selection in Motor Imagery Based Brain-computer Interface*. Proceedings of IEEE Engineering in Medicine and Biology 27th Annual Conference Shanghai, China, September, 2005.
- [106] Steven Lemm Motoaki Kawanabe Klaus-robert Muller Benjamin Blankertz, Ryota Tomioka. *Optimizing Spatial filters for Robust EEG Single-Trial Analysis*. IEEE Signal Processing Magazine. Volume:25, Issue:1, 2008.
- [107] Alexandre Barachant. *Common Spatial Pattern with MNE*. Kaggle, 2015. <https://www.kaggle.com/alexandrebarachant/common-spatial-pattern-with-mne>.
- [108] Benoni B Edin Matthew D Luciw, Ewa Jarocka. *Multi-channel EEG recordings during 3,936 grasp and lift trials with varying weight and friction*. Scientific Data volume 1, Article number: 140047, 2014.
- [109] Jason Brownlee. *Logistic Regression for Machine Learning*. MachineLearningMastery, 2016.

- [110] Dae-Ki Kang Ahmed El-Koka, Kyung-Hwan Cha. *Regularization parameter tuning optimization approach in logistic regression*. IEEE. International Conference on Advanced Communications Technology (ICACT), 2013.
- [111] Gary Wills Iwan Syarif, Adam Prugel-Bennett. *SVM Parameter Optimization Using Grid Search and Genetic Algorithm to Improve Classification Performance*. TELKOMNIKA, Vol.14, No.4. Pages: 1502-1509, 2016.
- [112] Yaoru Sun Huaping Zhu Jinhua Zeng Hongyu Sun, Yang Xiang. *On-line EEG classification for brain-computer interface based on CSP and SVM*. 3rd International Congress on Image and Signal Processing, 2010.
- [113] Issam El Ouakouak Mourad Gharbi Fakhita Regragui Mohamed Majid H Rihab Bousseta, Salma Tayeb. *EEG efficient classification of imagined hand movement using RBF kernel SVM*. 11th International Conference on Intelligent Systems: Theories and Applications (SITA), 2016.
- [114] Martin Hofmann. *Support Vector Machines — Kernels and the Kernel Trick*. Bamberg Uni, 2006.
- [115] Lecturer: Michael I. Jordan. Scribe: Romain Thibaux. *The Kernel Trick*. CS281B/Stat241B: Advanced Topics in Learning and Decision Making, 2004.
- [116] Koji Tsuda Jean-Philippe Vert and Bernhard Scholkopf. *A Primer on Kernel Methods*. Kernel Methods in Computational Biology, 2004.
- [117] F. Pedregosa, G. Varoquaux, A. Gramfort, V. Michel, B. Thirion, O. Grisel, M. Blondel, P. Prettenhofer, R. Weiss, V. Dubourg, J. Vanderplas, A. Passos, D. Cournapeau, M. Brucher, M. Perrot, and E. Duchesnay. *Scikit-learn: Machine Learning in Python*, volume 12. 2011.
- [118] Oswin Forstner David Steyrl, Reinhold Scherer and Gernot R. Muller-Putz. *Motor Imagery Brain-Computer Interfaces: Random Forests vs Regularized LDA*. Graz University of Technology Publishing House, 2014.
- [119] L. Breiman. *Random forests*. Mach. Learn. Volume: 45 Pages: 5–32, 2001.
- [120] Fahrendi Rizky NASUTION Muhammad Murtadha RAMADHAN, Imas Sukaesih SI-TANGGANG and Abdullah GHIFARI. *Parameter Tuning in Random Forest Based on Grid Search Method for Gender Classification Based on Voice Frequency*. 2017 International Conference on Computer, Electronics and Communication Engineering, 2017.
- [121] Kantardzic M. *Data Mining: Concepts, Models, Methods, and Algorithms*. IEEE Press and John Wiley, 2002.
- [122] Kak A. C. Martinez A. M. *PCA versus LDA*. IEEE Transactions on Pattern Analysis and Machine Intelligence, 2001.

- [123] K. Fukunaga. *Introduction to Statistical Pattern Recognition*. second ed. Academic Press, 1990.
- [124] Athanase Papadopoulos. *Physics in Riemann's mathematical papers*. hal.archives-ouvertes.fr/hal-01628080, 2017.
- [125] Marco Congedo Christian Jutten Alexandre Barachant, Stephane Bonnet. *Riemannian geometry applied to BCI classification*. 9th International Conference Latent Variable Analysis and Signal Separation. Saint-Malo, France, 2010.
- [126] João F. Henriques Fátima Silva Jorge Batista Rui Caseiro, Pedro Martins. *Rolling Riemannian Manifolds to Solve the Multi-class Classification Problem*. IEEE Conference on Computer Vision and Pattern Recognition, 2013.
- [127] Alexandre Barachant. *pyRiemann Documentation Release 0.2.5*. 2018. [https://pyriemann.readthedocs.io/en/latest/auto\\_examples/motor-imagery/plot\\_single.html](https://pyriemann.readthedocs.io/en/latest/auto_examples/motor-imagery/plot_single.html).
- [128] Andrzej Cichocki Maureen Clerc Marco Congedo et al Fabien Lotte, Laurent Bougrain. *A Review of Classification Algorithms for EEG-based Brain-Computer Interfaces*. Journal of Neural Engineering, IOP Publishing, 2007.
- [129] MAHER MOAKHER. *A DIFFERENTIAL GEOMETRIC APPROACH TO THE GEOMETRIC MEAN OF SYMMETRIC POSITIVE-DEFINITE MATRICES*. SIAM J. MATRIX ANAL. APPL. Volume: 26. Issue: 3, Pages: 735–747., 2005.
- [130] Andrzej Cichocki Maureen Clerc Marco Congedo et al Fabien Lotte, Laurent Bougrain. *A Review of Classification Algorithms for EEG-based Brain-Computer Interfaces*. Journal of Neural Engineering, IOP Publishing, 2007.
- [131] Krishnaswamy S Gaber M, Zaslavsky A. *A Survey of Classification Methods in Data Streams*. Aggarwal C. Editors. Data Streams, Advances in Database Systems. US: Springer. Pages: 39-59, 2007.
- [132] Ron Kohavi. *A Study of Cross Validation and Bootstrap for Accuracy Estimation and Model Selection*. International Joint Conference on Artificial Intelligence IJCA, 1995.
- [133] R. Kohavi. *A study of cross-validation and bootstrap for accuracy estimation and model selection*. Proceedings of the Fourteenth International Joint Conference on Artificial Intelligence. Volume: 2. Pages: 1137–1143, 1995.
- [134] Guy Lapalme Marina Sokolova. *A systematic analysis of performance measures for classification tasks*. 2009.
- [135] Jason Brownlee. *Classification Accuracy is Not Enough: More Performance Measures You Can Use*. MachineLearningMastery, 2014.
- [136] Sutskever Ilya Krizhevsky, Alex and Geoffrey E Hinton. *Imagenet classification with deep convolutional neural networks*. *Advances in neural information processing systems*. Advances in Neural Information Processing Systems 25, 2012.

- [137] Fernandez S Graves, Alex and Marcus Liwicki. *Unconstrained online handwriting recognition with recurrent neural networks*. Advances in Neural Information Processing Systems, 2008.
- [138] Andrej Karpathy and G Toderici. *Large-scale video classification with convolutional neural networks*. Computer Vision and Pattern Recognition (CVPR), 2014.
- [139] Andrew NG. *Machine Learning Yearning. Technical Strategy for AI Engineers, in the Era of Deep Learning*. deeplearning.ai, 2018.
- [140] Yoav Freund and Robert E. Schapire. *A Decision-Theoretic Generalization of On-Line Learning and an Application to Boosting*. Journal of Computer and System Sciences, 1997.
- [141] Hato E Shafique, M.A. *Use of acceleration data for transportation mode prediction*. Springer US, 2015.
- [142] Jerome H. Friedman. *Greedy Function Approximation: A Gradient Boosting Machine*. Institute of Mathematical Statistics IMS, Reitz Lecture, 1999.
- [143] Tong He Tianqi Chen. *Higgs Boson Discovery with Boosted Trees*. Journal of Machine Learning Research, 2015.
- [144] Cheryl L Dickter and Paul D Kieffaber. *EEG Methods for the Psychological Sciences*. SAGE, 2014.
- [145] Upasana Mehta Amarjeet Kaur, Pooja Chaturvedi. *Analyzing and Eliminating Artifacts in EEG Signal (using Independent Component Analysis)*. International Journal of Scientific and Engineering Research, Volume 4, Issue 5, 2013.
- [146] Gevins A. *The future of electroencephalography in assessing neurocognitive functioning*. Electroencephalogr Clin Neurophysiol, 1998.
- [147] Chris Lo. *The magic touch: bringing sensory feedback to brain-controlled prosthetics*. ANALYSIS, 2019.
- [148] Stuart Nathan. *Future Prosthetics: towards the bionic human*. the Engineer, 2018.
- [149] Geneviève Ruiz by Swiss National Science Foundation. *Database of natural movements to feed machine-learning algorithms for prostheses*. Neuroscience, 2016.
- [150] Ecole Polytechnique Federale de Lausanne. *When the neuroprosthetics learn from the patient*. Neuroscience, 2015.